



Government of **Western Australia**  
Department of **Mines and Petroleum**

RECORD 2015/10

# EUCLA BASEMENT STRATIGRAPHIC DRILLING RESULTS RELEASE WORKSHOP: EXTENDED ABSTRACTS

compiled by  
CV Spaggiari and RH Smithies



Geological Survey  
of Western Australia



EXPLORATION  
INCENTIVE SCHEME



Curtin University



Government of **Western Australia**  
Department of **Mines and Petroleum**

**Record 2015/10**

# **EUCLA BASEMENT STRATIGRAPHIC DRILLING RESULTS RELEASE WORKSHOP: EXTENDED ABSTRACTS**

**compiled by  
CV Spaggiari and RH Smithies**

**Perth 2015**



**Geological Survey of  
Western Australia**

**MINISTER FOR MINES AND PETROLEUM**  
**Hon. Bill Marmion MLA**

**DIRECTOR GENERAL, DEPARTMENT OF MINES AND PETROLEUM**  
**Richard Sellers**

**EXECUTIVE DIRECTOR, GEOLOGICAL SURVEY OF WESTERN AUSTRALIA**  
**Rick Rogerson**

#### **REFERENCE**

**The recommended reference for this publication is:**

(a) For reference to an individual contribution:

Wingate, MTD, Kirkland, CL, Spaggiari, CV, and Smithies, RH 2015, U–Pb geochronology of the Madura Province, *in* Eucla basement stratigraphic drilling results release workshop: extended abstracts *compiled by* CV Spaggiari and RH Smithies: Geological Survey of Western Australia, Record 2015/10, p. 14–16.

(b) For reference to the publication:

Spaggiari, CV and Smithies, RH (compilers) 2015, Eucla basement stratigraphic drilling results release workshop: extended abstracts: Geological Survey of Western Australia, Record 2015/10, 70p.

**National Library of Australia Card Number and ISBN 978-1-74168-646-3**

Grid references in this publication refer to the Geocentric Datum of Australia 1994 (GDA94). Locations mentioned in the text are referenced using Map Grid Australia (MGA) coordinates, Zones 51 and 52. All locations are quoted to at least the nearest 100 m.



U–Pb measurements were conducted using the SHRIMP II ion microprobes at the John de Laeter Centre of Isotope Research at Curtin University in Perth, Australia. Isotope analyses were funded in part by the Western Australian Government Exploration Incentive Scheme (EIS). Lu–Hf measurements were conducted using LA-ICPMS at the ARC National Key Centre for Geochemical Evolution and Metallogeny of Continents (GEMOC), via the ARC Centre of Excellence in Core to Crust Fluid Systems (CCFS), based in the Department of Earth and Planetary Sciences at Macquarie University, Australia.

#### **Disclaimer**

This product was produced using information from various sources. The Department of Mines and Petroleum (DMP) and the State cannot guarantee the accuracy, currency or completeness of the information. DMP and the State accept no responsibility and disclaim all liability for any loss, damage or costs incurred as a result of any use of or reliance whether wholly or in part upon the information provided in this publication or incorporated into it by reference.

**Published 2015 by Geological Survey of Western Australia**

This Record is published in digital format (PDF) and is available online at <[www.dmp.wa.gov.au/GSWApublications](http://www.dmp.wa.gov.au/GSWApublications)>.

**Further details of geological products and maps produced by the Geological Survey of Western Australia are available from:**

Information Centre  
Department of Mines and Petroleum  
100 Plain Street  
EAST PERTH WESTERN AUSTRALIA 6004  
Telephone: +61 8 9222 3459 Facsimile: +61 8 9222 3444  
[www.dmp.wa.gov.au/GSWApublications](http://www.dmp.wa.gov.au/GSWApublications)

## Contents

Preface .....	1
<i>by CV Spaggiari and RH Smithies</i>	
Cenozoic records of dynamic topography, neotectonics and eustasy from the Eucla Basin .....	4
<i>by M O'Leary, L Mounsher, M Barham, and N Timms</i>	
Stratigraphical and geochemical analysis of pre-Cenozoic sediments beneath the Nullarbor Plain and implications for basin and margin evolution .....	7
<i>by M Barham, S Reynolds, M O'Leary, CL Kirkland, H Allen, P Haines, and R Hocking</i>	
Drilling Techniques – getting through complex cover to basement .....	9
<i>by P Mander</i>	
Madura Province: lithological characteristics and structural evolution.....	10
<i>by CV Spaggiari, RH Smithies, and RN England</i>	
U–Pb geochronology of the Madura Province.....	14
<i>by MTD Wingate, CL Kirkland, CV Spaggiari, and RH Smithies</i>	
Madura Province: geochemistry and petrogenesis .....	17
<i>by RH Smithies, CV Spaggiari, CL Kirkland, MTD Wingate, and RN England</i>	
Madura Province: isotopes and crustal evolution .....	29
<i>by CL Kirkland, RH Smithies, CV Spaggiari, and MTD Wingate</i>	
Forrest Zone: lithological characteristics and structural evolution .....	30
<i>by CV Spaggiari, RH Smithies, and RN England</i>	
U–Pb geochronology of the Forrest Zone of the Coompana Province .....	37
<i>by MTD Wingate, CL Kirkland, CV Spaggiari and RH Smithies</i>	
Forrest Zone: geochemistry and petrogenesis.....	41
<i>by RH Smithies, CV Spaggiari, CL Kirkland, MTD Wingate, and RN England</i>	
Forrest Zone: isotopes and crustal evolution.....	52
<i>by CL Kirkland, RH Smithies, CV Spaggiari, and MTD Wingate</i>	
Eucla basement results: implications for geodynamics and mineral prospectivity .....	53
<i>by CV Spaggiari, RH Smithies, CL Kirkland, RN England, SA Occhipinti, and MTD Wingate</i>	
Appendix 1: Summary logs of the stratigraphic cores and Haig cores .....	59





# Preface

by

**CV Spaggiari and RH Smithies**

The Eucla basement stratigraphic drilling program, funded through the Exploration Incentive Scheme (EIS), was established to investigate the greenfields Madura and Coompana basement provinces that are completely overlain by up to 500 m of cover rocks belonging to the Cretaceous and Cenozoic Bight and Eucla Basins in Western Australia. Because of this cover, drill cores provide the only means of obtaining basement rocks for analysis. Combined with work on existing EIS co-funded and donated company cores, the new drill cores provide insight into the geodynamics and prospectivity of the vast region that lies beneath the Nullarbor Plain, and increases our knowledge of the hidden basement provinces that are missing links in understanding Proterozoic Australian geology.

The main objectives of the program were to:

- Obtain high quality, oriented drill cores for detailed logging, structural analysis, petrography, geochronology, geochemistry and isotope analysis
- Understand the geological evolution of the basement provinces beneath the Bight and Eucla Basins — regional mapping under cover
- Understand the links between the Albany–Fraser Orogen, the Musgrave Province and the Gawler Craton
- Assist mineral system studies and provide insight into prospectivity
- Give the exploration industry geological knowledge, rather than just geophysical targets

During 2013 and 2014 eight diamond holes were successfully drilled, providing 1,560 m of high quality, oriented HQ basement core (Table 1, Fig. 1). The locations of the holes were chosen to investigate and map distinct geophysical domains interpreted in magnetic and gravity data, rather than as specific geophysical targets. They were also chosen to investigate potential host rocks to known mafic intrusions in the Madura Province (i.e. Loongana, Haig and Serpent). The eight stratigraphic cores have successfully intersected a diverse array of basement rocks,

from mafic volcanics to a variety of gabbroic and granitic rocks, and have provided a wealth of new information. This is still a work in progress, and the first results and interpretations are summarized in this volume.

Prior to this program the first two diamond cores drilled in the Madura Province were by Helix Resources northwest of Loongana, and these interlayered granitic and gabbroic rocks provided dates of c. 1400 Ma. These crystallization ages did not correlate with any dates further west in the Albany–Fraser Orogen and were extremely rare in the context of the Proterozoic evolution of Australia. They pointed at a different history in the region beneath the Nullarbor Plain. Following the release of government regional aeromagnetic (200 m line-spacing) and gravity data a few years ago, Teck Australia drilled 4 diamond holes (Haig and Serpent prospects), Gunson Resources drilled 2 diamond holes (Burkin prospect) and Venus Resources drilled 2 diamond holes in the Mundrabilla Shear Zone (Moodini prospect) (Figure 1). These cores are all stored at the GSWA Perth Core Library and have provided valuable background information to the three stratigraphic holes drilled in the Madura Province. In contrast, no diamond cores existed in the Forrest Zone of the Coompana Province and the five stratigraphic holes provide the first information of the nature of that basement. Very few of the older petroleum wells in the Nullarbor region intersect basement, and in most cases only minor amounts of small chips were recovered.

In addition, the drilling program has provided valuable experience and knowledge of the drilling conditions in the Nullarbor region, and the challenges of getting through the variable cover sequences to basement. Both RC and mud-rotary techniques have been trialled and assessed. The cover comprises limestone formations (Eucla Basin) underlain by shale and siltstone, and locally sandstone and conglomerate (Bight Basin), some of which is unconsolidated. Cover rocks were sampled from specific sites (425 m PQ core, 148 m HQ core, RC chips; Table 1) and these cores and chips are the subject of collaborative work between Curtin University's Department of Applied Geology and the Basins and Energy Geoscience Section of GSWA.

Table 1. Location and collar information of the eight stratigraphic holes.

2013 Hole ID	Location	Longitude	Latitude	Zone	Easting	Northing	Drilled depth to basement (m)	Azimuth	Inclination (degrees)	Collar (m)	PQ basin cover core (m)	HQ basin cover core (m)	HQ basement core (m)	Total depth of hole (m)
FOR004	Northwest of Eucla	128.553960	-31.280080	52	457543	6539272	389.90	70	-80	137.7 (RC)	229.00	17.50	180.50	570.40
FOR011	North-northeast of Forrest	128.175830	-30.617160	52	421006	6612536	284.87	10	-80	88.6 (RC)	196.50	None	215.00	500.10
FOR010	Northeast of Forrest	128.366040	-30.518600	52	439176	6623576	357.60	140	-80	227 (RC)	None	130.60	170.20	52780
MAD014	North of Loongana	127.085710	-30.478610	52	316247	6626622	250.00	340	-80	270 (RC)	None	None	189.40	459.50
MAD002	Near Gunnadorrak homestead	125.831450	-30.975750	51	770428	6569645	389.10	290	-80	389.1 (MR)	None	None	202.50	591.60
2014 Hole ID	Location	Longitude	Latitude	Zone	Easting	Northing	Drilled depth to basement (m)	Azimuth	Inclination (degrees)	Collar (m)	PQ basin cover core (m)	HQ basin cover core (m)	HQ basement core (m)	Total depth of hole (m)
MAD011	Southeast of Loongana	127.123210	-31.029953	52	320871	6565566	440.40	140	-75	440.40	None	None	200.75	641.15
FOR012	Forrest-Mundrabilla Track	127.985770	-31.300655	52	403478	6536633	310.10	150	-75	310.10	None	None	200.50	510.60
FOR008	East of Reid	128.686140	-30.829034	52	469984	6589303	383.75	105	-75	383.75	None	None	201.70	585.45

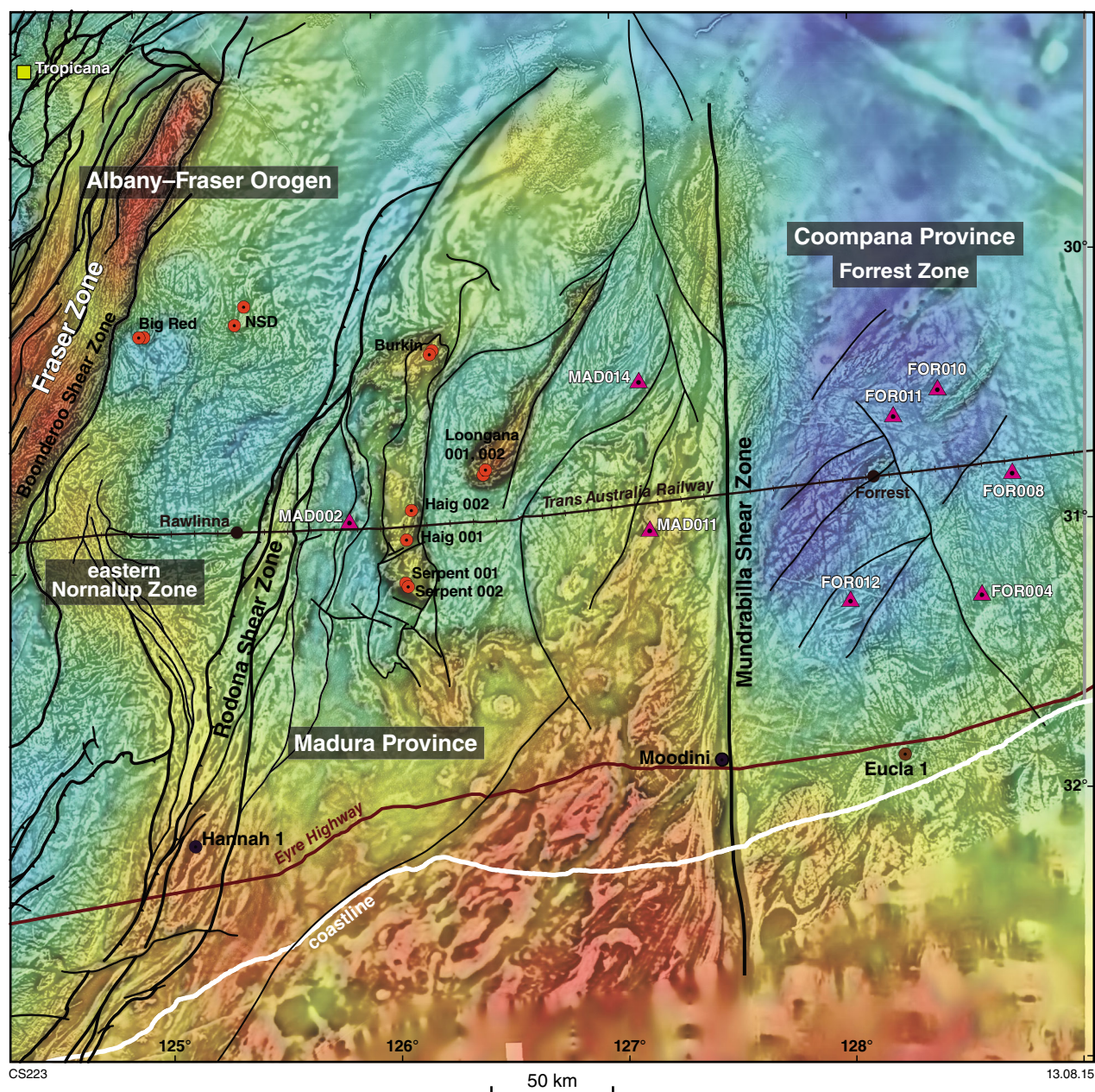


Figure 1. Simplified structures and drill site locations plotted on a drape image of gravity (colour) and reduced to pole, first vertical derivative aeromagnetic data (greyscale). The stratigraphic drill sites are shown with pink triangles, EIS co-funded drill sites with orange dots, donated core sites with purple dots, and the Eucla 1 petroleum well with a brown dot.

## Acknowledgements

GSWA thanks all of the Nullarbor locals for their invaluable assistance in making this drilling program a success. In particular we thank Colin and Brie from Mundrabilla Station and Cameron, Brett and Dot Day from Gunnadorrah Station for providing water carting and earthworks services, advice and hospitality. We thank Mark and Sandi of Forrest Airport for providing water and a friendly oasis. The Traditional Owners of the Ngadju and Spinifex people are thanked for Heritage Surveys of the proposed drilling sites.

# Cenozoic records of dynamic topography, neotectonics and eustasy from the Eucla Basin

by

M O'Leary<sup>1</sup>, L Mounsher<sup>2</sup>, M Barham<sup>3</sup>, and N Timms<sup>3</sup>

Vast areas of the Australian continental crust have traditionally been considered tectonically quiescent and largely unaffected by recent deformation processes. Indeed, modern crustal deformation within the Australian plate is difficult to resolve above background noise on a decadal timescale using GPS instrumentation (Tregoning, 2003). However, it is becoming apparent that deformation has occurred in parts of the Australian crust during the Cenozoic as a result of stress transfer from evolving plate-boundary dynamics during the extremely rapid northward drift of the Australian Plate (Sandiford, 2003; Keep et al., 2007; Clark et al., 2012; Babaahmadi & Rosenbaum, 2014; Holford et al., 2014). Despite increasing awareness, there remains a paucity of onshore field data quantifying timing and amplitude of Cenozoic deformation to better understand: (i) evolution of the Australian intra-plate stress field as well as cratonic stress-fields in general, (ii) the significance of strain structures in terms of their seismic hazard and influence on basin evolution, and (iii) the degree of tectonic overprinting on palaeoshoreline elevation data in supposedly "stable" locations.

The Eucla Basin for example, has traditionally been considered a tectonically quiescent domain, with very few early studies considering the onshore evidence of Cenozoic tectonic activity. More recently however, the Eucla Basin has yielded important evidence of: 1) continent-scale Cenozoic crustal deformation (Sandiford, 2007), 2) basin-wide tilting (Hou et al., 2008) and, 3) faulting (Clark et al., 2012). Sandiford (2007) noted a distinct latitudinal asymmetry in the geomorphology of the Australian landmass, expressed through a number of irregularities in the sedimentary record; Cenozoic marine sediments have been preserved up to 250 m above the present-day sea level, by comparison across northern Australia coeval marine sediments lie almost exclusively below present-day sea level. Hou et al. (2008) identified

east-down dynamic tilting of the Eucla Basin based on the relative height difference in coeval shoreline barriers situated on the eastern and western margins of the basin. Lastly, Clark et al. (2012) was able to show, using SRTM digital elevation data, an exquisite record of linear fault scarps, however due to the duration of basin emergence (~10 mya) and low rates of surface deflation (~5 m/mya), these scarps likely reflect the long-term tectonic stability of the underlying Proterozoic basement terrains.

Common to all these studies is they have relied heavily on remote sensed (SRTM) digital elevation models, with only limited ground truth or stratigraphic analysis, thus have had to make assumptions on the extent to which the original fault or deformation feature has been modified or masked through surface erosional/depositional processes. Here we attempt to redress the lack of field data in quantifying Cenozoic deformation of the Australian crust through reanalysis of tectonic features within the Eucla Basin in southern Australia.

In order to establish the degree of uplift and/or deformation of the Eucla Basin, a broad survey of older and higher Miocene age marine strata was undertaken. We surveyed the subsurface contact elevations of marine erosional unconformities exposed in caves, cliffs and dolines on the Nullarbor Plain (NP). We reason that these marine erosional unconformities would have originally formed broad quasi-horizontal contact surfaces, similar to modern shaved continental shelf morphologies, and have been unaffected by post depositional karst processes or surface deflation.

A total of 27 field sites were selected on the Nullarbor and Roe Plains. The suite of sites comprised 19 caves/rockholes, three road cuts, two coastal outcrops, two gullies along the Hampton Escarpment and one quarry. Horizons were constrained at each site based on the sedimentological parameters of the bounding limestones, and elevations were measured to a high degree of accuracy ( $\pm 15$  cm) through the use of a differential GPS and a laser total station. Sedimentological data were also recorded at each field site and all horizons were examined for evidence of karstification, erosion or irregular depositional topography. These records represented a means by which constant or step change in contact elevations could

1 Department of Environment and Agriculture, Curtin University, Bentley WA 6845

2 Woodside Energy Ltd., Perth WA 6000

3 Department of Applied Geology, Curtin University, Bentley WA 6845



be investigated. Given the vast geographic extent and remoteness of the Eucla Platform, supplementary data were sourced from online drilling records (63 sites – South Australian and Western Australian Geological Surveys), published literature (24 sites – Lowry, 1970) and logging archived drill core and chips (12 sites). In each case, the logged contact depths were converted to elevations using DEM values extracted for each site.

The investigation of subsurface horizons in the Cenozoic carbonate stratigraphy did highlight the effect that long-wavelength tilting has had on the basin's architecture. The degree of tilting measured on the basal Nullarbor Limestone horizon was shown to mirror that of the inboard Miocene palaeoshoreline, which supports the predefined notion that dynamic topography has been an important driver in the uplift of southwestern Australia over the last 15 million years.

New evidence of intrabasin warping is identified in the present-day expression of a Miocene planation surface, with approximately 25 m of uplift occurring in the region immediately north of the lower Pliocene age Roe Plain. Assuming linear deformation this equates to an approximate uplift rate of about 1.5 m/Mya. Possible drivers of this deformation include dynamic topography, or alternatively, the erosion and removal of around 1000 km<sup>3</sup> of limestone could have resulted in isostatic disequilibrium of the crust beneath the Roe Plain causing the area immediately north of the plain to bow up.

Analyses conducted on the suite of onshore faults suggest that they likely developed under a neotectonic compressional regime. A component of strike slip displacement or reverse reactivation is also inferred from anomalously low 'vertical displacement/scarp length' fault ratios. Colocation of the surface fault ruptures (mapped from DEM) with linear aeromagnetic anomalies that represent more substantial displacements and juxtaposition of basement geology subcrop, imply that the faults likely propagated along reactivated, pre-existing crustal weaknesses. Stress field heterogeneity, at the scale of the area studied, does not appear to have occurred across the expanse of the basin, as established by a comparison of fault characteristics and expression of planation benchmarks either side of the centrally located (and structurally significant at depth Mundrabilla–Lasseter Shear Zone) Mundrabilla Fault.

The vastness of Nullarbor Plain along with low rates of sedimentation and erosion make it an ideal location to study Cenozoic records of dynamic topography, neotectonics and eustasy. Evidence of multiple wavelength tectonic events, from fault ruptures to continental scale tilting have been identified, however establishing the timing, rates and amplitude of deformation are still uncertain and warrant further investigation.

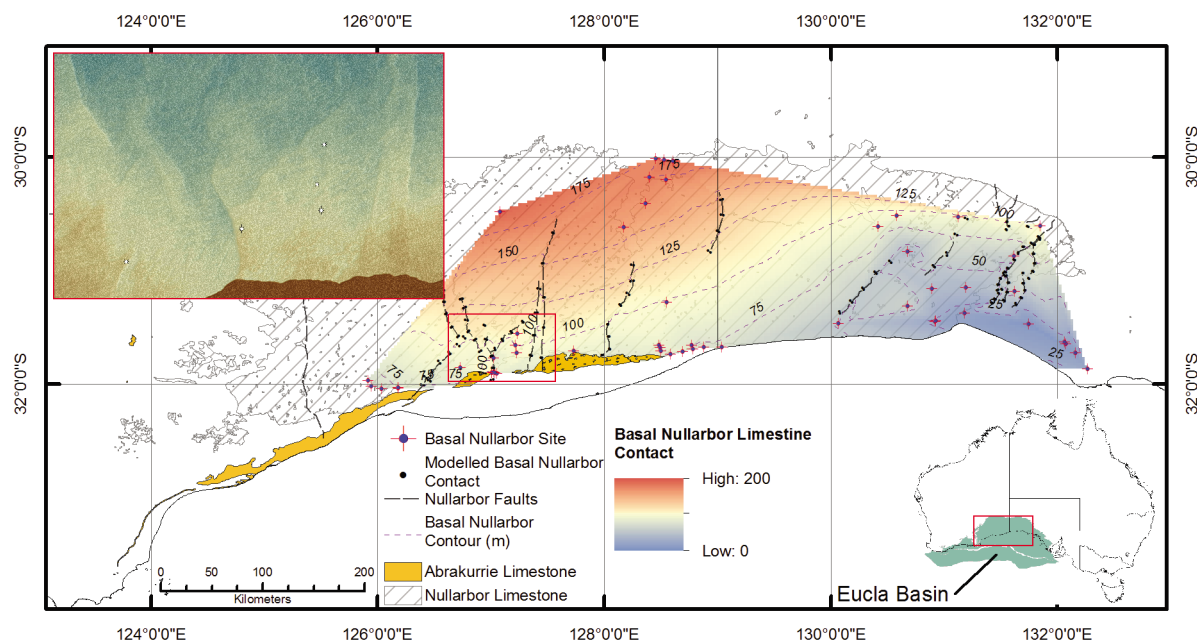


**Figure 1. Nullarbor Plain tectonics and deformation.** Coloured contours represent the basal Nullarbor Limestone contact, a transgressive quasi-horizontal marine abrasion platform. Elevations increase towards the central Nullarbor Plain suggesting this region has experienced significant uplift, while elevations decrease to the east suggesting this region has experienced significant subsidence. Where the Middle Miocene Abrakurrie Limestone is exposed at the surface indicates that there has been complete deflation/erosion of the overlying Nullarbor Limestone; this could be equivalent to tens of metres of karst dissolution and would suggest that the original Nullarbor Plain surface has been significantly modified through karst dissolution. Faults appear to be more common in the area north of Madura and may be the result of intra-plate stress fields reactivating deeper fault structures. Interestingly these faults occur within the region of identified localised uplift, so it is possible that faulting could also be the result of crustal flexure driven by isostatic forces as the Roe Plain developed.

## References

- Babaahmadi, A. & Rosenbaum, G. (2014) Late Cenozoic Intraplate Faulting in Eastern Australia. *Journal of Structural Geology*, 69, Part A, p. 59-74.
- Clark, D., McPherson, A. & Van Dissen, R. (2012) Long-Term Behaviour of Australian Stable Continental Region (Scr) Faults. *Tectonophysics*, 566-567, p. 1-30.
- Holford, S.P., Tuitt, A.K., Hillis, R.R., Green, P.F., Stoker, M.S., Duddy, I.R., Sandiford, M. & Tassone, D.R. (2014) Cenozoic Deformation in the Otway Basin, Southern Australian Margin: Implications for the Origin and Nature of Post-Breakup Compression at Rifted Margins. *Basin Research*, 26, p. 10-37.
- Hou, B., Frakes, L.A., Sandiford, M., Worrall, L., Keeling, J. & Alley, N.F. (2008) Cenozoic Eucla Basin and Associated Palaeovalleys, Southern Australia — Climatic and Tectonic Influences on Landscape Evolution, Sedimentation and Heavy Mineral Accumulation. *Sedimentary Geology*, 203, p. 112-130.
- Lowry, D.C. (1970) Geology of the Western Australian Part of the Eucla Basin. G. S. o. W. Australia, Geological Survey of Western Australia. Perth. Bulletin 122, 207p.
- Sandiford, M. (2003) Neotectonics of Southeastern Australia: Linking the Quaternary Faulting Record with Seismicity and in Situ Stress. *Geological Society of America Special Papers*, 372, p. 107-119.
- Sandiford, M. (2007) The Tilting Continent: A New Constraint on the Dynamic Topographic Field from Australia. *Earth and Planetary Science Letters*, 261, p. 152-163.
- Tregoning, P. (2003) Is the Australian Plate Deforming? A Space Geodetic Perspective. In: *Evolution and Dynamics of the Australian Plate* (Ed. by R. R. Hillis & R. D. Müller), p. 41-48. Geological Society of Australia Special Publication 22 and Geological Society of America Special Paper 372.



# Stratigraphical and geochemical analysis of pre-Cenozoic sediments beneath the Nullarbor Plain and implications for basin and margin evolution

by

M Barham<sup>1</sup>, S Reynolds<sup>1</sup>, M O'Leary<sup>1</sup>, CL Kirkland<sup>1</sup>, H Allen, P Haines, and R Hocking

Sediments of the Eucla and Bight Basins are extensively developed along the southern margin of Australia as a result of the separation of the Australian and Antarctic continents during the Mesozoic. Sediments along Australia's Southern margin preserve an important record of this rifting as well as the environmental conditions of the time. Furthermore, understanding the depositional architecture and controls of these sediments has implications for exploiting the significant economic potential for mineralisation in the basement and for petroleum systems in the Great Australian Bight. Unfortunately however, relatively little is known about the Mesozoic (and older) sequences due to the extensive development of blanketing Cenozoic carbonates and relatively limited exploration in the region.

Drilling by the GSWA through the Exploration Incentive Scheme in 2013 and 2014 has provided new data that has been incorporated with pre-existing, and recently made publicly available, well-data to revise our understanding of the geological history of the Madura Shelf (the onshore Bight Basin) and produce a 3D stratigraphic model within a GIS database. This talk will discuss the sedimentology and stratigraphy of the Madura Shelf sediments as well as present new palynology and U/Pb and Hf-isotope data of detrital zircons from throughout the sequences examined in WA.

New stratigraphic units have been identified disconformably underlying the Mesozoic sequence of the Madura Shelf, which testify to isolated pre-existing depocentres along the southern margin of Australia that may have influenced its later development. Through palynology, it has been possible to resolve the relative timing and environment of deposition of lithostratigraphical units across the Madura Shelf. Deposition commenced during the early Cretaceous with initial sedimentation characterised by non-marine sands and silts. Widespread marine conditions were established later, at least by the mid-Albian. Localised anomalies in the development of the Madura Formation suggest movement occurred during the Cretaceous along faults that may be correlated into 2D seismic lines offshore.

However, by the end of the Cretaceous, the Madura Formation had blanketed all significant pre-existing topography (Figures 1 and 2), with the preserved surface showing little evidence for any later disturbance. In-fact, enigmatically, neither the Madura Formation itself, nor its upper surface, show evidence of the extended periods of time they represent, with little variability/cyclicality or indicators of erosion preserved.

Analysis of detrital zircon age-populations recovered from the major stratigraphic units encountered beneath the Eucla Basin are consistent with the expected age signatures of the Musgrave Province and Albany-Fraser Orogen, implying these basement blocks are the likely source (via several older sedimentary basins). Hf-isotopes further refine this and suggest the Musgrave Province is the main primary source of the refractory mineral cargo. Detrital zircon U/Pb data from the Madura Shelf sediments are comparable to some of the newly identified older units as well as sediments from Cenozoic shorelines along the Eucla Basin that host world-class heavy mineral deposits. However, significant differences exist between the data recovered here and those documented from the Cretaceous Ceduna Delta.

This geochemical work suggests:

- (i) Dominance of Musgrave Province-sourced sediment.
- (ii) That these sediment pathways were long-lived (established pre-Cretaceous).
- (iii) That a partitioning/disconnection existed between the sediment systems operating in the eastern and western Bight Basin, with little to no sediment from the east being supplied to the west.
- (iv) That essentially syn-depositional mid-Cretaceous volcanism provides an absolute age constraint on the Madura sequence (based on a euhedral zircon population with distinct oscillatory zoning and an age contemporaneous with palynology). It is proposed that this population represents a distal air-fall from explosive super-eruptions along the eastern seaboard of Australia and confirms the dominant polar easterlies experienced by Australia at this time.

<sup>1</sup> Department of Applied Geology, Curtin University, Bentley WA 6845

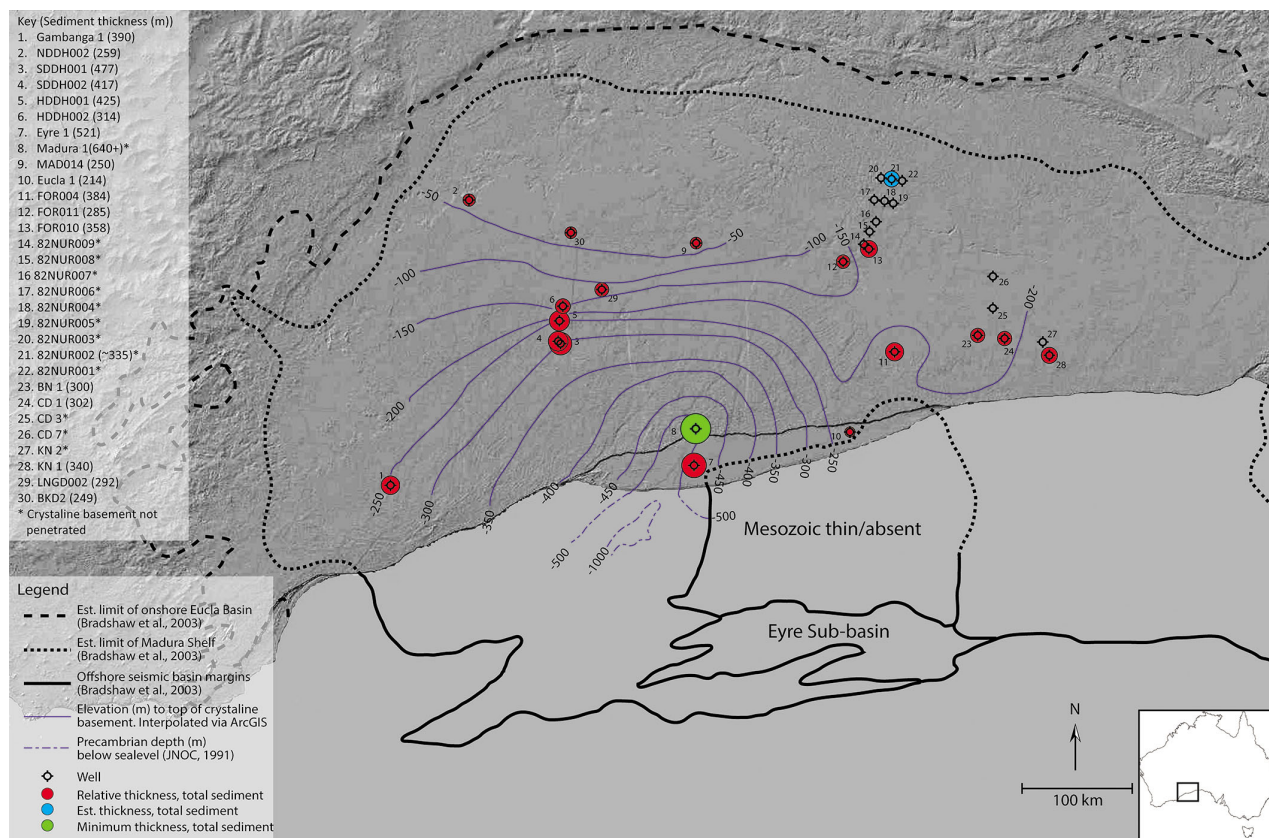


**Figure 1.** Dots represent the relative total sediment thickness above basement derived from the available borehole data. Contours are for the crystalline basement surface and are plotted in m relative to the Australian Height Datum.

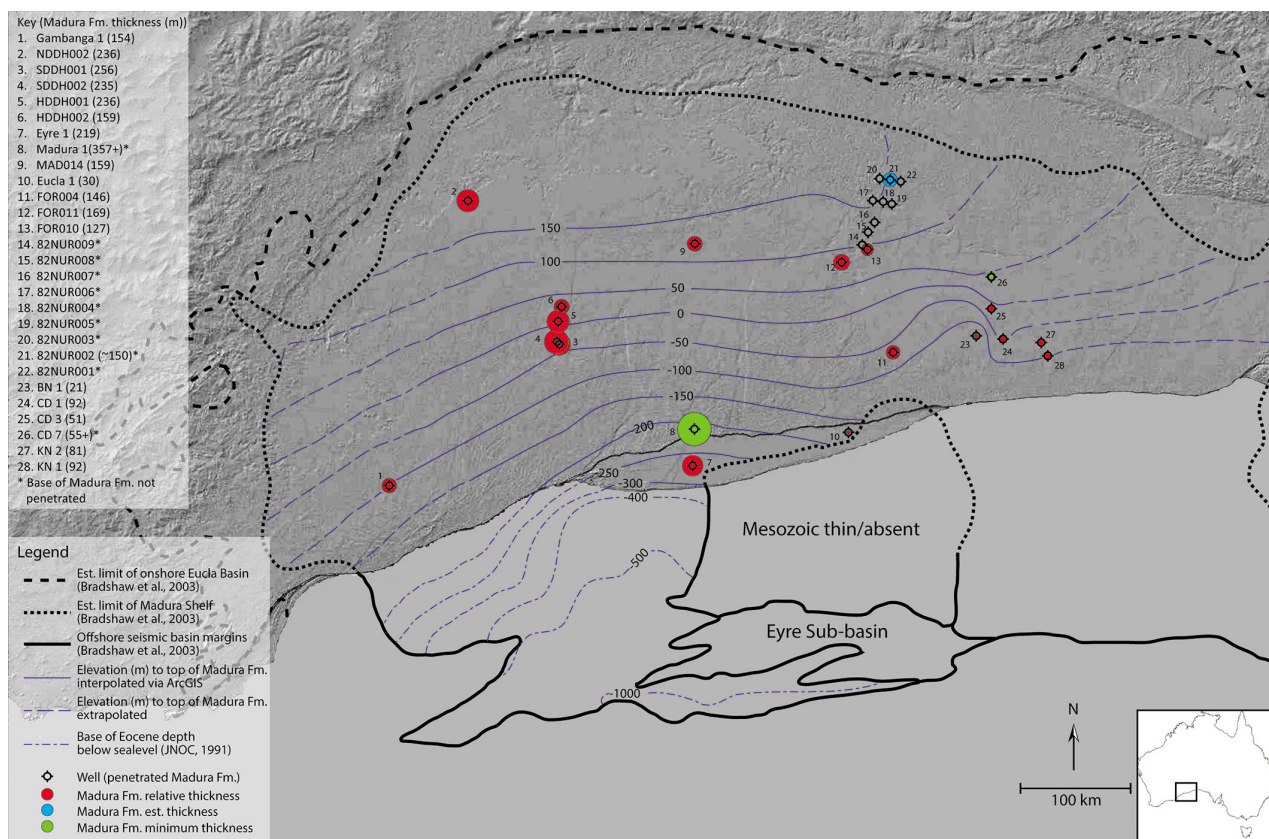


**Figure 2.** Dots show the relative thickness of the Madura Formation. Contours are for the top of the Madura Fm., which is the top of the known Cretaceous sediments on the Madura Shelf (shown in m above the Australian Height Datum).

# Drilling Techniques – getting through complex cover to basement

by

P Mander\*



Lessons learnt from two successful drilling campaigns by First Drilling during 2013 and 2014 are described below.

## Main Challenges:

- Access to drill locations
- Availability of water
- Keeping water up to the drill
- Hole stability whilst drilling through cover to basement
- Weather

Once drilling commenced, using mud rotary techniques, hole advancement and stability were achieved allowing successful casing of the hole into basement. From there, the target zones for the hole could be accurately drilled in competent rock using diamond drilling techniques.

Choosing a mud drilling system with flexibility to change to the nature of the ground conditions as the holes progressed was paramount to success. Generally using a Salt Water tolerant Gel and PAC based system enabled production whilst reducing hole degradation of the poorly consolidated sandstones, siltstones and shale formations of the Madura Formation. Inhibition of the shales was extremely important in maintaining rotation and reducing drilling torque. Constant adjustment of the fluids makeup was necessary due to the changing ground conditions.

Continuous 12 hour shifts are required with crews changing over on the rig. To avoid the risk of compromising the hole, consistent fluid pressure is needed to aid stability, so wherever possible the drilling process should not be stopped until case off.

Lost circulation through the early stages of the hole within the limestones poses an additional challenge as the crew work hard to maintain a water supply for drilling and then to prepare the drilling fluid to acceptable strengths and yields before pumping down the hole. Several other additives are required to try and maintain as much fluid circulation as possible.

A Solids Removal Unit (SRU) was employed on site to assist with recirculation of fluids when achievable. The most beneficial use of this equipment was during the diamond drilling phase as circulation at the top of the hole was rarely achieved even after attempts at cementing through the voids. An added advantage of the SRU is that it keeps the site clean and dry and makes rehabilitation much simpler.

Every hole drilled was a success in reaching basement and continuing through to end of hole depth, a significant achievement given that no prior drilling had taken place in the vicinity.

---

\* First Drilling Group, Unit 1/31 Hensbrook Loop, Forrestdale WA 6112

# Madura Province: lithological characteristics and structural evolution

by

CV Spaggiari, RH Smithies, and RN England<sup>1</sup>

## Introduction

The Madura Province lies between the Albany–Fraser Orogen and the Forrest Zone of the Coompana Province, where it is truncated by the subvertical Mundrabilla Shear Zone. It is separated from the Albany–Fraser Orogen by the Rodona Shear Zone, a complex, broad network of shear zones with a dominant, moderate easterly dip (Spaggiari et al., 2014a). Prior to the stratigraphic drilling program a total of 10 diamond cores existed (including Moodini; Fig. 1 in the Preface), drilled as exploration targets into either magnetic or gravity highs, or both. In contrast, the three new stratigraphic holes are located over regional magnetic and gravity domains to aid in regional interpretation of the basement geology. The cores provide important constraints on understanding the evolution of the Madura Province.

## Stratigraphic core MAD002

Drill hole MAD002 is located on a curving, generally north- to northeast-trending, locally folded, stripy magnetic fabric and moderate gravity response. The rocks the magnetic fabric relate to occur in the hanging wall of the Rodona Shear Zone, and are inferred to lie structurally above accreted oceanic-arc rocks to the east (Loongana, Haig and Serpent prospects, Haig Cave Supersuite; Spaggiari et al., 2014a), based on the dominant, moderate northwest dip of reflectors in seismic line 12GA-AF3 below the location of MAD002 (Spaggiari et al., 2014b). The lithological units in MAD002 are described below, and shown in the graphic log in Appendix 1.

The core comprises two main units: 1) fine-grained (average 1–2 mm), variably coloured, distinctly laminated to layered, foliated mafic amphibolite schist, interpreted as metabasalt, and 2) medium-grained, generally pale grey to white, thin leucogranite veins interpreted to be metamorphosed plagiogranite (adakite) (Fig. 1a,b). The

distinct layering in the metabasalt comprises assemblages of blue-green hornblende – plagioclase – titanite (sometimes replacing ilmenite), typically with variable quantities of epidote, biotite, and quartz, and locally with ilmenite, rutile, and magnetite. The assemblage blue-green hornblende – epidote – oligoclase – quartz – biotite – ilmenite – magnetite is likely to record a lower amphibolite facies metamorphic peak, with very minor indication of retrogression. Although speculative, the metabasalt could be interpreted as a mafic tuff, with the fine-grained, differentiated layering and laminations formed as an ash-fall sequence, possibly in a shallow-marine setting.

The leucogranite is composed of plagioclase–quartz–biotite, locally with hornblende and magnetite, and minor chlorite. The leucogranite veins are generally parallel to the main fabric in the metabasalt, but locally cross-cut the layering, and are therefore intrusive into the metabasalt.

## Sulfides

Sulfides are present in minor amounts throughout much of the core and in both metabasalt and leucogranite. They occur as disseminated grains, in stringers and veins with similar minerals to the host rocks (Fig. 1c), and along fracture fillings. The veins are generally mm-scale and cut the fabrics in both units. Some veins include calcite and chlorite, and may be younger, lower temperature veins. Thin veins are locally associated with small brittle faults, with offsets of a few millimeters to a few centimeters. Some of these veins also contain similar minerals to the host rock, suggesting they formed at similar metamorphic conditions.

The disseminated sulfides comprise anhedral pyrite (probably retrogressed pyrrhotite), variably pyritised pyrrhotite, and chalcopyrite. Stringers comprise pyrite, hornblende, titanite and minor anhedral chalcopyrite. One example in the metabasalt (GSWA 206767, 435.48–435.59 m) comprises plagioclase–biotite–pyrite–chalcopyrite–titanite–magnetite veinlets, interpreted to have been present at the metamorphic peak. Another example (GSWA 206769, 457.73–457.88 m; 15 cm ½ HQ

---

<sup>1</sup> Petrology Services, Duncraig, WA 6023



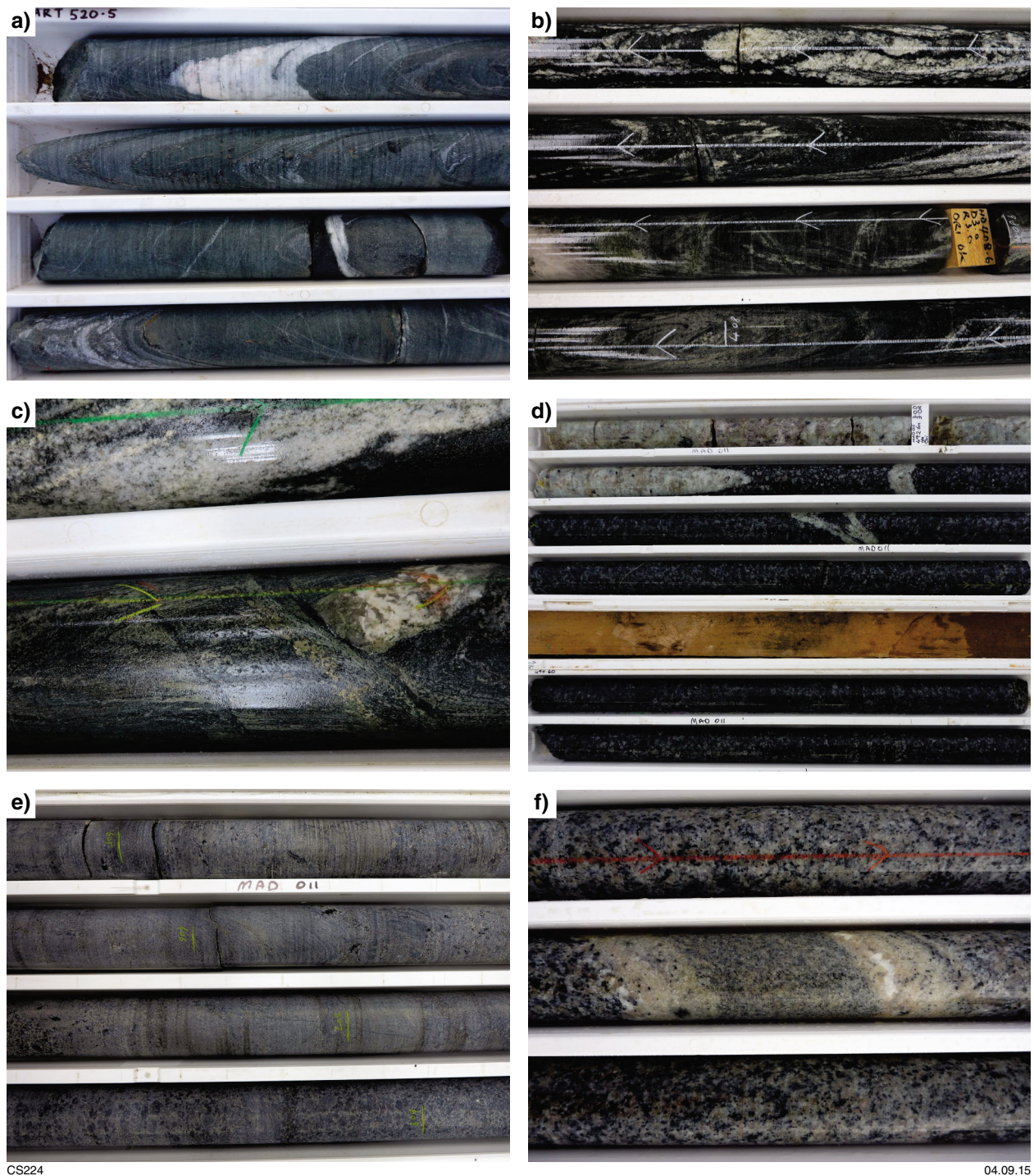


**Figure 1.** Photographs of Madura Province stratigraphic basement cores showing: a) distinct layering in metabasalt, intruded by plagiogranite veins (MAD002, photographed dry); b) metabasalt with wispy plagiogranite veins and quartz-epidote veins (MAD002, photographed wet); c) metabasalt and plagiogranite with sulfide veinlet (MAD002, photographed wet); d) undeformed, cumulate texture leucogabbro grading to blocky, coarse, plagioclase-rich leucogabbro (MAD011, photographed wet); e) rafts or xenoliths of fine-grained amphibolite interpreted as metabasalt within leucogabbro (MAD011, photographed dry); f) coarse-grained, equigranular biotite-hornblende granodiorite intruded by fine-grained, equigranular biotite-granite with coarse-grained margins (MAD014, photographed wet).

core, 1147 ppm Cu) comprises sericitised plagioclase, blue-green hornblende, tan biotite concentrated along the walls, and minor chlorite. Anhedral <1.5 mm pyrite, forming about 3% of the vein, is quite commonly rimmed with or partly surrounded by <0.1 mm granular magnetite and anhedral chalcopyrite. Chalcopyrite also forms a veinlet in a coarse, unaltered hornblende prism with no associated retrogression. This is similar to metabasalt GSWA 206770 (458.29–458.46 m; 17 cm  $\frac{1}{2}$  HQ core, 2146 ppm Cu), which comprises sericitised plagioclase-rich veins and quite strong pyrite–chalcopyrite mineralisation.

## Structural analysis

The layering in both units is folded into steeply northeast- to vertically-plunging, tight chevron and typically Z- or S-folds that have a hornblende-bearing, axial planar foliation. At 395.20 m drilled depth, a small-scale fold has an axis that plunges  $78^\circ$  to 042, and the enveloping surface is oriented  $82^\circ$  to 050 (dip, dip direction). The axial planar foliation is mostly subparallel to the layering, except in the hinges. Together, the foliation and the layering define the main fabric in the metabasalt, which has a predominant, steep northwest or southeast dip. Stereonet analysis of a best fit great circle from poles to planes of the main fabric gives a calculated fold axis of  $86^\circ$  to 356, similar to the measured fold. Fitting an axial plane to the poles gives an orientation of  $86^\circ$  to 029 (dip, dip direction). This suggests that the larger fold structure is relatively open, west-northwest trending, with the limbs comprising a series of steeply-plunging S- or Z-folds where the long limbs define the prevalent northwest and southeast steep dips observed in the core. Rare, small-scale refolded folds imply an earlier phase of folding. Given that it is difficult to produce steeply plunging primary (F1) folds, the steep plunges of the observed and calculated folds suggests they are secondary (F2) folds.

The folding is observed in both the metabasalt layering and the leucogranite veins however, thin leucogranite veins also locally transgress the fabric and folds. This suggests the leucogranite veins intruded either pre- and/or syn-folding. Alternatively, there may be a second generation of granitic veins that cut the folds, but no distinction can be made petrographically or geochemically, so this is unlikely. The preferred interpretation is that the veins intruded during the same event as the folding, with late injections or remobilisation of felsic material as the folds formed. This also fits with the formation of cross-cutting sulfide-bearing veins, described above.

## Stratigraphic core MAD011

Drill hole MAD011 is located on a prominent, northeasterly trending anomaly of coincident high magnetic and gravity response west of the Mundrabilla Shear Zone. The anomaly is similar to other coincident magnetic and gravity highs that wrap into the shear zone and indicate sinistral shear sense. The lithological units in MAD011 are described below, and shown in the graphic log in Appendix 1.

The core is dominated by medium- to coarse-grained, unfoliated leucogabbro (ferro-monzogabbro) with subhedral to euhedral plagioclase up to 1 cm. The leucogabbro generally has a cumulate texture, and appears undeformed. Locally, the leucogabbro grades to a blocky, coarse, plagioclase-rich leucogabbro (Fig. 1d). The leucogabbro comprises a typical assemblage of plagioclase, quartz, and mafic clots comprising aggregates with variable proportions of granoblastic dark blue-green strongly poikiloblastic metamorphic hornblende with small inclusions of quartz, and outer zones of anhedral biotite. Myrmekite is present in some samples. Magnetite (locally with pyrite) and ilmenite are locally heavily rimmed with or replaced by titanite. One example (GSWA 216212) has an assemblage of biotite–orthopyroxene (retrogressed to cummingtonite)–clinopyroxene (pigeonite)–apatite–quartz. Another example (GSWA 206783; 14 cm  $\frac{1}{2}$  HQ core, 253 ppm Cu) contains minor 1 mm anhedral grains of pyrite and <0.1 mm anhedral chalcopyrite associated with magnetite. The Cu may be magmatic, or could have been mobilised from the mafic country rock described below.

Entrained within the leucogabbro are rafts or xenoliths of fine-grained (1–2 mm), variably layered or laminated, locally foliated, mafic amphibolite, interpreted as a metabasalt that may have been metamorphosed to a mafic hornfels during intrusion of the leucogabbro (Fig. 1e). The fine grain size and fine dissemination of ilmenite suggest that they were flows, fragmentals, or chilled intrusives. These rocks typically contain the assemblage orthopyroxene–clinopyroxene–hornblende–plagioclase–ilmenite, and locally magnetite and biotite. Orthopyroxene and plagioclase typically have granoblastic textures. The foliation and layering has variable orientations, consistent with fragmentation by the intrusion of the leucogabbro. In the lower section of the core some of the metabasalt is unfoliated and has a globular texture that is disaggregated and chaotic, whereas in other sections the metabasalt is foliated and dominated by acicular amphibole. Both lithologies are cut by thin felsic veins, including quartz–epidote veins, and some of these contain sulfides.

## Stratigraphic core MAD014

Drill hole MAD014 is located in the center of an elongate, northeasterly trending area of low gravity response and low to moderate response magnetic fabric, cut by splays off the Mundrabilla Shear Zone. The core comprises unfoliated, mesocratic, medium- to coarse-grained, equigranular biotite–hornblende granodiorite to monzogranite (high-K series; see graphic log in Appendix 1). The typical assemblage is plagioclase–microcline–quartz–biotite–titanite, with possible allanite. Some samples contain hornblende, and fluorite. This is intruded by fine- to medium-grained, equigranular, biotite granite, commonly with 1–10 cm thick pegmatite margins, and similar assemblages to the coarse-grained host (Fig. 1f). These rocks appear to be undeformed, even though they occur within the regional, northeasterly trending magnetic fabric. It is feasible that the margins of the elongate magnetic zone are deformed, but the center is not. The granites are cut by minor quartz or quartz–epidote veins, locally with sulfide.

## Other rocks previously drilled in the Madura Province

The Loongana prospect (drilled by Helix Resources Ltd in 2003; Bunting and McIntyre, 2003) and the Haig and Serpent prospects (drilled by Teck Australia Pty Ltd in 2010–11, co-funded through the EIS; Tillick, 2011; Tillick and Hunt, 2010; Figure 1 in Preface) comprise a series of dominantly weakly layered, medium-grained, mafic cumulate rocks, locally with medium-grained, peridotitic cumulate rocks, intruded by medium- to coarse-grained trondhjemitic plagiogranite dated at c. 1400 Ma in the Loongana prospect (see summary and references in Spaggiari et al., 2014a). The Haig prospect has similar aged detritus in conglomerate above the basement unconformity (Reynolds, 2014; see graphic logs in Appendix 1 for Haig cores).

The Moodini prospect (Venus Metals) occurs on the eastern edge of the Madura Province within the Mundrabilla Shear Zone (Figure 1, in Preface). The cores contain metagranite with a strong subhorizontal fabric that yielded identical magmatic crystallization dates of  $1125 \pm 7$  Ma and  $1132 \pm 9$  Ma (GSWA 192565 and 192566, respectively; preliminary data). These dates are similar to the Eucla 1 granite crystallization date of  $1140 \pm 8$  (Kirkland et al., 2011) and provide a maximum age constraint on the timing of sinistral shearing on the Mundrabilla Shear Zone.

## References

- Bunting, JA and McIntyre, J R 2003, Loongana Project combined annual technical report C150/2001: Exploration Licences 69/1516, 1517, 1718, 1719 and 1720 for the period 11/8/2002 to 10/8/2003, Helix Resources Limited, 29p.
- Kirkland, CL, Wingate, MTD, Spaggiari, CV and Tyler, IM 2011, 194773: granitic rock, Eucla No. 1 drillhole; Geochronology Record 1001: Geological Survey of Western Australia, 4p.
- Reynolds, S, 2014, Stratigraphic evolution of the southern Australian onshore Bight Basin: a record for the breakup of Gondwana during the Cretaceous: Curtin University Honours thesis, unpublished.
- Spaggiari, CV, Kirkland, CL, Smithies, RH, and Wingate, MTD, 2014a, Tectonic links between Proterozoic sedimentary cycles, basin formation and magmatism in the Albany–Fraser Orogen: Western Australia Geological Survey of Western Australia Report 133, 63p.
- Spaggiari, CV, Occhipinti, SA, Korsch, RJ, Doublier, MP, Clark, DJ, Dentith, MC, Gessner, K, Doyle, MG, Tyler, IM, Kennett, BLN, Costelloe, RD, Fomin, T and Holzschuh, J 2014b, Interpretation of Albany–Fraser seismic lines 12GA-AF1, 12GA-AF2 and 12GA-AF3: implications for crustal architecture, in Albany–Fraser Orogen seismic and magnetotelluric (MT) workshop 2014: extended abstracts: compiled by CV Spaggiari and IM Tyler Geological Survey of Western Australia, Record 2014/6, p. 28–51.
- Tillick, D 2011, Final Report of Co-funded Government – Industry Drilling Program at the Haig Prospect, Eucla Project, August 2011, Teck Australia Pty Ltd, 24p.
- Tillick, D and Hunt, D 2010, Eucla Project, C283/2008, Combined Annual Report for the Period 1 April 2009 to 31 March 2010, Teck Australia Pty Ltd, 13p.



# U–Pb geochronology of the Madura Province

by

MTD Wingate, CL Kirkland, CV Spaggiari and RH Smithies

## Introduction

Four samples were collected for U–Pb geochronology from three new stratigraphic drillcores in the Madura Province. Previous geochronology results are available for eight samples from three industry drillcores in the Madura Province. Analytical methods are described in detail in Wingate and Kirkland (2015). Analyses >5% discordant are generally considered to be unreliable and, in most cases, are not included in determining the age of each sample. Results are described below in order of decreasing age. Except where noted otherwise, the dates discussed below are based on  $^{207}\text{Pb}^*/^{206}\text{Pb}^*$  ratios, and mean ages for samples, or groups of samples, are quoted with 95% confidence intervals ( $t\sigma\sqrt{\text{MSWD}}$ , where  $t$  is Student's  $t$ ). Results for all samples are listed in Table 1. During sampling, care was taken to document the geological context of each sample within the drillcore, and fractions of each geochronology sample were isolated for geochemistry and petrography. Interpretation of geochronology results takes into account relevant petrographic, geochemical, isotopic, and structural data for all samples and intervening drillcore material, as detailed elsewhere in this volume.

## Geochronology results

### Burkin gneiss (c. 1478 Ma)

The oldest sample (GSWA 182485) revealed so far in the Madura Province is a garnet-bearing felsic gneiss, sampled at c. 272 m depth in the Burkin prospect drillcore, BKD2 (EIS co-funded core, Benton, 2009), although interpretation of the nature of the protolith, and therefore of the geochronology, are equivocal. The zircons are mainly subhedral, variably rounded, and most exhibit concentric zoning in CL images. Fourteen analyses indicate a weighted mean date of  $1478 \pm 4$  Ma, interpreted here as the crystallization age of an igneous protolith.

Seven analyses fall into two groups, an older group of three dates at 2408–2293 Ma and a younger group with an average of  $1538 \pm 17$  Ma; these results are interpreted as the ages of inherited components. An alternative interpretation is that the  $1478 \pm 4$  Ma date is the age of migmatization during high-grade metamorphism, and that the older analyses are of detrital zircons, in which case the date of  $1538 \pm 17$  Ma represents a maximum age of deposition for deposition of a sedimentary precursor (Kirkland et al., 2012). A third alternative is that all the zircons are detrital in origin, in which case the age of  $1478 \pm 4$  Ma is the maximum age of deposition.

### Haig Cave Supersuite (c. 1410 Ma)

Five samples of recrystallized metagabbro and granitic gneiss in two drillcores from the Loongana prospect, LNGD0001 and LNGD0002 (drilled by Helix Resources; Bunting and McIntyre, 2003), yield dates of 1415–1403 Ma (Table 1; Nelson, 2005a,b,c; Kirkland et al., 2013a,b), and are assigned to the Haig Cave Supersuite. In contrast to the Burkin sample, interpretation of U–Pb results for these samples is straightforward. In each case, the data are single-component, mainly concordant, and well grouped, yielding precise protolith ages. The ages of five samples are in statistical agreement, and yield a weighted mean of  $1409 \pm 6$  Ma.

Sample GSWA 206754 is an adakite (plagiogranite), from the new GSWA stratigraphic drillcore, MAD002. The sample yielded anhedral to subhedral, concentrically zoned zircons, some of which contain older cores. Twenty-one analyses of 18 zircons yield a well defined weighted mean date of  $1389 \pm 7$  Ma, interpreted as the crystallization age of the granite. Seven analyses of seven zircon cores yield dates in four groups, at c. 2480, 1760, 1550, and 1475 Ma, interpreted as the ages of inherited components. Although the 1389 Ma age is significantly younger than the results from the Loongana samples, this granite is at present considered to be part of the Haig Cave Supersuite.

**Table 1. U–Pb zircon geochronology results for Madura Province drillcore samples**

Sample ID	Unit name	Rock type	Drillcore ID	Depth interval sampled (m)	Magmatic age (Ma)	Metamorphic age (Ma)	Inheritance (Ma)
182485	Burkin gneiss*	migmatitic gneiss	BKD2	271.38 – 272.08	1478 ± 4		2408–2293, 1538
178070	Haig Cave Supersuite	amphibolite	LNGD0001	637.60 – 640.00	1415 ± 7		
192558	Haig Cave Supersuite	tonalitic gneiss	LNGD0002	465.30 – 466.20	1411 ± 6		
178071	Haig Cave Supersuite	metatonalite	LNGD0001	611.80 – 612.50	1408 ± 7		
178072	Haig Cave Supersuite	tonalitic gneiss	LNGD0002	363.52 – 364.00	1407 ± 6		
192557	Haig Cave Supersuite	metagabbro	LNGD0002	371.00 – 371.50	1403 ± 6		
206754	Haig Cave Supersuite	adakite (plagiogranite)	MAD002	488.58 – 488.83	1389 ± 7		2487–1455
192595	Moodini Supersuite	granodiorite	MAD014	433.27 – 433.87	1181 ± 7		
206779	Moodini Supersuite	m/g monzogabbro	MAD011	562.01 – 562.32	1144 ± 7		
206778	Moodini Supersuite	c/g monzogabbro	MAD011	491.00 – 491.92	1143 ± 5		
192566	Moodini Supersuite	metagranite	MORC002	592.83 – 593.39	1132 ± 9		
192565	Moodini Supersuite	metagranite	MORC001	497.37 – 497.94	1125 ± 7		

NOTE: \* indicates an informal unit name. Ages are quoted with 95% confidence intervals.

## Moodini Supersuite (1181–1125 Ma)

The remaining five samples, from four drillcores in the Madura Province, yield igneous crystallization ages of 1181–1125 Ma, and are assigned to the Moodini Supersuite (Table 1). A granodiorite from GSWA drillcore MAD014 yielded a mean age of  $1181 \pm 7$  Ma. From c. 491 m depth in MAD011, a coarse-grained monzogabbro furnished high-uranium (median = 1750 ppm  $^{238}\text{U}$ ), low Th/U (median = 0.05), largely metamict zircons that nevertheless yielded a well defined mean 207-corrected  $^{238}\text{U}/^{206}\text{Pb}^*$  age of  $1143 \pm 5$  Ma, thanks to the high spatial resolution of the SHRIMP primary beam (c. 20 microns diameter), which allowed the damaged parts of the zircons to be avoided. From c. 562 m depth in the same core, a medium-grained monzogabbro provided much lower uranium (median = 94 ppm  $^{238}\text{U}$ ), high Th/U (median = 2.3), undamaged zircons that yielded an essentially identical 207-corrected  $^{238}\text{U}/^{206}\text{Pb}^*$  age of  $1144 \pm 7$  Ma. The last two Madura samples are metagranites from the Moodini prospect drillcores MORC001 and MORC002, which were drilled by Venus Metals to intersect a coincident magnetic and gravity anomaly in the Mundrabilla Shear Zone, and yielded well defined mean ages of  $1132 \pm 9$  and  $1125 \pm 7$  Ma.

## Comparison with the Albany–Fraser Orogen

Comparison of geochronology of the Madura Province with results for the eastern Albany–Fraser Orogen has been made previously by Spaggiari et al. (2012; 2014). Rocks equivalent in age to the 1478 Ma Burkin gneiss and the 1415–1389 Ma Haig Cave Supersuite (which includes the c. 1410 Ma Loongana oceanic arc; Spaggiari et al., 2014) are not known in the Albany–Fraser Orogen (Fig. 1). However, the ages of detrital zircons in the Arid Basin are dominated by a component at 1425–1375 Ma, indicating that the Haig Cave Supersuite of the Madura Province may have been a source of detrital material. Moodini Supersuite intrusive rocks, dated at 1181–1125 Ma, are broadly coeval with the 1200–1140 Ma Esperance Supersuite, which intruded the Albany–Fraser Orogen during Stage II events at 1225–1140 Ma.

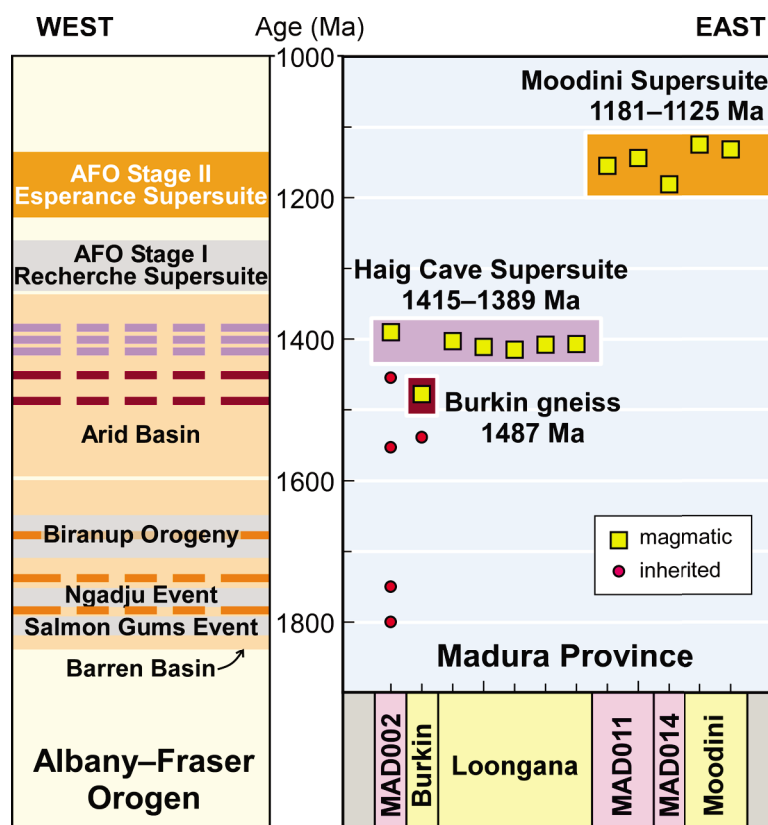


**Figure 1.** Graphic comparison of U–Pb ages of rock units in the Madura Province with those of rock units and geological events in the eastern Albany–Fraser Orogen. Thick dashed lines represent the ages of main detrital zircon components in the Barren and Arid Basins (Spaggiari et al., 2014).

## References

- Benton, J 2009, Diamond Drilling at E69/1972, 19 August 2009 – 16 September 2009, Holes BKD1 – BKD2, Gunson Resources Limited's Burkin Nickel Project, well completion report: Digirock Pty Ltd, Perth, Western Australia, 18p. (unpublished).
- Bunting, JA and McIntyre, J R 2003, Loongana Project combined annual technical report C150/2001: Exploration Licences 69/1516, 1517, 1718, 1719 and 1720 for the period 11/8/2002 to 10/8/2003, Helix Resources Limited, 29p. (unpublished).
- Kirkland, CL, Wingate, MTD and Spaggiari, CV 2012, 182485: migmatitic gneiss, Burkin prospect; Geochronology Record 1054: Geological Survey of Western Australia, 4p.
- Kirkland, CL, Wingate, MTD and Spaggiari, CV 2013a, 192557, metagabbro, Haig Cave; Geochronology Record 1140: Geological Survey of Western Australia, 4p.
- Kirkland, CL, Wingate, MTD and Spaggiari, CV 2013b, 192558, granitic gneiss, Haig Cave; Geochronology Record 1089: Geological Survey of Western Australia, 4p.
- Nelson, DR 2005a, 178070: amphibolite, Haig Cave; Geochronology Record 596: Geological Survey of Western Australia, 4p.
- Nelson, DR 2005b, 178071: recrystallized biotite microtonalite, Haig Cave; Geochronology Record 597: Geological Survey of Western Australia, 4p.
- Nelson, DR 2005c, 178072: tonalitic gneiss, Haig Cave; Geochronology Record 598: Geological Survey of Western Australia, 4p.
- Spaggiari, CV, Kirkland, CL, Smithies, RH and Wingate, MTD 2012, What lies beneath — interpreting the Eucla basement, in GSWA 2012 extended abstracts: promoting the prospectivity of Western Australia: Geological Survey of Western Australia, Record 2012/2, p. 1–2.
- Spaggiari, CV, Kirkland, CL, Smithies, RH and Wingate, MTD 2014, Tectonic links between Proterozoic sedimentary cycles, basin formation and magmatism in the Albany–Fraser Orogen: Geological Survey of Western Australia, Report 133, 63p.

# Madura Province: geochemistry and petrogenesis

by

RH Smithies, CV Spaggiari, CL Kirkland<sup>1</sup>, MTD Wingate, and RN England<sup>2</sup>

## Introduction

Apart from the three MAD-prefix stratigraphic drill cores GSWA has obtained geochemical data from several exploration drill cores, including EIS co-funded drill cores. These include Burkin, Hannah 1, Haig 1 and 2, Serpent 1 and 2, Loongana 1 and 2, and Moodini 1 and 2 (Figure 1 in Preface). Reference will also be made to samples from the NSD drill hole and outcrop samples from coastal exposures at Point Malcolm, east of Cape Arid, which are interpreted as pieces of the Madura Province thrust onto eastern edge of the Albany–Fraser Orogen, and preserved within the eastern Nornalup Zone. Collectively, this sample set can be divided into four major rock groups; basalts and fine-grained mafic rocks, gabbroic rocks and peridotites, sodic granites, and potassic granites. All samples are metamorphosed to at least greenschist facies. The samples represent the least altered and texturally and lithologically most homogeneous material available, covering the full lithological range encountered in each core. Where sampling of altered material has been unavoidable, geochemical interpretation has been mainly based on variations in typically fluid-immobile elements. In all cases, major element data (e.g.  $\text{SiO}_2$  wt%) has been recalculated volatile-free (e.g.  $\text{aSiO}_2$  wt%). Table 1 provides a summary of geochemical characteristics and of petrogenetic interpretations.

## Basalts and fine-grained mafic rocks

Basalts and fine-grained mafic rocks were sampled from MAD002, MAD011, Burkin, Point Malcolm and NSD (Table 1). All groups show general trends to increasing  $\text{FeO}^T$  with decreasing  $\text{Mg}^\#$  reflecting tholeiitic trends.

Samples from MAD002 can be divided between a low-Mg group ( $\text{SiO}_2 = 45.07 - 48.81$  wt%;  $\text{MgO} = 8.37 - 4.8$  wt%;  $\text{Mg}^\# = 54-40$ ;  $\text{Ni} < 91$  ppm;  $\text{Cr} < 225$  ppm) and a high-Mg group ( $\text{SiO}_2 = 51.03 - 43.93$  wt%;  $\text{MgO} = 17.81 - 13.54$  wt%;  $\text{Mg}^\# = 75-67$ ;  $\text{Ni} = 1430-315$  ppm;  $\text{Cr} = 2520-770$  ppm) (Fig. 1). The high-Mg basalts have compositions that reflect near-primary mantle melts. Of the other basalts, those from MAD011 and Point Malcolm include samples with  $\text{MgO} > 10$  wt% (MAD011:  $\text{Cr}$  to 558 ppm,  $\text{Ni}$  to 157 ppm; Point Malcolm:  $\text{Mg}^\#$  to 76,  $\text{Cr}$  to 1751 ppm,  $\text{Ni}$  to 279 ppm). There are only a few samples each from the NSD and Burkin drill cores, and these lie in a  $\text{MgO}$  range from 6.46 to 4.75 wt% ( $\text{Mg}^\#$  42–35).

At a given  $\text{Mg}^\#$  the basalts can also be divided into high-Ti (MAD002 and NSD) and low-Ti groups (Fig. 1). High-Ti basalts have high Nb concentrations, primitive mantle (PM)-normalized trace element patterns between those of E-MORB and OIB (Fig. 2) and show very little evidence for crustal contamination. Their high Ti/Yb ratios suggest melting of a deep garnet-lherzolite source.

The PM-normalized trace element patterns for the low-Ti basalt (Burkin, Point Malcolm, MAD011) are relatively flat (Fig. 2). Ratios of high field strength elements ( $\text{HFSE} = \text{Nb, Zr, Ti}$ )/Yb are typically close to N-MORB values reflecting a depleted mantle source. In the case of MAD011 basalts, negative Zr (Hf) anomalies suggest a source more depleted than the source of N-MORB. For all low-Ti groups, however,  $\text{HFSE}/\text{REE}$  and  $\text{HFSE}/\text{Th}$  ratios are  $\gg$  N-MORB values requiring an enriched, or crustal, component. These patterns closely resemble those of arc tholeiitic basalts derived from a weakly subduction modified depleted mantle source region (e.g. forearc or backarc).

Samples taken from the Burkin drill core included fine-grained, layered, plagioclase–chlorite–hornblende–epidote rocks, interpreted to be metamorphosed and deformed mafic sedimentary or volcanosedimentary rocks, and fine magnetite layers. Previous geochemical data identified several horizons of anomalous Cu (up to ~1000 ppm). Our analyses additionally show the banded magnetite layers to have up to 8.6 wt% MnO – potentially pointing to an exhalative origin.

<sup>1</sup> Centre for Exploration Targeting – Curtin Node, Department of Applied Geology, Curtin University, Bentley WA 6845

<sup>2</sup> Petrology Services, Duncraig, WA 6023

Table 1. Geochemical characteristics and petrogenetic interpretations of rocks of the Madura Province

<i>Drill/sampling site</i>	<i>Rock type</i>	<i>Geochemical characteristics</i>	<i>Age</i>	<i>Formal unit</i>	<i>Tectonic interpretation</i>
Moodini	Quartz-diorite to Monzogranite	High-KFe series	1132–1125 Ma	Moodini Supersuite	Mixed mafic lower crustal melts and asthenospheric melts at base of thinned crust
MAD011	Basalt	Weakly enriched N-MORB and mixing with evolved crust	>1155 Ma – possibly c. 1400 Ma	Haig Cave Supersuite?	Melting weakly subduction-enriched N-MORB source and contamination by more-evolved crust
	Ferro-monzogabbro to ferro-monzodiorite	High-KFe series	1155–1145 Ma	Moodini Supersuite	Mixed mafic lower crustal melts and asthenospheric melts at base of thinned crust
Hannah	Ferro-monzodiorite	High-KFe series	c. 1174 Ma	Moodini Supersuite	Mixed mafic lower crustal melts and asthenospheric melts at base of thinned crust
MAD014	Monzogranite	High-KFe series	c. 1181 Ma	Moodini Supersuite	Mixed mafic lower crustal melts and asthenospheric melts at base of thinned crust
Loongana	Gabbro and peridotite	Weakly enriched N-MORB	c. 1403 Ma	Haig Cave Supersuite	Melting of variably subduction-modified N-MORB source
	Leucogranite	Sodic plagiogranite	c. 1411 Ma	Haig Cave Supersuite	Low- to medium-pressure melting of mafic crust
Haig	Gabbro	Unenriched to weakly enriched N-MORB	Undated – likely to be c. 1400 Ma	Haig Cave Supersuite	Melting of variably subduction-modified N-MORB source
	Leucogranite	Sodic plagiogranite	Undated – likely to be c. 1400 Ma	Haig Cave Supersuite	Low- to medium-pressure melting of mafic crust
Serpent	Gabbro	Weakly enriched N-MORB	Undated – likely to be c. 1400 Ma	Haig Cave Supersuite	Melting of variably subduction-modified N-MORB source
Point Malcolm	Basalt	Weakly enriched N-MORB	Undated – but between c. 1450 Ma and c. 1315 Ma	Malcolm Metamorphics	Melting weakly subduction-enriched N-MORB source in fore- or back-arc region
Burkin	Basalt	Weakly enriched N-MORB	Undated – likely between c. 1478 Ma and c. 1400 Ma	Malcolm Metamorphics	Melting weakly subduction-enriched N-MORB source in fore- or back-arc region
MAD002	Basalt	Transitional E-MORB/OIB	Undated - likely 1600–1400 Ma	none	Asthenospheric upwelling during lithospheric extension – continental or OCT
NSD	Leucogranite	Adakite	c. 1389 Ma	Haig Cave Supersuite	Melting of subducted slab with slab-sediment contamination
	Basalt	Transitional E-MORB/OIB	Undated - likely 1600–1400 Ma	none	Asthenospheric upwelling during lithospheric extension – continental or OCT

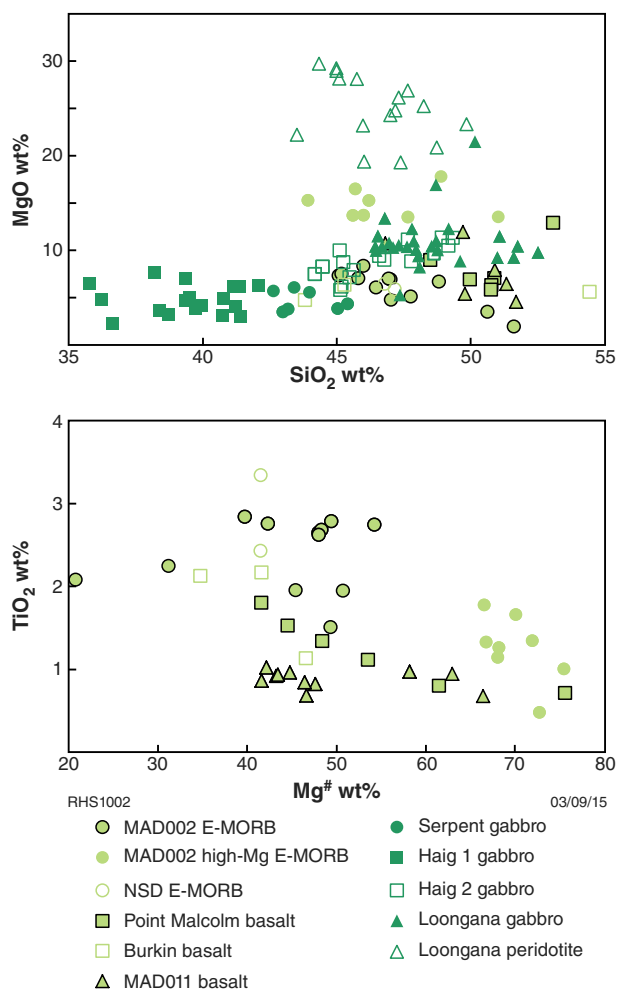


**Figure 1. Variation in MgO vs SiO<sub>2</sub> and TiO<sub>2</sub> vs. Mg<sup>#</sup> for mafic rocks of the Madura Province [Mg<sup>#</sup> = mol Mg/(Mg+FeT)].**

## Gabbroic rocks and peridotites

Mafic and mafic-ultramafic rocks have been drilled at Loongana (LNGD001 and LNGD002), Haig (HDDH001 and HDDH002), and Serpent (SDDH001 and SDDH002) (Table 1). One gabbro sample from Loongana has been dated at c. 1403 Ma. Fe-enrichment trends and low K<sub>2</sub>O contents, show that these intrusions are derived from low- to medium-K, tholeiitic parental magmas. Two anomalously high-Ti samples from Haig 1 are magnetite cumulates. With Mg<sup>#</sup> > 60, the Loongana and Haig 2 rocks crystallised from near primary magmas, whereas the compositions in Haig 1 and Serpent are strongly evolved. Peridotites were sampled mainly from the upper parts of Loongana 1 (Fig. 3). Mafic intrusive rocks are also found in MAD011 and Hannah 1. These are distinctive high-FeO, -K<sub>2</sub>O (high-FeK) monzodiorites and monzogabbro (petrographically quartz-monzodiorite to quartz-monzogabbros) and are discussed later.

The two Haig intrusions are mineralogically distinct, Haig 1 having an essentially anhydrous, pyroxene-dominated mafic mineralogy, while Haig 2 contains abundant hornblende. These differences correspond to significant differences in major element compositions, with the compositions of Haig 1 reflecting crystallisation from a much more evolved magma with a significantly better developed tholeiitic Fe-enrichment trend. Normalized trace element plots for the Loongana and Haig intrusions show the ‘spiky’ patterns typical of mafic cumulate rocks, including pronounced negative Nb (Ta) and Zr (Hf) anomalies. In most cases, there is a systematic increase in normalized concentrations in the order Nb, Zr, Ti, Yb, with patterns likely reflecting a mantle source more depleted than the source of N-MORB (i.e. Nb/Yb etc. < N-MORB values). Gabbros from Haig 1 have HFSE/Yb, Th/Nb and La/Nb ratios closer to N-MORB values, possibly reflecting a mantle source essentially free of any significant subduction (or crustal) influence. In contrast, much higher Th/Nb ratios and, at least in the case of Haig 2, a hydrous primary mineralogy likely reflects a crust-contaminated bulk source — potentially a subduction-enriched mantle source.

## Sodic granites

Granites in the compositional range of tonalite to trondhjemite intrude gabbro in Loongana 1 and 2, and Haig 1 and 2, and intrude the basaltic rocks (E-MORB) in MAD002 (Table 1). They form only a minor component of the Haig cores, dominate sections of Loongana 1 and MAD002, and are the primary lithology in Loongana 2. Sodic granite from Loongana has been dated at c. 1411 Ma (but within analytical uncertainty of the host gabbro) while sodic granite from MAD002 has been dated at c. 1389 Ma.

Sodic granites from Loongana (1 and 2) are distinctive in that they range to higher K<sub>2</sub>O contents (up to 1.7 wt%) at higher SiO<sub>2</sub> contents and have the highest K<sub>2</sub>O/Na<sub>2</sub>O ratios of up to 0.41 (i.e. still very sodic) (Fig. 4). Samples from MAD002 show distinctly more Al-rich trends and are distinctly enriched in Na<sub>2</sub>O (5.48 – 6.05 wt%), with maximum K<sub>2</sub>O/Na<sub>2</sub>O ratios of 0.1.

The sodic granites are mostly depleted in LREE, HFSE and Rb and have variable concentrations of Ba, following trends in K<sub>2</sub>O. They share these features with sodic felsic magmas from a range of tectonic settings, including ‘oceanic plagiogranites’ from ophiolite complexes. Rocks from Loongana, in particular, show major element trends resembling oceanic plagiogranites, and additionally show an extended silica range typical of such rocks.

In terms of the behaviour of Sr, Y and HREE, however, the sodic granites show a range of patterns. Rocks from MAD002 and Haig contain very high concentrations of Sr (MAD002 = 1055–849 ppm; Haig 1 = 835–420 ppm; Haig 2 = 618–258 ppm) compared with the other Madura Province sodic granites (Fig. 4) and with plagiogranites from oceanic settings. Again, samples from Loongana have Sr concentrations more typical of the low-pressure

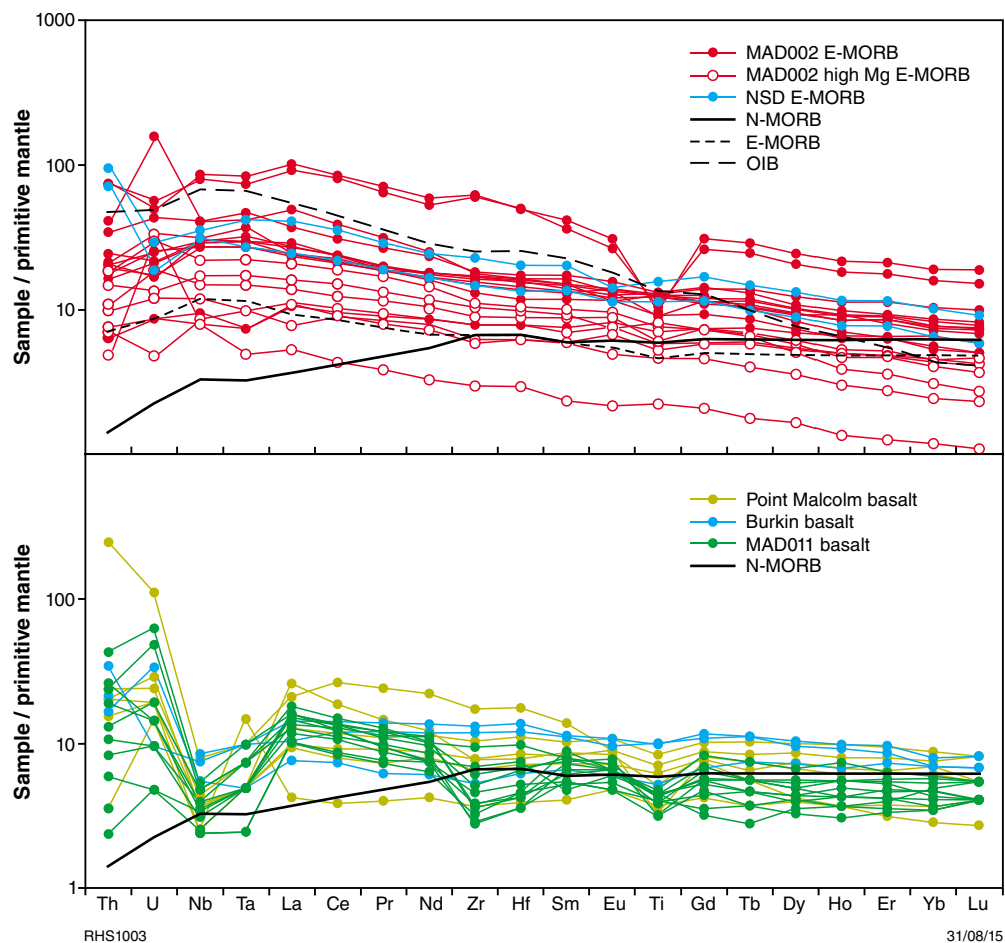


**Figure 2.** Primitive mantle normalized trace element diagrams for basalts from MAD002, NSD, Point Malcolm and Burkin. Normalization factors and compositions of N-MORB, E-MORB and OIB are from Sun and McDonough (1989).

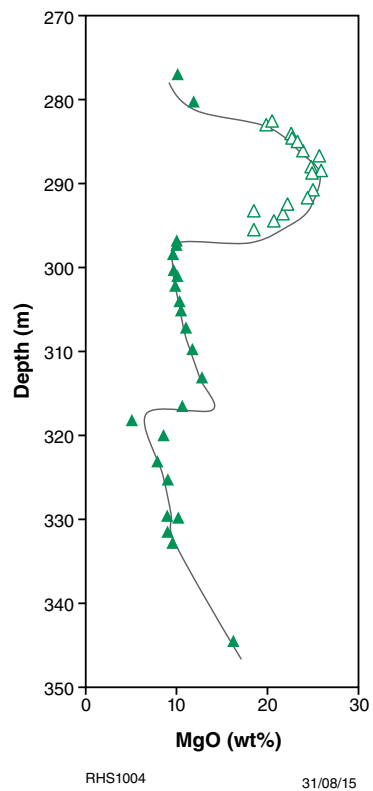


**Figure 3.** Variation in MgO content of gabbros and peridotites with depth in Loongana drill core LNGD001.



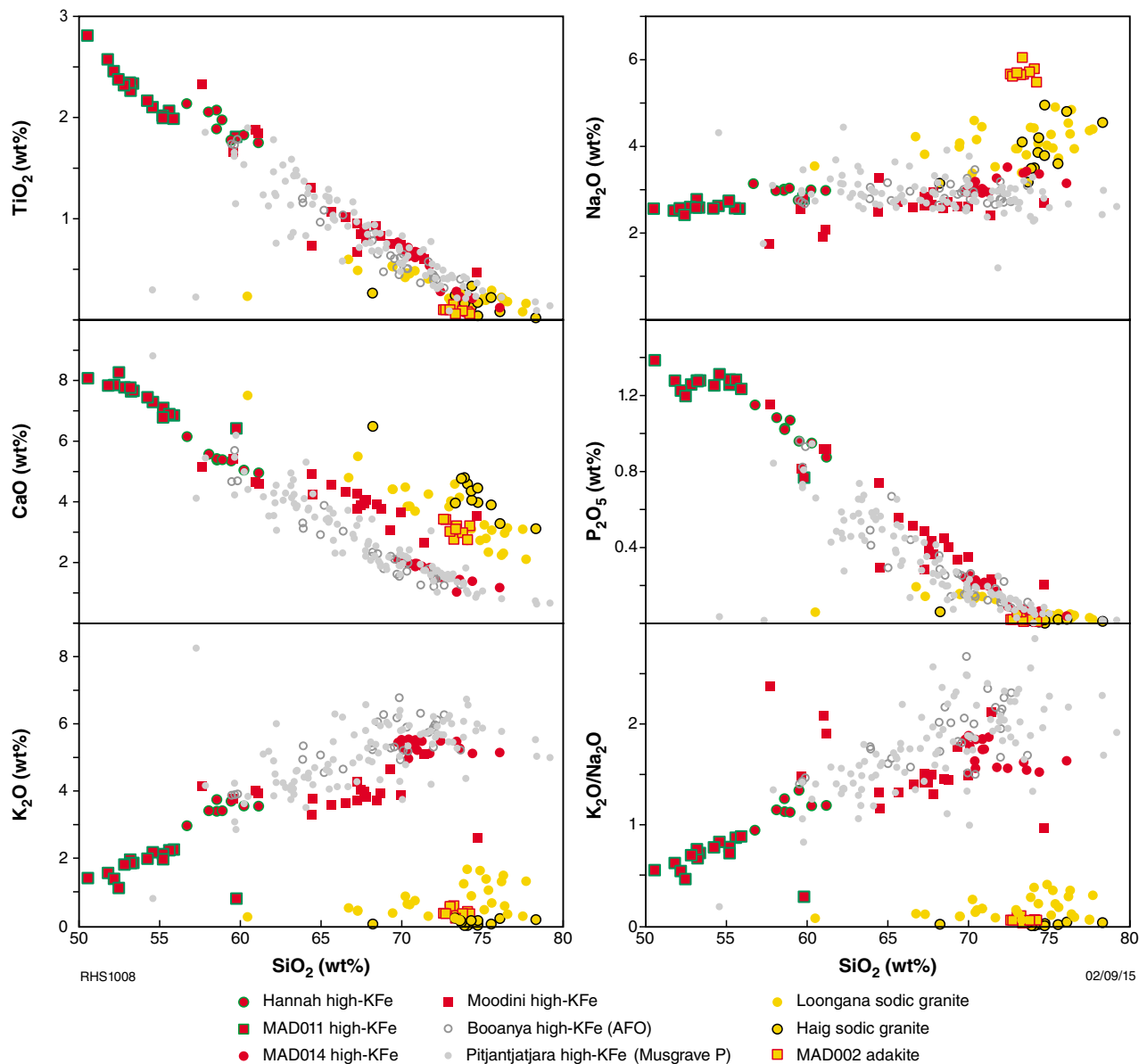


**Figure 4. Major element variation vs  $\text{SiO}_2$  for felsic rocks of the Madura Province. Also shown for comparison are high-KFe series rocks from the Albany–Fraser Orogen (AFO) and from the Musgrave Province.**

processes through which most sodic plagiogranites form in oceanic settings. Conversely, concentrations of HREE and Y are anomalously low in sodic granites from MAD002 ( $\text{Yb} = 0.29 - 0.08$  ppm), Haig 1 ( $\text{Yb} = 0.4 - 0.2$  ppm) and Haig 2 ( $\text{Yb} = 0.6 - 0.17$  ppm) compared with concentrations in those from Loongana 1 ( $\text{Yb} = 5.41 - 0.28$  ppm) and Loongana 2 ( $\text{Yb} = 1.5 - 0.28$  ppm) (Fig. 4), which are more representative of the range for oceanic plagiogranites.

Viewing the composition of the sodic granites alongside the composition of the mafic crust that they intrude (Fig. 5) shows that the high Sr and low Yb characteristics of the Haig sodic granites are shared by the Haig gabbro

and similarly, the Loongana sodic granites and gabbros share low Sr high Y characteristics. The high Sr, low Yb characteristics of the MAD002 sodic granites, however, is opposite to that of the E-MORB-like basalts into which it intrudes.

Plagiogranites represent low-fraction partial melts of variably hydrated mafic crust or are the results of extended fractional crystallisation of mafic magmas. In either case, distinctive compositional features of their mafic parents will be inherited. This would explain the similarities in trace element patterns between sodic granites and gabbros at Loongana and Haig, particularly the extreme Sr concentration seen in the Haig sodic granites.

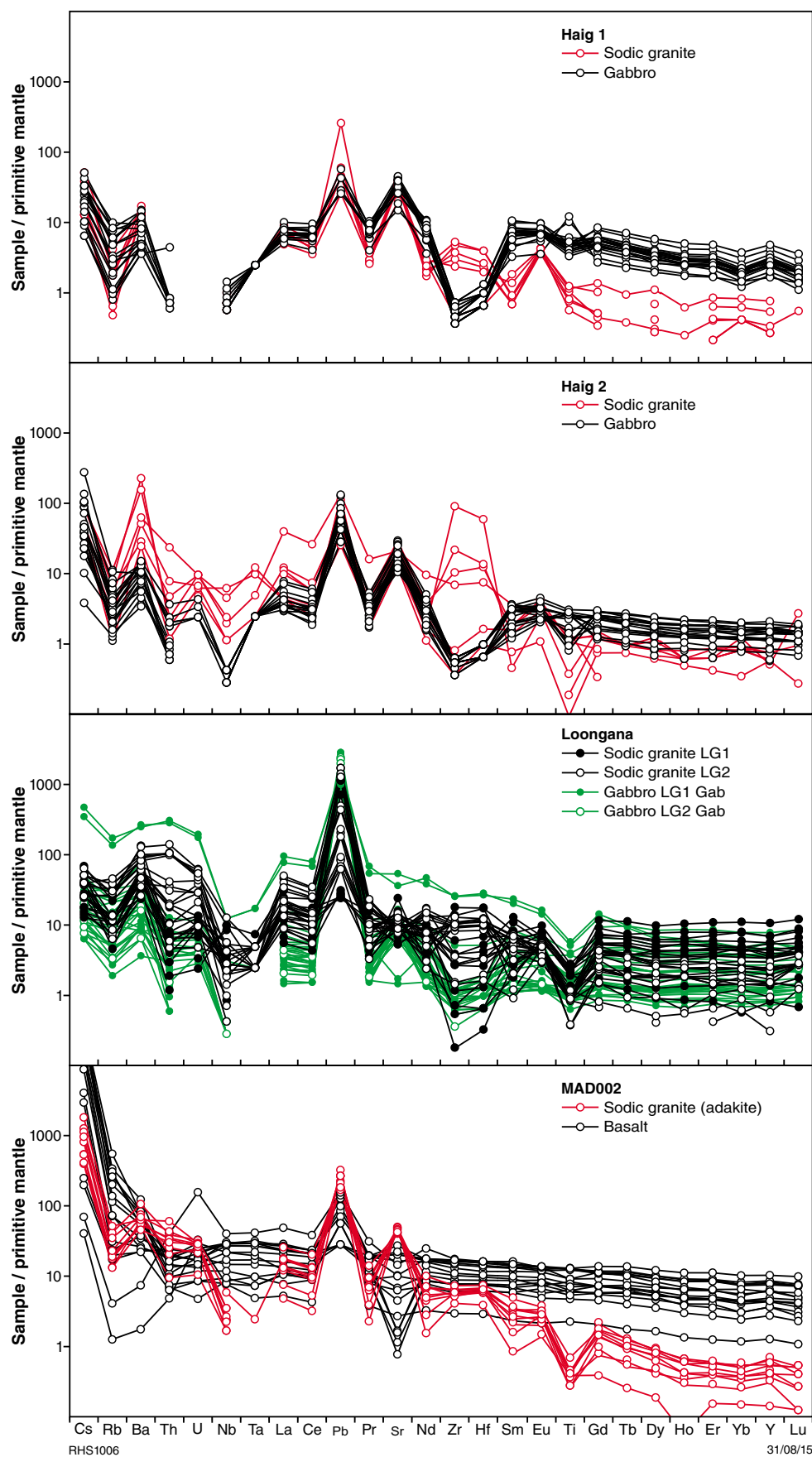


**Figure 5.** Primitive mantle normalized trace element diagrams for intrusive mafic rocks and spatially associated sodic leucogranites from MAD002, and from the Loongana and Haig prospects. Normalization factors are from Sun and McDonough (1989).

In the case of Loongana, the strong similarities between the sodic granites and oceanic plagiogranites typical of ophiolite complexes might favour a similar tectonic setting. Oceanic leucogranites in ophiolite sequences are commonly intruded at or near the interface between the lower gabbroic sequence of the ophiolite stratigraphy and the overlying sheeted dyke complex.

The patterns for MAD002 sodic granites strongly contrast with those of the associated basalts, particularly in terms of the very high La/Yb ratios and strongly developed negative Nb and Ti anomalies seen in the granites (Fig. 5). The notably  $\text{Al}_2\text{O}_3$ - and  $\text{Na}_2\text{O}$ -enriched compositions of these sodic granites along with the very high Sr and very low Y and HREE concentrations (very high Sr/Y ratios) are characteristics of adakites, resulting through high-pressure (>10 kbar), garnet-present, melting of mafic crust. The high Sr/Y ratios of Haig 1, however, can be better explained in terms of compositional inheritance from compositionally similar gabbroic melting sources. Indeed, relatively flat HREE patterns with low Dy/Yb ratios (Figs 5 and 6) ranging to values lower than associated gabbros and other oceanic leucogranites are consistent with low-pressure fractionation or source retention of hornblende rather than with equilibrium with peritectic garnet.

## Potassic granites and associated mafic rocks – high-KFe rocks

K-rich granites are the sole basement lithology encountered in MAD014 and in the two cores from Moodini (Table 1). The rocks in Moodini range from quartz-diorite and granodiorite to biotite-hornblende monzogranite while those from MAD014 are mainly biotite monzogranite. They have been dated at c. 1125–1135 Ma (Moodini) and c. 1181 Ma (MAD014). Samples from Moodini cover a much wider silica range (57.64 – 74.68 wt%) than those from MAD014 ( $\text{SiO}_2$  = 69.77 – 76.08 wt%). With increasing  $\text{SiO}_2$  contents, concentrations of all major element oxides decrease, except for  $\text{K}_2\text{O}$ , which increases, and  $\text{Na}_2\text{O}$ , which increases in the MAD014 rocks and is constant in the Moodini rocks (Fig. 7). The MAD014 rocks are enriched in both  $\text{K}_2\text{O}$  and  $\text{Na}_2\text{O}$  and have distinctly lower CaO than the Moodini rocks, resulting in MAD014 rocks being mainly alkali-calcic whereas the Moodini rocks are mainly calc-alkalic. However, these rocks all form part of a distinctly  $\text{TiO}_2$ - and  $\text{P}_2\text{O}_5$ -rich trend of mainly metaluminous, ferroan composition) – referred to here as the Madura high-KFe series.

All rocks of the Madura high-KFe series have clear A-type (high-K) characteristics. This can be seen in terms of their high Ga/Al ratios, high HFSE, Ga, Zn concentrations, and their ferroan compositions. Within the general A-type classification, the distinct high- $\text{TiO}_2$  and - $\text{P}_2\text{O}_5$  trends identify these rocks as probable members of a ‘charnockite-series’ (e.g. Kilpatrick and Ellis, 1992)

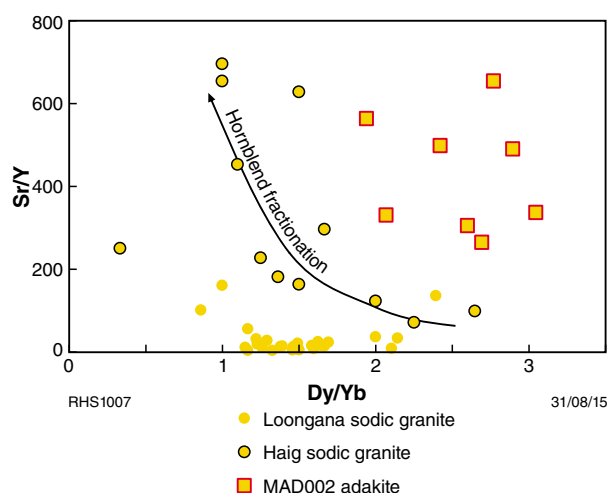


Figure 6. Variation of Sr/Y with Dy/Yb for the sodic leucogranites of the Madura Province.

although only the orthopyroxene-bearing mafic end-members (see MAD011, below) preserve mineralogical affinities with charnockites. These are typically very high temperature magmas derived from dry and reduced lower crustal source regions incorporating a large mantle component. Zirconium-saturation thermometry (Watson and Harrison, 1983) on these rocks confirms high emplacement temperatures (Fig. 8).

As discussed previously, the younger mafic intrusions sampled from MAD011 (c. 1144 Ma) and Hannah 1 (c. 1180 Ma) are monzogabbros, monzodiorites and monzonites distinctly different in composition from the older (c. 1400 Ma) mafic intrusions sampled from Haig, Loongana and Serpent. Compared with these older gabbro intrusions at a given silica content, these younger intrusions have unusually high FeO,  $\text{K}_2\text{O}$ ,  $\text{TiO}_2$ , and  $\text{P}_2\text{O}_5$  concentrations. They form part of the same 1181–1125 Ma Madura high-KFe series as the more silicic rocks from MAD014 and Moodini. They show normal systematic igneous trends but are strongly enriched in LILE, HFSE and REE. The primary mineralogy of these rocks included orthopyroxene and possibly also pigeonite. Such compositions and mineralogy are characteristic of high-temperature, Fe-rich orthopyroxene-monzonite (jotunite) suites (e.g. Vander Auwera et al., 1998).

## Potential tectonic settings based on geochemistry and relationships established from drill cores.

This is always a dangerous practise – particularly for units in isolation – but confidence is increased when common themes emerge from otherwise independent sources.

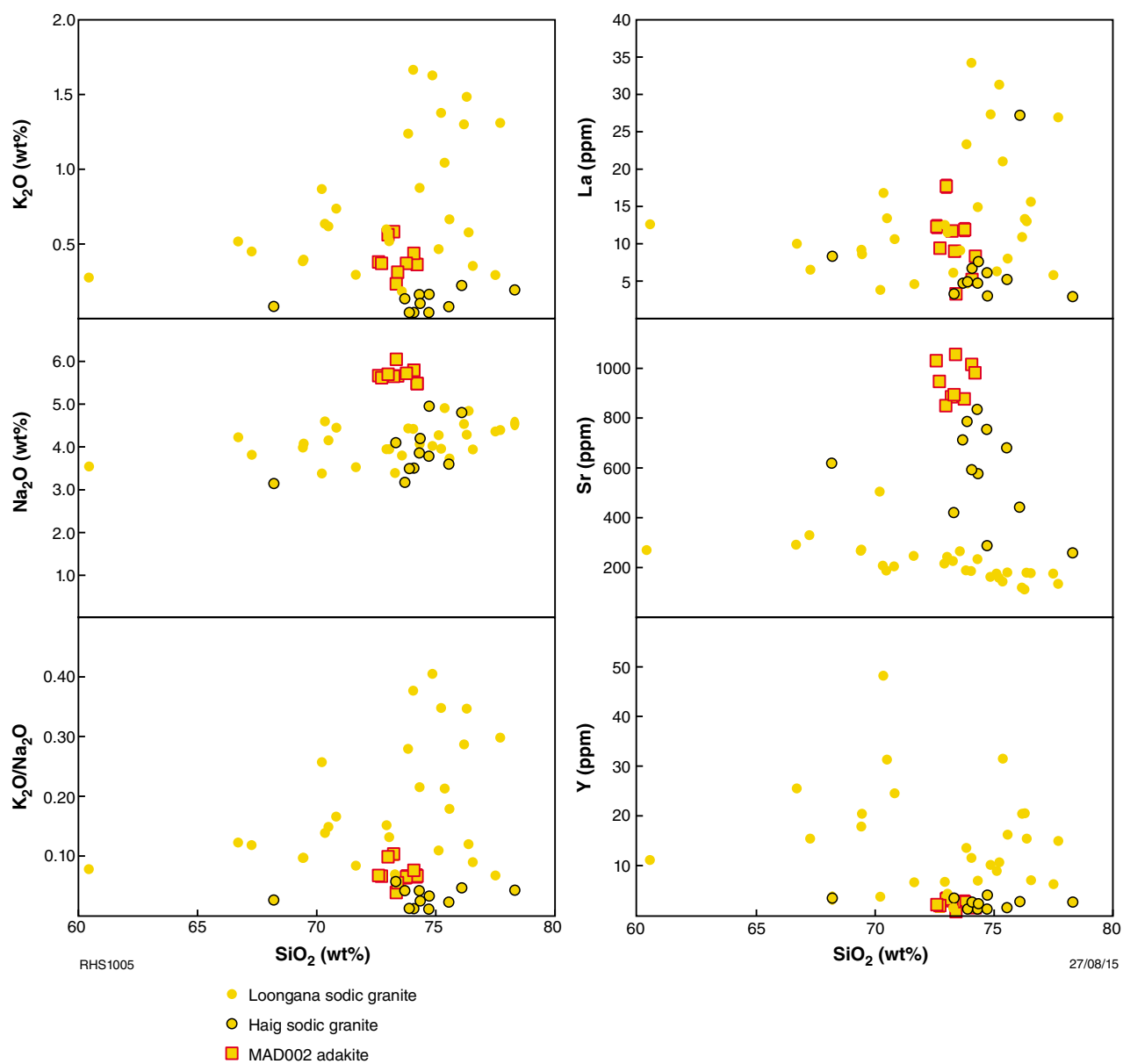


Figure 7. Results of zircon-saturation thermometry for rocks of the high-KFe series of the Madura Province.

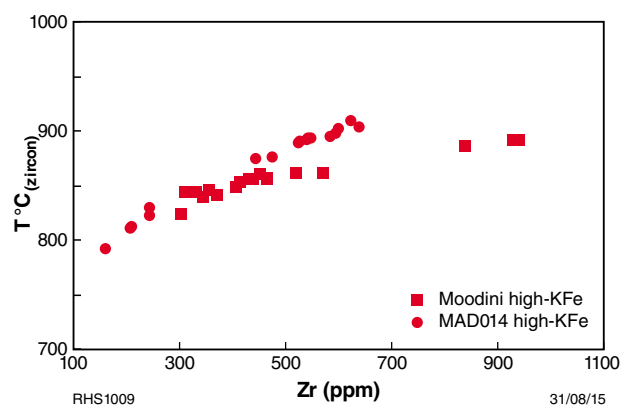
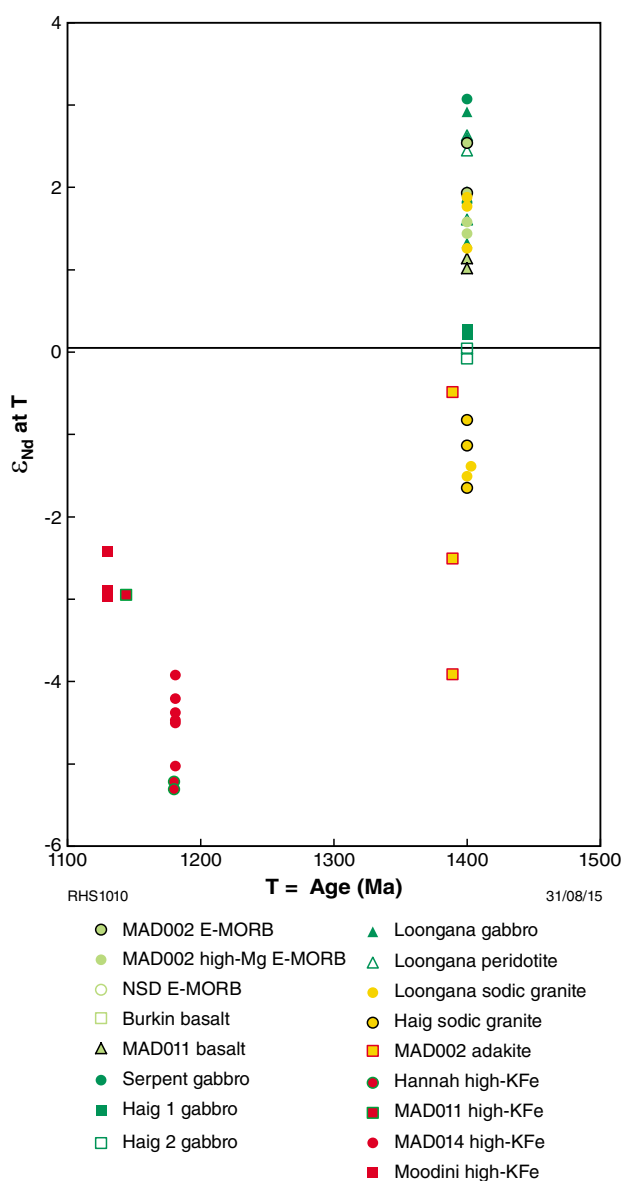


Figure 8. Results of Zr saturation thermometry vs Zr concentrations for high-KFe series rocks from Moodini and MAD014

## MAD002 – c. 1389 Ma hot subduction beneath OCT-related lithosphere capped by E-MORB/OIB crust.

MAD002 can be subdivided lithologically into two broad units — high-Ti basalts and adakites. The sole firm age constraints come from the adakites, which intruded the basalts at c. 1389 Ma. Trace element patterns for the basalts are transitional between E-MORB and OIB and suggest low-degree melting of a fertile (or at least non-depleted) mantle source. The compositions permit only a small degree of crustal contamination (or source input) — suggesting an oceanic or proto-oceanic environment. High Ti/Yb ratios in the most primitive compositions confirm melting of a deep (>2.8 GPa = > 100 km) garnet-bearing mantle source.



**Figure 9. Nd-isotope compositions for rocks of the Madura Province**

Hence the basalts can be interpreted as the result of decompression melting during upwelling of relatively deep and fertile asthenospheric mantle — with only limited subsequent assimilation of crustal material. More likely scenarios for this include a mantle plume (including plume-ridge interaction) beneath either oceanic or transitional continental lithosphere, perhaps forming an oceanic plateau, or mantle upwelling beneath the extending crust of an ocean-continent transition (OCT) zone. On the one hand, there is no other regional evidence for pre- c. 1400 Ma plume activity. On the other hand, an independently developed tectonic interpretation of the region at this age has inferred an OCT environment (Spaggiari et al., 2015) — and we note that this interpretation itself could represent evidence for plume activity! Hence, the favoured model here is one of E-MORB/OIB proto-oceanic crust formation during lithospheric extension (with or without a mantle plume) associated with an OCT phase that began at or before c. 1600 Ma. The maximum age of the basalt is the age of OCT initiation and the minimum age is constrained by adakite intrusion at c. 1389 Ma.

Adakite formation reflects garnet-present melting of lithosphere with basaltic compositions at pressures of ~1.5 GPa (52 km depth), typically low degree partial melting of subducted mafic lithosphere leaving a garnet±rutile (eclogite) residual. The Nd-isotope composition of the MAD002 adakite ( $\epsilon_{Nd(1400Ma)}$  -3.79 – -0.36) (Fig. 9) is significantly less radiogenic than that of the host basaltic crust ( $\epsilon_{Nd(1400Ma)}$  +2.54 – +1.44) and  $T_{2DM}$  ages for the adakites (2.2 – 1.9 Ga) require a bulk source that included material that was c. 2 Ga or older. Hence, it seems likely that the subducted lithosphere was not related to the E-MORB/OIB crust that the adakites intruded and that slab-melting incorporated a large amount of exotic, less radiogenic, sediment — potentially belonging to the Arid Basin (see Spaggiari et al., 2014, 2015).

## Loongana and Haig – c. 1400 Ma oceanic arc crust

This series of tholeiitic intrusions ranges from hornblende-bearing gabbro (Haig 2) to olivine and pyroxene-bearing gabbros and peridotites (Haig 1 and Loongana 1 and 2; Table 1).  $Mg^\#$  are high in Haig 2 and Loongana and reflect values in equilibrium with mantle peridotite. Haig 1 has more fractionated compositions. Gabbros from Haig 1 are also distinct from the other intrusions in that their trace element ratios more closely approximate N-MORB (Fig. 10) (although we need to be cautious about Th and Nb values close to detection limits) whereas the other bodies have Th/Nb ratios consistent with either a subduction addition to their mantle source or assimilation of older crust (Fig. 10) (again – we need to be cautious with the low Th and Nb concentrations).

Despite having trace-element compositions approximating N-MORB, Haig 1 gabbros have similar Nd-isotopic compositions ( $\epsilon_{Nd}$  0.21– 0.27) to Haig 2 gabbros ( $\epsilon_{Nd}$  -0.08 – 0.04) and both have less radiogenic Nd



isotopic compositions than the Loongana intrusions ( $\epsilon_{\text{Nd}}$  1.33 – 2.92) (Fig. 9). Although the Loongana intrusions (and likely also the Haig intrusions) are dominantly cumulates, the observed degree of Nd-isotope variability within the Loongana intrusions ( $>1.5 \epsilon$  units) reflects an open system. Magmas forming the cumulates were extracted from a chamber itself either undergoing progressive wall-rock contamination or replenished by magmas extracted from an isotopically variable mantle source.

All of the intrusions show a significant negative Zr anomaly (i.e.  $\text{Zr}/\text{Zr}^* < 1$ ), most prominent in Haig 1 (Fig. 5). These are not seen in basaltic units in MAD002, Burkin, Point Malcolm, or NSD, but are seen in basaltic rocks from MAD011. Both positive and negative Zr (and Hf) anomalies are a notable feature of arc-related magmas. This has often been ascribed to the relative immobility of HFSE compared with REE in fluids during subduction, but more recently to the stability of low-Al clinopyroxene during melting of variably depleted mantle sources or low-pressure fractionation of low-Al clinopyroxene and Ti-magnetite (e.g. Woodhead et al., 2011). The Zr anomalies in the Madura rocks become more prominent with decreasing MgO but show no correlation with Zr or Sc concentration and cannot be related to early zircon removal or clinopyroxene fractionation. They are also unlikely to result through crustal contamination – which would require crust with an extremely low  $\text{Zr}/\text{Zr}^*$  ratio.

Thus, the Madura Province gabbros show a range of features consistent with a bulk source dominated by a juvenile depleted mantle component, but also requiring a small amount of more evolved material. The amount of evolved material is significantly less in Haig 1 than in the other intrusions. The mantle source component appears to have varied slightly from similar to N-MORB source (e.g. Haig 1) to a source more depleted than N-MORB source, based on trends in HFSE depletions and possibly

also the low  $\text{Zr}/\text{Zr}^*$  ratios. The evolved material added might not have been ‘continental’ since Nd-isotope evidence for more of the evolved component correlates with trace element evidence for less of the evolved component. In addition, large variations in incompatible trace element ratios occur over relatively small variations in Nd-isotope composition. It is possible, therefore, that the evolved component was variably re-worked juvenile crust. Evidence for a refractory mantle source component along with Th/Nb ratios forming a broad band of high values that parallel the MORB-OIB array favour a subduction setting. Although it is possible that the evolved component represents crustal contamination, this would require isotopically juvenile crust, and the inferred setting would remain most likely subduction-related, or at least ‘oceanic’.

An additional feature that favours an oceanic subduction setting for the Madura Province gabbros is that they are intruded, near contemporaneously, by sodic plagiogranite. These are often minor components of arc stratigraphy and their sodic compositions reflect their generally basaltic parental compositions – either as basaltic crust or as basaltic parental melts (e.g. Brophy, 2008). The plagiogranites from Loongana, in particular, resemble the low-K plagiogranites from ophiolite complexes.

Some of the sodic plagiogranites in the Madura Province have a Nd-isotopic range ( $\epsilon_{\text{Nd}(1400\text{Ma})}$  1.88 – 1.26) within that of the gabbros ( $\epsilon_{\text{Nd}(1400\text{Ma})}$  2.92 – -0.08) they intrude (Fig. 9), and their extremely low  $\text{K}_2\text{O}$  contents (mainly  $< 1.0 \text{ wt\%}$  but up to 1.65 wt%) (Fig. 4) clearly indicate that any evolved component within the melting source of the granites was itself extremely minor and low-K (i.e. not ‘continental’). Nevertheless, two higher-K ( $\sim 1.6 \text{ wt\% K}_2\text{O}$ ) sodic plagiogranites from Loongana have significantly less radiogenic Nd-isotopic compositions ( $\epsilon_{\text{Nd}}$  -1.5 – -1.39) than their gabbro host ( $\epsilon_{\text{Nd}}$  +1.33) and the combined Nd-isotope data for Loongana plagiogranites shows a clear negative correlation with  $\text{K}_2\text{O}$  concentration (Fig. 11).

These trends show that whilst the crustal melting source for the Loongana sodic granites was dominantly very low-K and mafic (i.e. dominated by deeper equivalents of the gabbro itself), it must also have included a small component of relatively K-rich crust (? previously reworked juvenile/arc crust) with slightly less radiogenic compositions. It is also likely that any such component was very fusible (i.e. fertile) and so was also likely very over-represented as a source component in the granites. However, it is also interesting to note that all gabbros from Loongana are more radiogenic than the granites and gabbros from Haig – despite the Haig granites having lower  $\text{K}_2\text{O}$  than the Loongana granites.

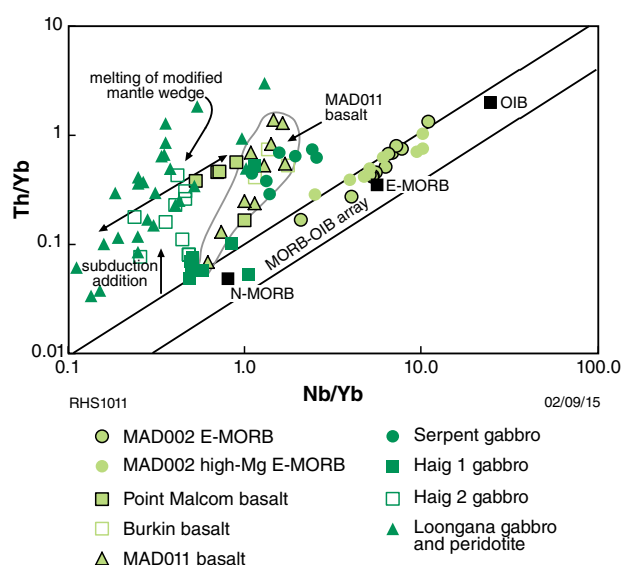


**Figure 10. LogTh/Yb vs log Nb/Yb diagram (after Pearce, 2008) for mafic rocks of the Madura Province.**

## Point Malcolm and Burkin – c. 1400 Ma fore-arc or back-arc tholeiite (N-MORB) magmatism

Both Point Malcolm and Burkin include low-Ti basalt with compositions similar to N-MORB but that show evidence

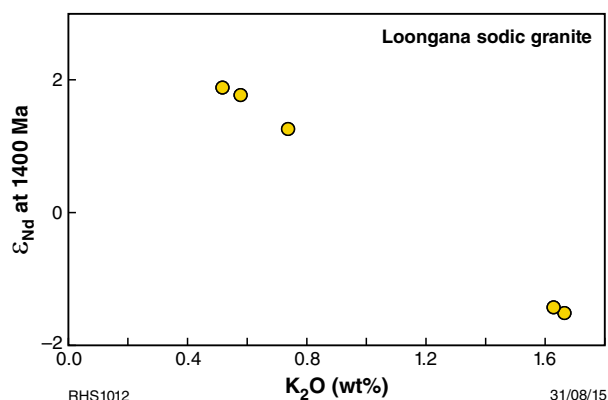


**Figure 11. Variation in Nd isotope composition with K<sub>2</sub>O content for sodic leucogranites from the Loongana prospect.**

for incorporation of minor amounts of an enriched component. The nature of the observed enrichment is equally compatible with subduction enrichment of a mantle source or crustal contamination of N-MORB. Favouring the former suggestion is that the Th/Nb ratio of these basalts is similar to that of the Loongana-Haig gabbros (Fig. 10), which are interpreted to have formed in an oceanic arc. If this is the case, the limited degree of enrichment and tholeiitic nature of magmatism favour a fore-arc or back-arc setting.

Basalts at both localities are locally interleaved with metasedimentary rocks. At Point Malcolm, detrital zircon and monazite data from these metasedimentary rocks indicate a maximum depositional age (for both sediments and basalt) of c. 1450 Ma and metamorphic age of c. 1315 Ma (Adams, 2012). This places basalt magmatism within the same age range as the evolution of the c. 1400 Ma Loongana oceanic arc. A c. 1478 Ma date from quartzofeldspathic gneiss in the Burkin core possibly also represents a maximum age of sedimentation. These similarities in age and, in the case of Burkin the present proximity to Haig and Loongana, lends support to the suggestion that the basaltic magmatism was indeed arc-related.

Comparing the Madura Province gabbro with the basalts on a plot of Th/Yb vs Nb/Yb (e.g. Pearce, 2008) (Fig. 10) identifies two main trends – both paralleling the mantle (MORB-OIB) array. A MORB-like trend includes Haig 1 and basalts from MAD002. A higher Th/Nb “subduction-source” trend contains all other groups. The one anomaly is for basalts from MAD011. These are isotopically and geochemically distinct from the MAD011 monzogabbro that intrudes them – they cannot be co-genetic. They form a trend to increasing Th/Nb, but the low Th/Nb samples also have significantly negative Zr-anomalies ( $Zr/Zr^*$  as low as 0.37), similar to many of the gabbros, and these anomalies decrease both with increasing  $Mg^\#$  and increasing Th/Nb. On this basis, it might be concluded that the MAD011 basalts were derived from a similar refractory source as the gabbros. In terms of their Nd-isotopic composition, the MAD011 basalts also fall within the radiogenic range of the other basalts and gabbros (Fig. 9).

## High-KFe series (mafic to felsic) – c. 1200–1125 Ma high-temperature reworking

It is interesting to note that felsic rocks throughout the Madura Province are either primitive c. 1400 Ma sodic granites (including adakites) or, perhaps more commonly, form part of the Madura high-KFe series. Apart from the obvious differences in K<sub>2</sub>O/Na<sub>2</sub>O (Fig. 7), these two granite groups have strongly contrasting compositions that clearly reflect contrasting petrogenetic processes and possibly also different source regions.

Similar high-KFe series rocks are relatively rare, except in some ‘Grenvillian’ aged Mesoproterozoic terrains where they are intimately associated with massif-style anorthosite batholiths and with charnockitic A-type granites (AMC suite) (e.g. Vander Auwera et al., 1998; Bogaerts et al., 2006; Duchesne et al., 2006). The Madura jotunitic rocks (MAD011) are associated with A-type granites but they lack any association with massif-style anorthosite bodies. However, high-KFe A-type granites occur elsewhere with no obvious connection to either anorthosite or jotunitic (e.g. west Musgrave Province; Smithies et al., 2010; Howard et al., 2015). The mineralogy of the mafic end-members of the Madura high-KFe series, and zircon-saturation thermometry on the felsic rocks, point to very high melting temperatures (>900°C) under dry and relatively reducing conditions. Although very rare, high-KFe suite rocks are very compositionally distinctive and in all known occurrences similarly high crustal-melting temperatures (>1000°C – see Kilpatrick and Ellis, 1992) have been determined or inferred. In the case of high-KFe series rocks from the Musgrave Province, crustal melting was synchronous with extended (>80 Ma) ultrahigh-temperature metamorphism involving regional lithospheric removal (Smithies et al., 2010). Volcanic equivalents to high-KFe series intrusions include continental latites, genetically related to flood basalts (e.g. the Mesozoic Karro latites, Kilpatrick and Ellis., 1992) and whether related to anorthosites or not, there appears to be a potential link with continental flood basalt style magmatism (e.g. Bogaerts et al., 2006).

In the absence of any link to AMC-style suites (including massif-style anorthosites), it is most likely that the jotunitic (MAD011) to A-type granite high-KFe series involves reworking of earlier mafic crust associated with significant juvenile mantle input. The crustal component involved was the same isotopically juvenile crust formed during the earlier evolution of the Madura Province, which remained geochemically primitive (basaltic to andesitic). The regional extent of this high-KFe province can be extended if similarly aged rocks from the Musgrave Province (Pitjantjatjara Supersuite) and Albany–Fraser Orogen (Booanya Suite) are also considered. This represents and extraordinarily large region of specialised magmatism involving extremely high temperature lower crustal melting facilitated by thermal and material input from shallow asthenosphere.

The Madura high-KFe series show regional compositional variation and this is also the case in terms of their Nd-isotopic compositions. Rocks of the Booanya Suite



(Hannah) marginal to the Madura Province are less radiogenic ( $\epsilon_{\text{Nd}(1200\text{Ma})}$  -4.95 – -7.34) than those from MAD014 ( $\epsilon_{\text{Nd}(1200\text{Ma})}$  -3.7 – -4.8), which are less radiogenic than rocks from Moodini and MAD011 ( $\epsilon_{\text{Nd}(1200\text{Ma})}$  -1.85 – -2.7). This represents a systematic west-northwesterly increase in the proportion of non-radiogenic source material, a trend continued into the eastern Nornalup Zone of the Albany–Fraser Orogen (Smithies et al., 2015). It is also interesting to note that the more juvenile magmatism in the east-southeast of the Madura Province (MAD011 and Moodini) is significantly younger (c. 1144–1125 Ma) than magmatism to the west-northwest (Booanya, Hannah and MAD014; c. 1181–1172 Ma), reflecting a greater mantle contribution with decreasing age.

## References

- Adams, M 2012, Structural and geochronological evolution of the Malcolm Gneiss, Nornalup Zone, Albany–Fraser Orogen, Western Australia: Geological Survey of Western Australia, Record 2012/4, 122p.
- Bogaerts, M, Scaillet, B, and Vander Auwera, J 2006, Phase equilibria of the Lyngdal Granodiorite (Norway): Implications for the origin of metaluminous ferroan granitoids: *Journal of Petrology*, v. 47, p. 2405–2431.
- Brophy, JG 2008, A study of rare earth element (REE)–SiO<sub>2</sub> variations in felsic liquids generated by basalt fractionation and amphibole melting: a potential test for discriminating between the two different processes: *Contributions to Mineralogy and Petrology*, v. 156, p. 337–357.
- Duchesne, JC, Shumlyanskyy, L, and Charlier, B 2006, The Fedorivka layered intrusion (Korosten Pluton, Ukraine): An example of highly differentiated ferrobasic evolution: *Lithos*, v. 89, p. 353–376.
- Frost, BR, Barnes, CG, Collins, WJ, Arculus, RJ, Ellis, DJ and Frost, CD 2001, Ageochemical classification for granitic rocks: *Journal of Petrology*, v. 42, p. 2033–2048.
- Kilpatrick, JA and Ellis, DJ 1992, C-type magmas: igneous charnockites and their extrusive equivalents: *Transactions of the Royal Society of Edinburgh, Earth Sciences*, v. 83, p. 155–164.
- Pearce, JA 2008, Geochemical fingerprinting of oceanic basalts with applications to ophiolite classification and the search for Archean oceanic crust: *Lithos*, v. 100, p. 14–48.
- Smithies, RH, Howard, HM, Evins, PM, Kirkland, CL, Kelsey, DE, Hand, M, Wingate, MTD, Collins, AS and Belousova, E 2011 High-temperature granite magmatism, crust–mantle interaction and the Mesoproterozoic intracontinental evolution of the Musgrave Province, central Australia: *Journal of Petrology*, v. 52(5), p. 931–958.
- Spaggiari, CV, Kirkland, CL, Smithies, RH, and Wingate, MTD 2014, Tectonic links between Proterozoic sedimentary cycles, basin formation and magmatism in the Albany–Fraser Orogen: Geological Survey of Western Australia, Report 133, 63p.
- Spaggiari, CV, Kirkland, CL, Smithies, RH, Wingate, MTD, and Belousova, EA 2015, Transformation of an Archean craton margin during Proterozoic basin formation and magmatism: The Albany–Fraser Orogen, Western Australia: *Precambrian Research*, v. 266, p. 440–466.
- Sun, S-S and McDonough, WF 1989, Chemical and isotopic systematics of oceanic basalts: implications for mantle compositions and processes, in *Magmatism in the Ocean Basins edited by AD Saunders and MJ Norry*: Geological Society, London, Special Publication 42, p. 313–345.
- Vander Auwera, J, Longhi, J, and Duchesne, J-C 1998, A liquid line of descent of the jotunite (hypersthene monzodiorite) suite: *Journal of Petrology*, v. 39, p. 439–468.
- Watson, EB and Harrison, MT 1983, Zircon saturation revisited: temperature and composition effects in a variety of crustal magma types: *Earth and Planetary Science Letters*, v. 64, p. 295–304.
- Woodhead, J, Hergt, J, Greig, A, and Edwards, L 2011, Subduction zone Hf-anomalies: Mantle messenger, melting artefact or crustal process?: *Earth and Planetary Science Letters*, v. 304, p. 231–239.

# Madura Province: isotopes and crustal evolution

by

**CL Kirkland<sup>1</sup>, RH Smithies, CV Spaggiari, and MTD Wingate**

The Precambrian crystalline basement beneath the Eucla and Bight Basins represents a frontier greenfields region with very little known about its age, composition, and geodynamic evolution. Recent Exploration Incentive Scheme (EIS) stratigraphic and co-funded drilling, and donated cores (Fig. 1 in Preface), provide a unique sample set that can have a range of cutting edge isotopic techniques applied in an effort to reveal its geological evolution and enhance its exploration potential. Isotope geology is perhaps uniquely placed to see through overprinting events to expose both the timing and nature of early crust formation processes.

The Madura Province, the area of basement bounded by the Rodona Shear Zone and the Mundrabilla Shear Zone, lies adjacent to the Albany–Fraser Orogen but preserves a startlingly different geological history to its western neighbour. The Madura Province records at least two broad phases of magmatic activity. Zircon U–Pb geochronology from metagabbros and plagiogranites constrain one phase to 1411–1389 Ma, whereas younger metagranites and metagabbros indicate crystallization ages of 1180–1125 Ma (see Wingate et al., this volume). Zircon crystals from all these magmatic rocks cluster along an apparent evolution array intersecting depleted mantle at 2.0 – 1.9 Ga. Scatter in this apparent evolution array indicates clear evidence of new mantle input during the initial phase of 1411–1389 Ma magmatism, where Hf isotopic values extend to the model depleted mantle.

Nd isotopic data from granitic rocks of both phases of magmatism defines isotopic and geochemical mixing arrays between a radiogenic phase with high Nd concentrations and a radiogenic phase with low Nd concentration. The radiogenic phase with high Nd concentrations has a similar isotopic and geochemical signature to Pitjantjatjara Supersuite charnockitic granites in the Musgrave Province, which also dominantly record juvenile crust formed at c. 2.0 – 1.9 Ga. This component also dominates the c. 1400 Ma gabbros of the Madura Province. We interpret this 2.0 – 1.9 Ga primitive isotopic array to reflect a complex mix of oceanic-plate magma sources. In addition to this primitive array new addition of mantle material at c. 1400 Ma is recorded in granitic rocks which in some cases indicate greater juvenile mantle influence than in coeval gabbros. Such petrogenetic processes match aspects of oceanic arc magmatism and demonstrate that the Rodona Shear Zone is a fundamental suture now separating reworked rocks of Yilgarn heritage from new substrate of oceanic affinity lying between the Yilgarn and Gawler Cratons.

---

<sup>1</sup> Centre for Exploration Targeting – Curtin Node, Department of Applied Geology, Curtin University, Bentley WA 6845

# Forrest Zone: lithological characteristics and structural evolution

by

CV Spaggiari, RH Smithies, and RN England<sup>1</sup>

## Introduction

The Forrest Zone is inferred to be the westernmost part of the Coompana Province, which extends into South Australia and links to the Gawler Craton to the east (Korsch et al., 2014). To the west, the Forrest Zone is truncated by the subvertical Mundrabilla Shear Zone, separating it from the Madura Province. The eastern extent of the Forrest Zone, and its relationship with other parts of the Coompana Province are unknown, but are currently being investigated as part of the interpretation of the Eucla–Gawler deep crustal seismic reflection line. Prior to this drilling program no basement drilling had been undertaken in the Forrest Zone, so the tectonic subdivisions described above are tenuous. The five new stratigraphic cores provide important constraints on understanding the evolution of the Forrest Zone and Coompana Province, and its relationship to the Madura Province and Gawler Craton. These cores are described below.

## Stratigraphic core FOR011

Drill hole FOR011 is located within a series of northeasterly trending, moderate response magnetic features that appear to be cut by northwesterly trending, probable reverse faults, and potentially younger granitic intrusions pre-dating those faults. The region surrounding FOR011 is of low gravity response, although there are subtle features of moderate gravity response that are aligned parallel to the northeasterly trending magnetic fabric. These are likely to be due to the mafic to intermediate rocks that occur in both FOR011 and FOR010. The lithological units in FOR011 are described below, and shown in the graphic log in Appendix 1.

This core is dominated by interlayered, pink to red, seriate to equigranular metamonzogranite and metasyenite with distinct but irregular, mafic and felsic layering.

The felsic layers vary from fine- to coarse-grained, and are dominated by assemblages of plagioclase (locally myrmekitic), orthoclase (locally microcline), quartz, and olive-brown to dark biotite (locally overgrown by chlorite). The proportions of these minerals vary with the layering. The mafic layers are fine- to medium-grained, and are rich in dark green hornblende and dark biotite. Titanite is a common accessory mineral throughout. Some of the mafic rocks are chemically classified as shoshonites (see Smithies et al., this volume), and contain biotite and green hornblende aligned in the foliation, anhedral oligoclase mainly included in or at the margins of interstitial alkali feldspar, titanite and apatite. There is one distinct amphibolite layer that lacks quartz at 385.50 – 386.10 m (GSWA 213837), and possibly a second one at about 439.90 m. This rock contains abundant deep green hornblende (up to 4 mm), lightly illitised plagioclase (about An<sub>25</sub>), and dark brown biotite. The texture and hornblende colour are typical of Fe-rich amphibolites of the middle amphibolite facies. The lithologies described above, and the foliation in them, are cut by thin pegmatitic veins (Fig. 1a).

## Sulfides

Disseminated pyrite and chalcopyrite are reasonably common in minor quantities throughout. The pyrite could be a late hypogene alteration product of pyrrhotite, and the chalcopyrite is commonly altered to bornite. Pyrite also occurs along fractures and biotite cleavages where it may be a mobilised retrograde alteration product of early pyrrhotite. One sample of biotite monzogranite (GSWA 206733; 7 cm ½ HQ core, 143.4 ppm Mo, 172.4 ppm Cu) contains minor <0.45 mm molybdenite flakes, disseminated subhedral <0.5 mm pyrite forming about 1% of the rock in thin section, and disseminated anhedral <0.1 mm chalcopyrite. The molybdenite suggests a fairly high-T origin for the sparse sulfides from magmatic fluid, and the presence of unaltered biotite associated with some sulfides suggests they pre-date chlorite.

---

<sup>1</sup> Petrology Services, Duncraig, WA 6023

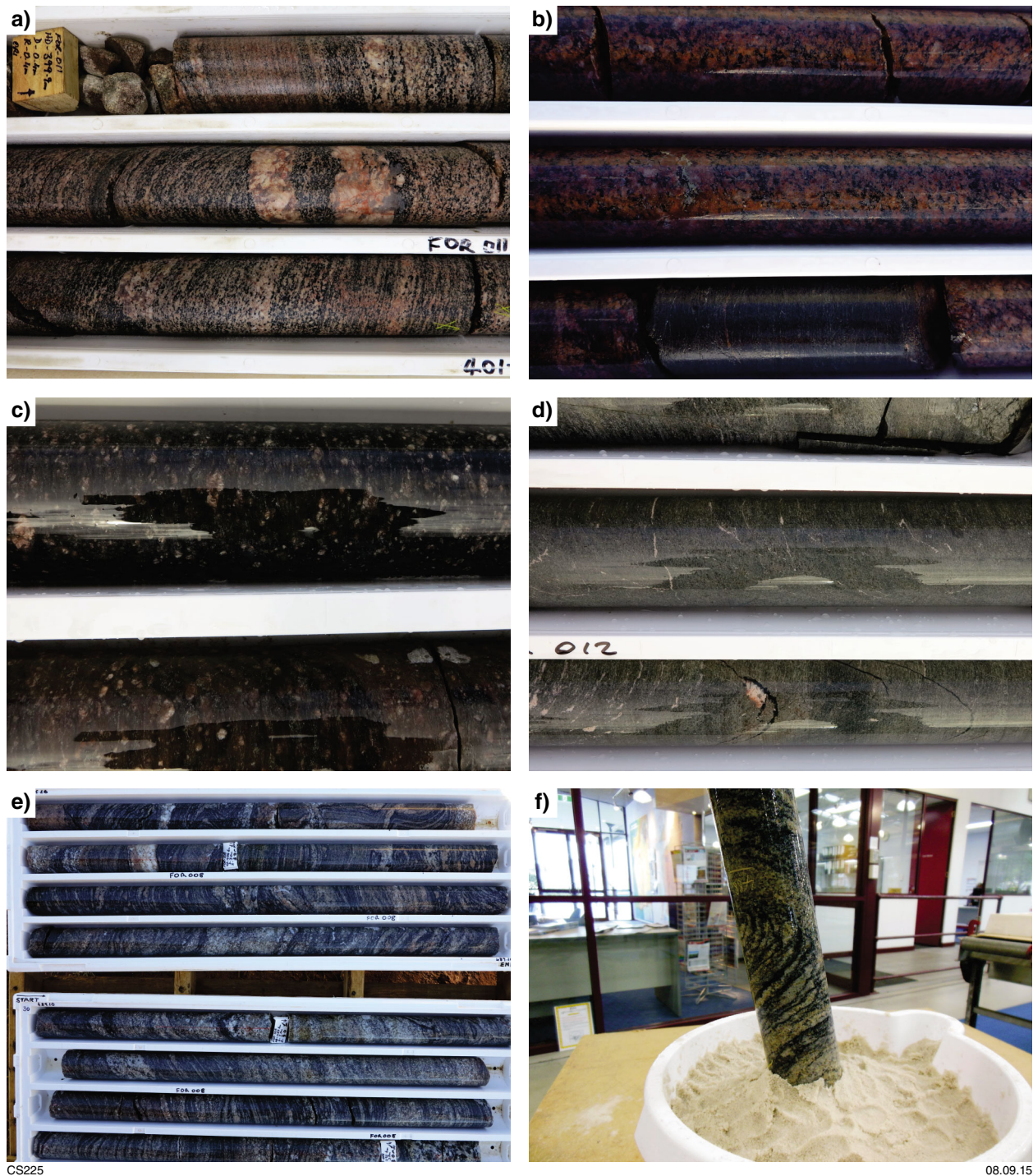


**Figure 1.** Photographs of Forrest Zone stratigraphic basement cores showing: a) layered seriate to equigranular metasyenite cut by coarse pegmatite veins (FOR011, photographed wet); b) porphyritic biotite monzogranite gneiss with sulfide, and shoshonite (lower part of photo) (FOR010, photographed wet); c) mylonitic metagranite (FOR012, photographed wet); d) grey felsic schist that is possibly a metavolcanic, with wispy carbonate veins (FOR012, photographed wet); e) migmatitic granite gneiss (FOR008, photographed wet); f) fold in granite gneiss measured in bucket of sand by orienting the core to its drilled position (FOR004, photographed wet).

## Structural analysis

Layering in the mafic and felsic rocks is subparallel to a well-developed, dominantly moderate intensity foliation (S1), that dips either northwest or southeast in the upper part of the hole, and predominantly northwest in the lower part of the hole. The foliation and layering are folded into a small-scale, shallowly northeast-plunging, tight fold at 409.3 m drilled depth. This observation is in agreement with stereonet analysis of a best fit great circle from poles to planes of the S1 foliation, which gives a calculated fold axis of 6° to 061. The fold hinge this represents is estimated to lie at about 398 m drilled depth, corresponding with measurements of S1 of 9° to 068 and 6° to 036 (dip, dip direction of hinge zone), and the change to a dominant northwest dip direction below. The foliation is cut by thin granitic or pegmatitic veins, abundant thin quartz–carbonate veins, and locally by zones of brecciation, typically with chlorite alteration.

## Stratigraphic core FOR010

Drill hole FOR010 is located on a distinct, northeasterly trending fabric of moderate magnetic response, and within a large area of low gravity response. About 10 km to the southeast is a northeasterly trending ridge of moderate gravity response coincident with a slightly stronger magnetic fabric. This ridge is inferred to include mafic to intermediate rocks described in FOR011 and in this core.

This core is complex and comprises five lithological units. In order of relative ages determined by cross-cutting relationships in the core these are, from oldest to youngest: 1) porphyritic biotite monzogranite gneiss, 2) foliated tonalitic metagranite, 3) mafic to intermediate hornblende-bearing metagranite (shoshonite), 4) unfoliated porphyritic syenogranite (evolved Si-rich shoshonite), and 5) unfoliated equigranular syenogranite (evolved Si-rich shoshonite). In the core itself the porphyritic biotite monzogranite gneiss appears to be the oldest phase, although this is not certain as layers of tonalitic metagranite occur locally within it, and the contacts are parallel to the foliation. In contrast, the shoshonite clearly intrudes the biotite monzogranite gneiss and the tonalitic metagranite, and the unfoliated porphyritic and equigranular syenogranites intrude all of the above. The five units are described below, and shown in the graphic log in Appendix 1.

## Monzogranite gneiss and tonalitic metagranite

The porphyritic biotite monzogranite gneiss is medium- to coarse-grained, greyish brown to red, and generally has a strong gneissic foliation in which the recrystallized feldspars form elongate aggregates or porphyroclasts. The porphyroclasts are either microcline or aggregates of anhedra K-feldspar (orthoclase in various stages of strain-inversion to microcline) with subordinate quartz, granular oligoclase, and rare small flakes of biotite. The porphyroclasts occur in a finer-grained, more mafic matrix

dominated by plagioclase (An<sub>20</sub>) and biotite, minor quartz and interstitial K-feldspar, and anhedra green hornblende locally. Fine-grained anhedra titanite, stubby euhedral zircon, and anhedra magnetite locally rimmed with titanite are common. The feldspars are locally altered to hematite, contributing to the red colour.

The tonalitic metagranite is grey, medium- to fine-grained, and moderately to strongly foliated. It comprises anhedra plagioclase (An<sub>20</sub>) distinctly flattened into a foliation defined by the preferred orientation of dark, Fe-rich biotite and subhedra prismatic to anhedra dark green hornblende, both of which are concentrated into streaky lenses parallel to the foliation, which also contain anhedra quartz. Anhedra magnetite is mostly altered to hematite. The mineral assemblage reflects metamorphic conditions around the lower amphibolite facies. The tonalitic metagranite is strongly deformed and altered near the top of the core (387.5 – 400.3 m and 429.2 – 430.2 m) where it is finer-grained, thinly layered, and dark greenish grey due to modification into a chloritised biotite–epidote schist. The presence of biotite and the plagioclase composition suggests this deformation and alteration took place at low amphibolite facies metamorphic conditions.

## Shoshonite

Fine- to medium-grained, mesocratic hornblende-bearing metagranite is classified as a shoshonite (Smithies et al., this volume). It typically contains 4–8 mm long (up to 15 mm) aligned mafic lenses of variable composition comprising columnar prismatic dark green hornblende commonly wrapped in biotite, which were probably originally mafic phenocrysts. These occur in a fine-grained groundmass of hornblende, biotite, K-feldspar, plagioclase, and titanite, typically with abundant prismatic apatite. Fine-grained quartz occurs locally with (metamorphic) hornblende reaction rims. One example (GSWA 213868) is slightly altered and contains subhedra stubby prismatic 0.3–2 mm pale green actinolitic hornblende, chloritised similar-sized biotite, 2 mm subhedra blocky K-feldspar, and anhedra <2 mm plagioclase (about An<sub>25</sub>) that is locally albitised. The assemblages described above indicate metamorphism in the low amphibolite or upper greenschist facies, and GSWA 213868 indicates the shoshonite was locally retrogressively altered (chloritising biotite) at low or subgreenschist facies.

## Structural analysis

The shoshonite contains a variably developed foliation that is for the most part parallel to the shallow to moderate northeasterly dip in the monzogranite gneiss and the tonalitic metagranite, both of which the shoshonite intrudes. Stereonet analysis of a best fit great circle from poles to planes of the foliation in the monzogranite gneiss and tonalitic gneiss gives a calculated fold axis of 20° to 061, similar to measured small-scale folds and the calculated fold axis in core FOR011 (6° to 061). Although the data are limited, the foliation in the shoshonite gives similar results however, in various places, veins



of shoshonite cut the foliation in both the monzogranite gneiss and the tonalitic metagranite. This suggests that the deformation took place during pulses of shoshonite intrusion (recorded in both cores FOR010 and FOR011), resulting in earlier shoshonite veins bearing a foliation (potentially magmatic), and later shoshonite veins cross-cutting the earlier ones. This would not preclude the monzogranite gneiss and tonalitic metagranite containing relicts of an older fabric. An alternative interpretation is that two, subparallel foliations may have formed in different events, with the earlier foliation in the monzogranite gneiss and tonalitic metagranite undergoing recrystallization in a similar orientation when the second foliation formed in the shoshonite, with strain partitioning resulting in variable development of the foliation in the shoshonite.

## Late syenogranite veins (evolved Si-rich shoshonite)

Unfoliated medium- to coarse-grained, red porphyritic syenogranite occurs as veins of variable thickness throughout the core. It typically has an assemblage of subhedral <8 mm orthoclase phenocrysts (commonly inverted to microcline), euhedral oligoclase phenocrysts, and anhedral quartz in a groundmass of subhedral plagioclase, interstitial anhedral quartz, partly chloritised dark (Fe-rich) biotite, minor microcline, titanite, magnetite, and rare subhedral dark olive hornblende.

The youngest unit is an unfoliated, fine-grained, red equigranular syenogranite that also occurs as veins of variable thickness throughout the core. It typically has an assemblage of partly chloritised plagioclase–microcline–biotite–quartz. Biotite is dark (Fe-rich) and partly chloritised. Accessories include granular and prismatic apatite, subround sphenoidal titanite, and mainly interstitial magnetite that is largely altered to hematite.

## Sulfides

Sulfides occur in minor amounts in the monzogranite gneiss and both types of syenogranite veins, and along the contacts of the phases the veins intrude (Fig. 1b). Minor disseminated pyrite and chalcopyrite occur in the monzogranite gneiss. In GSWA 213862 (447.94 – 448.20 m) disseminated subhedral <0.6 mm pyrite (0.5%) is weakly associated with very minor <0.3 mm subhedral epidote and <0.2 mm grains of chalcopyrite. In GSWA 206748 (492.60 – 492.74 m; ½ HQ core, 200 ppm Cu) sulfides present in trace amounts comprise <0.3 mm chalcopyrite and <0.1 mm galena. A couple of <8 mm irregular masses of greenish brown very fine sheet silicates that may have been coarse hornblende are speckled with <0.2 mm subhedral pyrite, and near their rims with leucoxene.

In the red, hematite-stained syenogranite veins sulfides comprise pyrite, chalcopyrite, and rare galena. In GSWA 206743 (441.98 – 442.10 m; ½ HQ core, 147 ppm Pb, 15.8 ppm Mo) a couple of 30 micron galena grains

adhere to a much larger subhedral grain of pyrite. Other sulfides are scarce chalcopyrite and pyrite with minor, late <0.3 mm magnetite on its margins. GSWA 206741 (441.12 – 441.25 m) contains disseminated, anhedral to subhedral <1mm pyrite forming about 2% of the rock, and traces of chalcopyrite. The tan colour of the slightly degraded pyrite, and the approximately 0.2 mm stubby rutile suggest that pyrite (or a pyrrhotite precursor) might have been present at the metamorphic peak.

## Stratigraphic core FOR012

Drill hole FOR012 is located on a northeasterly trending, distinct wedge about 50 km long and 12 km wide defined in a moderate response magnetic fabric, and within a broad area of low gravity response. The drill site lies just south of a west-northwesterly trending mafic dyke, interpreted in magnetic data, which may be part of the c. 825 Ma Gairdner Dyke Suite (Wingate et al., 1998). This hole was drilled to help test whether there was a tectonic boundary between combined sites FOR011–FOR010 and FOR004, which yielded different primary ages (see Wingate et al., this volume). The core is described below, and shown in the graphic log in Appendix 1.

Drill core FOR012 contains two texturally distinct units. The top section of the core (310–377 m) is dominated by a fine- to medium-grained (1–4 mm) dark grey, felsic mylonite with abundant pink, rounded feldspar porphyroclasts on average about 4 mm but up to 1 cm, and abundant quartz (or felsic aggregates) eyes and ribbons (Fig. 1c). Dark layers generally 1–2 cm thick occur locally, and could be biotite-rich or ultramylonite layers. In thin section the porphyroclasts are mostly subrounded mesoperthite with less than half K-feldspar, some of which show fine microcline twinning. Locally, albitised plagioclase porphyroclasts have coarse albite twinning that is lightly crackle-brecciated into subgrains with slightly disrupted orientations. Masses of fine-grained leucoxene, titanite, and magnetite (possibly after titanomagnetite) microphenocrysts occur locally. The groundmass is a mixture of anhedral quartz, tabular to anhedral muscovite, biotite, and aggregates of very fine-grained K-feldspar, albite and quartz. Disseminated metamorphic magnetite occurs mainly in the fine-grained quartzofeldspathic aggregates. Fine, anhedral acid-resistant carbonate (probably ankerite) occurs locally in the groundmass, and tiny carbonate inclusions are disseminated in most feldspar porphyroclasts. This section of core is interpreted as mylonitic to ultramylonitic metasyenogranite.

The lower unit is a fine-grained (1–3 mm), grey to dark grey schist with anastomosing, fine dark layering of variable thickness and abundance, and wispy pale veinlets that are subparallel to the foliation but locally transgress it (Fig. 1d). This schist is also strongly deformed, and mostly mylonitic. It comprises 0.5 – 5 mm, mostly eye-shaped, albitised plagioclase porphyroclasts wrapped by the foliation, which is dominated by variable proportions of white mica and locally chloritised biotite. Fine quartz, albite and titanite are minor phases. Magnetite is common, and occurs as microphenocrysts or is concentrated into



<2 mm layers parallel to the foliation. One example (GSWA 219003) contains porphyroclasts of <2 mm recrystallised bipyramidal and round quartz. In this sample the matrix comprises fine white mica and minor, partly chloritised biotite, quartz, minor albite and titanite. Minor acid-resistant carbonate is probably ankerite, and metamorphic magnetite is locally altered to hematite and possibly ankerite. Very minor wispy lenses of fine rutile are probably relics of igneous Fe-Ti oxide microphenocrysts. Thin veins that cut the foliation at a high angle consist of chlorite, K-feldspar, calcite, and minor ankerite or mixes of chlorite, epidote and quartz.

This unit is tentatively interpreted as a felsic volcanic, possibly a rhyolite, based on the overall fine-grainsize, and variable texture that could be inherited to some degree from the protolith. In thin section there are no coarse grains or masses of fine grains that could have been relicts of coarse igneous biotite. Alternatively, the unit is a strongly deformed to mylonitic metamonzogranite, and has virtually the same granitic protolith as the unit above, but is less porphyritic. Geochemically, there is little distinction between these two units (Smithies et al., this volume).

Below the upper metasyenogranite are several discrete horizons of mafic to intermediate schist that is similar in composition to the grey schist, but contains a greater proportion of micaceous minerals, and possibly some fine amphibole. It is also strongly deformed, and locally folded, and contains thin pale wispy carbonate veins.

Acid-resistant carbonate consistently present throughout FOR012 probably sets an upper limit to the metamorphic grade at the greenschist–amphibolite transition, and the biotite zone of the greenschist facies is the best estimate for the metamorphic grade of the shear zone this core has intersected.

## Sulfides

Minor disseminated fine pyrite and associated anhedral chalcopryrite occur locally in the schistose matrix, and are also typically associated with magnetite. Sulfides also occur in thin veins, for example, GSWA 206800 (435.23 – 435.46 m) contains a carbonate–quartz–pyrite–magnetite–chalcopryrite veinlet. In GSWA 206795 (394.67 – 394.92 m) minor disseminated <0.2 mm pyrite and associated anhedral chalcopryrite occur in the schistose white mica-dominated matrix. This sample contains 1172 ppm Cu (25 cm  $\frac{1}{2}$  HQ core). In GSWA 206797 (406.61 – 406.77 m) disseminated lightly hematized octahedral <1 mm magnetite forms about 1% of the rock. Cube-shaped <1 mm pyrite is concentrated in quartz-carbonate rich lenses parallel to the foliation. Rarer <0.2 mm chalcopryrite is associated with pyrite and magnetite. Finer pyrite in a cross-cutting 0.2 mm ankerite-quartz veinlet is probably later. In GSWA 206799 (422.07 – 422.29 m) disseminated <1 mm roughly cube-shaped pyrite is rare compared with disseminated magnetite hematized at its margins and associated with fine rutile or anatase. Rare <0.1 mm anhedral chalcopryrite is associated with pyrite, but also occurs in and near

sheeted veinlets that cut the foliation and contain acid-resistant carbonate (probably ankerite) and also calcite, locally contain <0.2 mm roughly prismatic to anhedral quartz, and are lined with fine chlorite.

## Structural analysis

The metasyenogranite in the upper part of the core has a mylonitic foliation with a dominant, moderate northwesterly dip and less common southeasterly dip, and a subhorizontal to shallow northeasterly plunging mineral lineation, measured at 15° to 060. This lineation is rodded to some degree, so the mylonite is between an L-tectonite and L-S tectonite. The asymmetry of the porphyroclasts indicate both sinistral and dextral shear sense, suggesting a strong flattening and/or stretching component. Minor folding visible in this unit has a measured fold axis of 5° to 040 and axial plane of 60° to 130 (dip, dip direction). The relatively minor switches in dip, from northwest to southeast, are likely to be due to S-folds.

The lower felsic unit also has a mylonitic foliation with moderate dip to both the southeast and northwest, and a measured mineral lineation of 3° to 050. The layers of mafic schist contain similar structures, with a dominant, moderate southeasterly dipping foliation, measured mineral lineation of 10° to 049, and tight folds plunging 5–10° to 045–060. Stereonet analysis of a best fit great circle from poles to planes of the foliation in each unit gives calculated fold axes of 2° to 048 (metasyenogranite), 1° to 046 (grey schist), and 3° to 226 (mafic schist). These data suggest all units have seen the same deformation event, consistent with similar metamorphic conditions and alteration of the matrix assemblages as the mylonite was formed. The mylonite itself appears to be folded about an upright, shallow northeasterly plunging axis, subparallel to the mineral lineation, with a shallow to moderate southeasterly dipping axial plane. Stereonet analysis of a best fit great circle from poles to planes of the foliation in all units gives a calculated fold axis of 2° to 047. This suggests shallowly inclined to subhorizontal folding with the core intersecting an upper limb dipping predominantly to the northwest (upper part of the core), and a lower limb dipping to the southeast, with a fold closure to the northwest. This geometry may be indicative of the overall shape of the northeasterly trending wedge that is visible in the aeromagnetic data.

## Stratigraphic core FOR008

Drill hole FOR008 is located on a fairly non-descript area of subtly northwesterly trending fabric of moderate magnetic response, but within a broad area of moderate, northeasterly trending gravity response. A northeasterly trending gravity low lies to the northwest of this site. The core is described below, and shown in the graphic log in Appendix 1.

This core is dominated by medium- to locally coarse-grained, red to grey, seriate-textured to porphyritic (up to 4 cm), biotite-rich, locally hornblende-bearing, migmatitic,

granodiorite to monzogranite gneiss (Fig. 1e). This gneiss has a well-developed, moderate to strong, anastomosing foliation that is locally folded. It comprises anhedral to blocky subhedral plagioclase (locally antiperthite or myrmekite), anhedral orthoclase (in various stages of strain-inversion to microcline), anhedral olive green hornblende (typically poikilitic and up to 10 mm), anhedral quartz, and weakly tabular biotite, locally in clots up to several millimeters. Porphyroclasts of microcline up to 10 mm locally enclose <4 mm euhedral blocky microcline grains in other orientations. As common as microcline in the groundmass is anhedral to blocky subhedral plagioclase (albite–oligoclase). Accessory minerals include anhedral to roughly octahedral magnetite that is mainly altered to coarse hematite, anhedral titanite (some with cores of ilmenite, some rimming magnetite), subround stubby prismatic zircon, and rare chlorite–epidote altered possible allanite. The accessories are unevenly distributed and all associated with hornblende and biotite. Foliation-parallel, cm- to m-scale quartzofeldspathic layers are generally coarser-grained, locally have biotite-rich selvages, and are interpreted as partial melt patches and veins. These are also folded but locally transgress the gneissic foliation.

The granodiorite gneiss is locally interlayered with medium-grained, monzodiorite gneiss. This gneiss is similar to the granodiorite gneiss but is much richer in hornblende and biotite. It also contains anhedral to blocky subhedral plagioclase, and anhedral orthoclase. The hornblende is fresh and green and tends to be interstitial to plagioclase. Accessories include octahedral magnetite and stubby prismatic apatite. These more mesocratic layers appear to be less migmatized than the more leucocratic layers, which were most likely more susceptible to anatexis during metamorphism.

The presence of metamorphic biotite and hornblende suggests amphibolite facies, and the partial melt patches and veins suggest upper amphibolite or possibly granulite facies. The assemblage in the granodiorite gneiss shows local retrogression to the low greenschist facies. Plagioclase is moderately altered to sericite, biotite to chlorite and epidote, and hornblende to chlorite and sericite.

## Sulfides

Sulfides are sparse in this core, but do occur locally, and assays indicate the presence of Cu. Granitic gneiss GSWA 219009 (448.16 – 448.36 m; ½ HQ core, 101 ppm Cu, 10 ppb Pd) contains a mm-scale stockwork consisting of <0.1mm-thick veinlets of chalcopyrite. This is near dark brown Fe-rich biotite concentrated along a stringer a couple of millimeters wide, with abundant subordinate <2 mm anhedral magnetite that has been completely altered to hematite. Hematite alteration is a common feature in this core, and some sections are distinctly reddish in colour. Coarse-grained porphyritic granite gneiss sample GSWA 219012 (565.60 – 565.81 m; ½ HQ core) contains 1154 ppm Cu, although no sulfide was identified in thin section. The section of core shows patchy chlorite (from biotite) and sericite (from plagioclase)

alteration, and hematite staining. This is just above a zone of increased chlorite–epidote alteration and cm-scale calcite veins with white, zoned, euhedral 5–8 mm crystals. GSWA 219013 (570.45 – 570.65 m, ½ HQ core) is similar to GSWA 219012 and contains 166 ppm Cu.

## Structural analysis

All rock types in this core have a well-developed, moderate to strong gneissosity that has a variable, dominantly shallow dip. This gneissosity is locally folded into flat-lying, small-scale Z-folds and curvilinear folds. These are locally cut by migmatitic patches and veins, indicating the folding took place prior to or during high temperature metamorphism. A weak to moderate intensity mineral lineation is subhorizontal, and is probably anastomosing like the gneissosity (measured at 6–10° to 096 or 196). Stereonet analysis of a best fit great circle from poles to planes of the gneissosity gives a calculated fold axis of 5° to 070, similar to measured fold axes and the mineral lineation. The folds also have subhorizontal folds axes, and flat-lying axial planes that are subparallel to the gneissosity. This suggests recumbent folding.

Localised high strain zones contain small, flat-lying kink bands that indicate top to the west or southwest transport. Throughout much of the core, the asymmetry of feldspar porphyroclasts indicate top to the northwest shearing. A small shear zone at 484 m is oriented 50° to 104 (dip, dip direction) and offsets the layering with top to the northwest displacement. The asymmetric feldspar porphyroclasts occur within the gneissosity, which is folded. The relationships indicate a history of top to the west or northwest transport (prior to or during migmatization), localised folding and probable thickening, closely followed by partial melting.

## Stratigraphic core FOR004

Drill hole FOR004 is located on an area of subtly northwesterly trending fabric of low to moderate magnetic response, and within an area of moderate gravity response. The drill site is situated just north of a northeasterly trending belt of magnetic granites, intersected in the Eucla 1 petroleum well (Fig. 1 in Preface). The site is also about 10 km east of a northwesterly trending fault, which is possibly a reverse fault. The core is described below, and shown in the graphic log in Appendix 1.

Drill core FOR004 is dominated by medium-grained (2–4 mm), mesocratic, mostly equigranular, granodioritic to monzogranitic gneiss (Fig. 1f). It contains anhedral to subhedral blocky plagioclase (An<sub>33</sub>), anhedral orthoclase inverted to microcline, interstitial anhedral quartz, anhedral dark olive-green hornblende, anhedral to roughly tabular dark-brown biotite, and subordinate anhedral to subhedral titanite. Titanite occurs locally with biotite in clots. Minor magnetite, some up to 4 mm, is also locally interstitial to feldspar, and zircon and apatite are common accessories.

This granite gneiss appears to be intruded by fine- to medium-grained, equigranular to seriate-textured, biotite leucogranite, which includes wisps and schleiren of fine-grained metadiorite and metagranodiorite. The two granites have gradational or cusped contacts, suggesting they were coeval. Interlayered with these granites is a metadiorite with cm-scale layering with the grainsize ranging from very fine to medium. The metadiorite contains plagioclase (around An<sub>35</sub>), green hornblende, dark tan biotite, minor quartz and titanite.

## Sulfides and alteration

The gneissic rocks in FOR004 locally show retrograde alteration with biotite altered to chlorite and locally sericite, and plagioclase overgrown by sericite. Thin chlorite–epidote–quartz veins cut the foliation and coarse interstitial magnetite is locally altered on fractures to chlorite and locally calcite. GSWA 213829 (548.16 – 548.38 m), a mesocratic monzodiorite to granodiorite gneiss, contains clustered chalcopyrite and rare bornite. GSWA 206717 (436.10 – 436.20 m) is a sericite–carbonate–albite–chlorite altered leucocratic granite with coarse mesothermal quartz. Minor <1 mm roughly tabular to anhedral biotite is completely altered to chlorite (epitaxially) and sericite, both dusted with prominent minor leucoxene or fine rutile. Irregular <2 mm masses of sericite are moderately abundant, some of which have replaced parts of plagioclase grains, and some of which partly enclose <1.5 mm prisms of hydrothermal quartz. Muscovite flakes up to 0.2 mm occur with the sericite. Rare <0.5 mm anhedral to subhedral pale buff-pink garnets probably belong to the alteration assemblage. GSWA 213834 (569.84 – 570.00 m) is described as a gneissic clotty biotite tonalite and contains partly chloritised <2 mm anhedral biotite, coarse magnetite, and a 1 mm anhedral grain or mass of chalcopyrite with biotite and plagioclase that appears to have undergone only minor disturbance since the metamorphic peak. There is no associated alteration of the host rock.

## Structural analysis

The rocks in FOR004 generally have a gneissic foliation that has a predominant, shallow to moderate, west-southwesterly dip. Stereonet analysis of a best fit great circle from poles to planes of the foliation in all units gives a calculated fold axis of 1° to 349, indicating that if the gneissic foliation is folded on a larger scale, the fold probably has a shallow plunge. In the core the gneissic layering is locally folded (Fig. 1f) into shallowly inclined folds with shallow plunges mostly around 20° towards 280. The upper part of the core is dominated by a west to southwest dip, and could be part of a larger fold nose, plunging to the west. Below the hinge zone the dip is more variable and generally switches between southeast and west-southwest. At around 525 m drilled depth the more mesocratic rocks contain small-scale refolded folds, with second generation (F2) west-plunging folds similar to those described above. These F2 folds are cut by the veins and alteration.

## Previous drilling

Prior to this drilling program the only information from the Forrest Zone was from granitic chips from the base of the Eucla 1 petroleum well, which contain oscillatory zoned zircons that yielded a date of  $1140 \pm 8$  Ma, interpreted as the magmatic crystallization age of the granite (GSWA 194773, Kirkland et al., 2011). This well overlies a distinct ovoid feature with high magnetic intensity, interpreted to be part of a distinct belt of northeasterly trending granitic intrusions truncated by, and dragged into, the Mundrabilla Shear Zone. The magnetic signature is similar to intrusions with high magnetic response belonging to the Booanya Suite of the c. 1200–1130 Ma Esperance Supersuite in the Albany–Fraser Orogen (Smithies et al., 2105).

In South Australia, granodiorite gneiss from the Coompana Province (sampled from the Mallabie 1 drillhole in South Australia) has been dated at  $1505 \pm 7$  Ma, interpreted as the igneous crystallization age of the granite protolith, which intruded into an unknown basement (Wade et al., 2007). The granodiorite is described as an intensely foliated gneiss locally with quartzofeldspathic and hornblende–biotite-bearing mafic layering.

## References

- Kirkland, CL, Wingate, MTD, Spaggiari, CV and Tyler, IM 2011, 194773: granitic rock, Eucla No. 1 drillhole; Geochronology Record 1001: Geological Survey of Western Australia, 4p.
- Korsch, RJ, Spaggiari, CV, Occhipinti, SA, Doublier, MP, Clark, DJ, Dentith, MC, Doyle, MG, Kennett, BLN, Gessner, K, Neumann, NL, Belousova, EA, Tyler, IM, Costelloe, RD, Fomin, T and Holzschuh, J 2014, Geodynamic implications of the 2012 Albany–Fraser deep seismic reflection survey: a transect from the Yilgarn Craton across the Albany–Fraser Orogen to the Madura Province, *in* Albany–Fraser Orogen seismic and magnetotelluric (MT) workshop 2014: extended abstracts compiled by CV Spaggiari and IM Tyler, Geological Survey of Western Australia, Record 2014/6, p. 142–173.
- Smithies, RH, Spaggiari, CV and Kirkland, CL 2015, Building the crust of the Albany–Fraser Orogen: constraints from granite geochemistry: Geological Survey of Western Australia, Report 150, 49p.
- Wade, BP, Payne, JL, Hand, M and Barovich, KM 2007, Petrogenesis of ca 1.50 Ga granitic gneiss of the Coompana Block: filling the 'magmatic gap' of Mesoproterozoic Australia: Australian Journal of Earth Sciences, v. 54, p. 1089–1102.
- Wingate, MTD, Campbell, IH, Compston, W and Gibson, GM 1998, Ion microprobe U–Pb ages for Neoproterozoic basaltic magmatism in south-central Australia and implications for the breakup of Rodinia: Precambrian Research, v. 87: 135–159.

# U–Pb geochronology of the Forrest Zone of the Coompana Province

by

MTD Wingate, CL Kirkland<sup>1</sup>, CV Spaggiari and RH Smithies

## Introduction

Fourteen samples were collected for U–Pb geochronology from five new GSWA stratigraphic drillcores in the Forrest Zone of the Coompana Province. Previous geochronology results are available for one sample from the Eucla 1 drillcore (Kirkland et al., 2011). Analytical methods are described in detail in Wingate and Kirkland (2015). Analyses >5% discordant are generally considered to be unreliable and, in most cases, are not included in determining the age of each sample. Results are described below in order of decreasing age. Except where noted otherwise, the dates discussed below are based on  $^{207}\text{Pb}^*/^{206}\text{Pb}^*$  ratios, and mean ages for samples, or groups of samples, are quoted with 95% confidence intervals ( $t\sqrt{\text{MSWD}}$ , where  $t$  is Student's  $t$ ). Results for all samples are listed in Table 1. During sampling, care was taken to document the geological context of each sample within the drillcore, and fractions of each geochronology sample were isolated for geochemistry and petrography. Interpretation of geochronology results takes into account relevant petrographic, geochemical, isotopic, and structural data for all samples and intervening drillcore material, as detailed elsewhere in this volume.

## Geochronology results

### Toolgana Supersuite (c. 1610 Ma)

Four samples for geochronology were collected from two drillcores, FOR004 and FOR008, in the eastern Forrest Zone (Table 1). The samples in FOR004 consist of layered granodioritic to monzogranitic gneiss (GSWA 192594), and weakly foliated schleiric biotite tonalite (GSWA 213822). The two samples (GSWA 216261 and 216276) in FOR008 are of migmatitic granodiorite

gneiss. In tonalite sample GSWA 213822, the zircons consist of concentrically zoned cores overgrown by high-uranium rims; in the three gneissic samples, zoned zircon cores are overgrown by rims of low-uranium zircon that also fills fractures in many crystals. Zircon cores in the four samples yield dates between 1613 and 1604 Ma, interpreted as the ages of granitic protoliths. These ages agree to within uncertainty, with a weighted mean of  $1611 \pm 7$  Ma. In three samples, analyses of zircon rims indicate Th/U ratios of 0.001 – 0.01, and provide dates of 1179, 1158, and 1150 Ma, interpreted as the ages of zircon growth during high-grade metamorphism. Analyses of three zircon rims, and one zircon core, in the fourth sample, GSWA 192594, yield unreliable, discordant results that suggest formation of zircon rims and loss of radiogenic Pb was younger than c. 1611 Ma. Two zircon cores in GSWA 192594 provide dates of 1724 and 1671 Ma, interpreted as the ages of inherited components. All four samples are assigned to the c. 1610 Ma Toolgana Supersuite.

### Undawidgi Supersuite (c. 1490 Ma)

Four samples of metagranite and one sample of felsic schist (possibly a metavolcanic rock) in three drillcores, FOR010, FOR011, and FOR012, yield dates of 1505–1487 Ma (Table 1), and are assigned to the Undawidgi Supersuite. The zircons are subhedral to euhedral, and concentrically zoned. With one exception (described below) none of the samples exhibits zircon rims. Apart from minor Pb-loss apparent in all samples, interpretation of U–Pb results for these samples is straightforward. In each case, most data indicate a mainly well grouped, concordant component, yielding a precise protolith age. Excluding the 1505 Ma date, four results (1499–1487 Ma) are in statistical agreement, and yield a weighted mean of  $1490 \pm 7$  Ma; including the older date increases the mean age to  $1492 \pm 9$  Ma. In sample GSWA 206730 (Table 1), zircon cores with a mean age of 1488 Ma are overgrown by thin zircon rims, six analyses of which indicate very low Th/U ratios (0.01 – 0.07) and yield a concordia age of  $1174 \pm 12$  Ma, interpreted as the age of high-grade metamorphism.

<sup>1</sup> Centre for Exploration Targeting – Curtin Node, Department of Applied Geology, Curtin University, Bentley WA 6845

**Table 1. U–Pb zircon geochronology results for Madura Province drillcore samples**

Sample ID	Unit name	Rock type	Drillcore ID	Depth interval sampled (m)	Magmatic age (Ma)	Metamorphic age (Ma)	Inheritance (Ma)
216276	Toolgana Supersuite	migmatitic gneiss	FOR008	552.21 – 552.91	1613 ± 13	1150 ± 10	
213822	Toolgana Supersuite	schleiric leucogranite	FOR004	484.54 – 485.10	1613 ± 4	1179 ± 10	
192594	Toolgana Supersuite	granitic gneiss	FOR004	497.67 – 498.18	1611 ± 7		1724, 1671
216261	Toolgana Supersuite	migmatitic gneiss	FOR008	476.31 – 476.81	1604 ± 6	1158 ± 12	
216239	Undawidgi Supersuite	monzogranite	FOR012	341.59 – 342.05	1505 ± 8		
206788	Undawidgi Supersuite	felsic schist	FOR012	433.00 – 433.50	1499 ± 9		
206751	Undawidgi Supersuite	metagranite	FOR010	432.75 – 433.10	1492 ± 9		
206730	Undawidgi Supersuite	metagranite	FOR011	419.20 – 419.40	1488 ± 4	1174 ± 12	
192592	Undawidgi Supersuite	porphyritic metagranite	FOR010	474.32 – 475.09	1487 ± 9		
206753	Moodini Supersuite	granite	FOR010	490.14 – 490.48	1192 ± 13		1576–1511
213838	Moodini Supersuite	granitic vein	FOR011	388.02 – 388.26	1189 ± 6		1552–1462
206752	Moodini Supersuite	porphyritic granite	FOR010	482.42 – 483.02	1184 ± 8		1554
206729	Moodini Supersuite	bio-hb metagranite	FOR011	415.80 – 416.19	1180 ± 6		
192593	Moodini Supersuite	hornblende metagranite	FOR010	459.77 – 460.25	1175 ± 5		
194773	Moodini Supersuite	granite	Eucla 1	215.00 – 221.00	1140 ± 8		

NOTE: Ages are quoted with 95% confidence intervals.

## Moodini Supersuite (1192–1140 Ma)

The remaining six samples in the Forrest Zone are granites in three drillcores: FOR010, FOR011, and Eucla 1 (Table 1). Zircons from these samples yield well defined igneous crystallization ages of 1192–1140 Ma, and are assigned to the Moodini Supersuite. As is the case with the Moodini Supersuite samples in the Madura Province (1181–1125 Ma; Wingate et al., this volume), the mean ages for the samples are dispersed well beyond analytical precision, indicating that Moodini Supersuite magmatism was protracted. However, the four oldest results in the Forrest Zone agree to within uncertainty, with a weighted mean of  $1185 \pm 8$  Ma.

In FOR010, sample GSWA 206752 contains a zircon core dated at 1554 Ma, and three cores in GSWA 206753 yield ages of 1576–1511 Ma; these are older than the c. 1490 Ma mean age of the two Undawidgi Supersuite samples in the same drillcore (Table 1). Sample GSWA 194773 from Eucla 1 also contains a zircon core, dated at 1598 Ma (Kirkland et al., 2011). Although inherited cores are very minor components in the FOR010 and Eucla 1 zircons, sample GSWA 213838 in FOR011 is dominated by zoned cores with dates of 1552–1462 Ma (Table 1), and a mean age of 1488 Ma.

Sample GSWA 213838 is a coarse-grained granite vein that clearly crosscuts the foliation in its c. 1488 Ma Undawidgi Supersuite metagranite host (GSWA 206730). The Undawidgi-age zircon cores in GSWA 213838 are overgrown by c. 1189 Ma zircon rims with Th/U ratios of 0.004 – 0.03. These Th/U ratios are more similar to those in metamorphic zircon rims in some Toolgana and Undawidgi Supersuite samples (see above), whereas the remaining five Moodini Supersuite samples exhibit Th/U ratios in magmatic zircons (i.e. excluding zircon cores) that are highly variable, ranging from 0.02 to 3.4. This variability to very high values is observed also in Moodini Supersuite samples from the Madura Province (0.03 – 3.5). Although Th/U ratios in GSWA 213838 appear to be more consistent with metamorphic rather than magmatic zircon growth, the c. 1189 Ma zircons in this sample are interpreted to date crystallization of the granite vein. Not only does the vein crosscut the foliation in its Undawidgi Supersuite host rock, but similar granite veins also crosscut foliations in rocks assigned to the Moodini Supersuite.

In the Forrest Zone, high-grade metamorphism that involved growth of zircon rims was broadly coeval with Moodini Supersuite magmatism, and occurred at c. 1179 Ma in FOR004, c. 1174 Ma in FOR011, and at 1158–1150 Ma in FOR008 (Table 1).



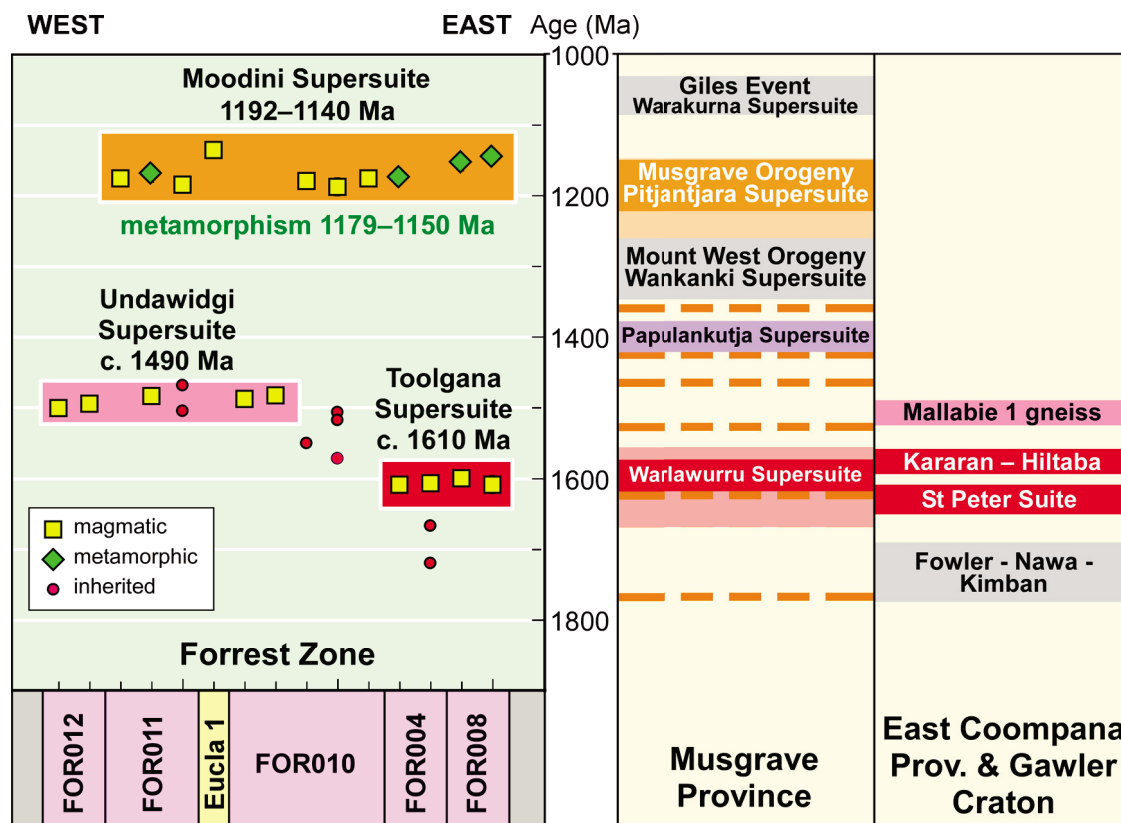


Figure 1. Graphic comparison of U–Pb ages of rock units in the Forrest Zone of the Coompana Province with those of rock units and geological events in the Musgrave Province and the eastern Coompana Province and Gawler Craton. Thick dashed lines represent the ages of the main detrital zircon components in the Ramarama Basin (Evins et al., 2012).

## Comparisons between the Forrest Zone, Madura and Musgrave Provinces, and the western Gawler Craton

A comparison of Madura Province geochronology with results for the eastern Albany–Fraser Orogen and the Moodini Supersuite granite in Forrest Zone drillcore Eucla 1 was made previously by Spaggiari et al. (2012; 2014). The range of Moodini Supersuite ages in the Forrest Zone (1192–1140 Ma) is broadly similar (Fig. 1) to that in the Madura Province (1181–1125 Ma), and to the age range of the Esperance Supersuite (1200–1140 Ma) in the eastern Albany–Fraser Orogen (Spaggiari et al., 2014; c.f. Fig.1 of Wingate et al., this volume). The 1505–1487 Ma age range of the Undawidgi Supersuite is a close match with the  $1478 \pm 4$  Ma age for granitic gneiss in Burkin drillcore BKD2 in the Madura Province (Kirkland et al., 2012; Wingate et al., this volume). Rocks equivalent in age to the 1415–1389 Ma Haig Cave Supersuite of the Madura Province are not known in the Forrest Zone, and equivalents of the c. 1610 Ma Toolgana Supersuite of the Forrest Zone are not known in the Madura Province.

The 1192–1140 Ma ages of Moodini Supersuite granites in the Forrest Zone also correlate with ages of 1220–1150 Ma for the granites of the Pitjantjara Supersuite in the western Musgrave Province (Smithies et al., 2010; Kirkland et al., 2015). However, the 1345–1293 Ma Wankanki Supersuite of the western Musgrave Province is not similar in age to any rocks known in the Madura Province or Forrest Zone, but does correlate with the 1330–1280 Ma Recherche Supersuite of the Albany–Fraser Orogen (Spaggiari et al., 2014). The Papulankutja Supersuite granite of the western Musgrave Province, dated at c. 1400 Ma, is equivalent in age to the 1415–1389 Ma Haig Cave Supersuite of the Madura Province, but has no temporal equivalent in the Forrest Zone, the eastern Coompana Province, or the Gawler Craton. The 1505–1487 Ma age range of the Undawidgi Supersuite overlaps with a date of  $1505 \pm 7$  Ma, interpreted as the age of the granitic protolith, for granitic gneiss in Mallabie 1 in the eastern Coompana Province (Wade et al., 2007). The oldest rocks identified in the Forrest Zone, the c. 1610 Ma Toolgana Supersuite, are similar in age to the newly defined 1615–1575 Ma Warlawurru Supersuite of the western Musgrave Province (Wingate et al., 2015, and references within) and to the 1640–1610 Ma St Peter Suite granites in the western Gawler Craton.

In the South Australian portion of the Musgrave Province, magmatic protolith ages of 1665–1565 Ma have been reported by Jagodinsky and Dutch (2013) for several orthogneiss samples.

## References

- Evins, PM, Kirkland, CL, Wingate, MTD, Smithies, RH, Howard, HM, and Bodorkos, S 2012, Provenance of the 1340–1270 Ma Ramarama Basin in the west Musgrave Province, central Australia: Geological Survey of Western Australia, Report 116, 39p.
- Jagodinsky, EA and Dutch, R 2013, SHRIMP U-Pb geochronology of the Teyon (5645) 1:100 000 mapsheet: Geological Survey of South Australia, Report Book 2013/00006, 223p.
- Kirkland, CL, Smithies, RH, Woodhouse, AJ, Howard, HM, Wingate, MTD, Belousova, EA, Cliff, JB, Murphy, RC and Spaggiari, CV 2012, A multi-isotopic approach to the crustal evolution of the west Musgrave Province, central Australia: Geological Survey of Western Australia, Report 115, 47p.
- Kirkland, CL, Wingate, MTD, Spaggiari, CV and Tyler, IM 2011, 194773: granitic rock, Eucla No. 1 drillhole; Geochronology Record 1001: Geological Survey of Western Australia, 4p.
- Smithies, RH, Howard, HM, Evins, PM, Kirkland, CL, Kelsey, DE, Hand, M, Wingate, MTD, Collins, AS, Belousova, E and Allchurch, S 2010, Geochemistry, geochronology and petrogenesis of Mesoproterozoic felsic rocks in the western Musgrave Province of central Australia and implication for the Mesoproterozoic tectonic evolution of the region: Geological Survey of Western Australia, Report 106, 73p.
- Spaggiari, CV, Kirkland, CL, Smithies, RH and Wingate, MTD 2012, What lies beneath — interpreting the Eucla basement, in GSWA 2012 extended abstracts: promoting the prospectivity of Western Australia: Geological Survey of Western Australia, Record 2012/2, p. 1–2.
- Spaggiari, CV, Kirkland, CL, Smithies, RH and Wingate, MTD 2014, Tectonic links between Proterozoic sedimentary cycles, basin formation and magmatism in the Albany–Fraser Orogen: Geological Survey of Western Australia, Report 133, 63p.
- Wade, BP, Payne, JL, Hand, M and Barovich, KM 2007, Petrogenesis of ca 1.50 Ga granitic gneiss of the Coompana Block: filling the 'magmatic gap' of Mesoproterozoic Australia: Australian Journal of Earth Sciences, v. 54, p. 1089–1102.
- Wingate, MTD, Kirkland, CL, Quentin De Gromard, R, Howard, HM and Smithies, RH 2015, 208455: foliated metasyenogranite, Yulun–Kudara Waterhole; Geochronology Record 1251: Geological Survey of Western Australia, 5p.

# Forrest Zone: geochemistry and petrogenesis

by

RH Smithies, CV Spaggiari, CL Kirkland<sup>1</sup>, MTD Wingate, and RN England<sup>2</sup>

## Introduction

Geochemical data was obtained from all five FOR-prefix stratigraphic drill holes. The rocks ranged in composition from mafic to felsic, in metamorphic grade from greenschist facies (typically the youngest rocks – c. 1180 Ma) to upper amphibolite or granulite facies (typically the oldest, c. 1610 Ma migmatites) and in fabric from massive (igneous-textures) to gneissic or mylonitic. The samples represent the least altered and texturally and lithologically most homogeneous material available, covering the full lithological range encountered in each core. Where sampling of altered material has been unavoidable, geochemical interpretation has been mainly based on variations in typically fluid-immobile elements. In all cases, major element data (e.g. SiO<sub>2</sub> wt%) has been recalculated volatile-free (e.g. aSiO<sub>2</sub> wt%).

Rocks from the five FOR-prefix cores will be discussed mainly in terms of decreasing age rather than by individual hole or geographically, although the age-groups do show a distinct geographical distribution. Table 1 provides a summary of geochemical characteristics and of petrogenetic interpretations.

## c. 1610 Ma rocks from FOR004 and FOR008

### Granites

Both FOR004 and FOR008 contain foliated feldspar-porphyritic granites dated at 1613–1604 Ma which are interleaved with fine- to medium-grained monzodiorite (petrographically quartz–diorite to quartz monzodiorite).

This package has undergone amphibolite to possibly granulite facies metamorphism at 1180–1150 Ma ranging from formation of a gneissic fabric, to incipient melt formation with discrete leucosomes to veins and sheets of leucogranite (though probably not extracted from the level sampled). Inherited zircon is found in FOR004 and this material is c. 1724–1671 Ma in age. All components of these cores show a rather narrow range of relatively juvenile Nd-isotopic compositions ( $\epsilon_{\text{Nd}(1600\text{Ma})} +1.49 - -0.86$ ) (Fig. 1), with the monzodiorite lying in the middle of this range.

The granites are all magnesian and mainly calc-alkalic (terminology of Frost et al., 2001). Those from FOR008 are mainly high-K while those from FOR004 are medium-K at lower silica contents (57–65 wt%) and high-K at higher silica contents (Fig. 2). Granites from FOR008 show an extended silica range from 62.51 to 75.29 wt%. Samples from FOR004 show more compositional scatter than in FOR008 and include a group with lower silica (57.02–61.7 wt%) (texturally transitional with the monzodiorites) and a smaller group with a high and narrow silica range (72.19–72.88 wt%).

Compared with the other FOR-prefix granite groups, the c. 1610 Ma granites typically have low TiO<sub>2</sub>, K<sub>2</sub>O and Na<sub>2</sub>O, low K<sub>2</sub>O/Na<sub>2</sub>O, and high CaO (Fig. 3), with variations typical of normal calc-alkaline granites and similar to other central and southern Australian Proterozoic suites thought to be subduction-related (e.g. c. 1300 Ma Wankanki Supersuite of the Musgrave Province, Smithies et al., 2010). A plot of Zr vs SiO<sub>2</sub> (Fig. 4) contrasts the potentially subduction-related suites (low Zr) from more extreme suites derived through high-temperature crustal melting (see later). The c. 1600 Ma FOR-prefix granites do show considerable scatter in LILE concentrations and are particularly depleted in Ba (Fig. 4). This is probably at least partly attributable to metamorphism, likely involving biotite breakdown (i.e. biotite  $D_{\text{Ba} > \text{Rb, Sr, La}}$  etc.).

The Nd isotopic composition for most of the c. 1610 Ma granites varies only slightly (within ~1.7  $\epsilon$  units) over a wide SiO<sub>2</sub> range (53.6–68.37 wt%) (Fig. 5), becoming less radiogenic with increasing SiO<sub>2</sub>. This suggests progressive contamination (i.e. AFC processes)

1 Centre for Exploration Targeting – Curtin Node, Department of Applied Geology, Curtin University, Bentley WA 6845

2 Petrology Services, Duncraig WA 6023

Table 1. Geochemical characteristics and petrogenetic interpretations of rocks of the Forrest Zone

<i>Drill/sampling site</i>	<i>Rock type</i>	<i>Geochemical characteristics</i>	<i>Age</i>	<i>Formal unit</i>	<i>Tectonic interpretation</i>
FOR008	Granite	Magnesian, alkali-calcic, high-K, weakly peraluminous	c. 1150		Intra-plate low-pressure anatectic melts
FOR004	Granite	Magnesian, calc-alkalic to alkalic, high-K to shoshonitic, weakly peraluminous	1185–1179 Ma		Intra-plate low-pressure anatectic melts
FOR011	Granite	Magnesian, calc-alkalic, low- to medium-K, weakly peraluminous	Undated but <1180 Ma based on cross-cutting relationships		Low- to medium-pressure melting of mafic crust
FOR011	Silica-rich shoshonite (syenogranite)	Magnesian, alkali-calcic to alkali, high-K to shoshonitic, weakly peraluminous	Undated – likely c. 1180 Ma	Moodini Supersuite (Bottle Corner Shoshonite)	Melting of old, previously subduction-enriched, lithosphere
FOR011	Shoshonite		c. 1180 Ma	Moodini Supersuite (Bottle Corner Shoshonite)	Melting of old, previously subduction-enriched, lithosphere
FOR010	Silica-rich shoshonite (syenogranite)	Magnesian, alkali-calcic to alkali, high-K to shoshonitic, mainly weakly peraluminous	1192–1184 Ma	Moodini Supersuite (Bottle Corner Shoshonite)	Melting of old, previously subduction-enriched, lithosphere
FOR010	Shoshonite		c. 1180 Ma	Moodini Supersuite (Bottle Corner Shoshonite)	Melting of old, previously subduction-enriched, lithosphere
FOR010	Granite	Magnesian, alkali, high-K, metaluminous	c. 1487 Ma	Undawidgi Supersuite	Melting of rifted lower mafic crust with mantle input
FOR011	Syenite	Magnesian, alkali, shoshonitic, weakly peraluminous	c. 1488 Ma	Undawidgi Supersuite	Melting strongly metasomatised lower crust
FOR010	Granite	Magnesian, calcic to calc-alkalic, low- to medium-K, mainly weakly peraluminous	c. 1492 Ma	Undawidgi Supersuite	Low- to medium-pressure melting of mafic crust
FOR012	Granite and possible rhyolite	Magnesian to ferroan, alkali-calcic, high-K, metaluminous to peraluminous	1505 – 1499 Ma	Undawidgi Supersuite	Melting of rifted lower mafic crust with mantle input
FOR008	Granite	Magnesian, calc-alkalic, high-K, metaluminous to peraluminous	c. 1604 Ma	Toolgana Supersuite	Primitive arc
FOR008	Monzodiorite	High-K, calc-alkalic	Undated – likely to be c. 1610 Ma	Toolgana Supersuite	Near primary melt of subduction-modified mantle source – primitive arc
FOR004	Monzodiorite	High-K, calc-alkalic	Undated – likely to be c. 1610 Ma	Toolgana Supersuite	Near primary melt of subduction-modified mantle source – primitive arc
FOR011	Monzodiorite and granodiorite	Magnesian, alkali-calcic, high-K, metaluminous	Undated – likely to be c. 1610 Ma	Toolgana Supersuite	Melt of subduction-modified mantle and lower crust – primitive arc
FOR011	High-K gabbro	High-K to shoshonitic	Undated – likely to be c. 1610 Ma	Toolgana Supersuite	Melting of shallow-subduction enriched N-MORB source
FOR004	Granite	Magnesian, calc-alkalic, medium- to high-K, metaluminous to peraluminous	1613 – 1611 Ma	Toolgana Supersuite	Primitive arc

and the presence of older  $\text{SiO}_2$ -rich material (perhaps the 1724–1671 Ma inherited signature), but either the amount of progressive contamination is very small or the contaminant itself is only slightly less radiogenic and/or is mafic. The associated monzodiorites are isotopically similar (Fig. 5) to the main population of c. 1600 Ma granites and are likely to be co-genetic based on mineralogically and texturally transitional contacts and on continuous geochemical trends.

## Monzodiorites

The monzodiorites also show quite a wide scatter of data, probably at least in part due to metamorphism, but are generally quite similar in composition. The most primitive samples from both FOR008 and FOR004 have  $\text{MgO} > 9.0$  wt%,  $\text{Mg}^\# > 65$  (Fig. 3), and Ni concentrations  $> 130$  ppm (up to 187 ppm). Such near primary compositions rule out significant fractionation and contrast with considerable enrichments in incompatible trace elements. These enrichments include high LILE/HFSE ratios (Fig. 6) indicative of a subduction, or crustal, contribution to the bulk source – consistent with Nd-isotopic requirement for a non-radiogenic source component. If this enriched component was added at a crustal level, then it is unlikely to have been the same component producing the AFC trends in the c. 1610 Ma granites. An alternative that is more consistent with the primitive nature of the monzodiorites is that the mantle source itself was contaminated (i.e. subduction enrichment).

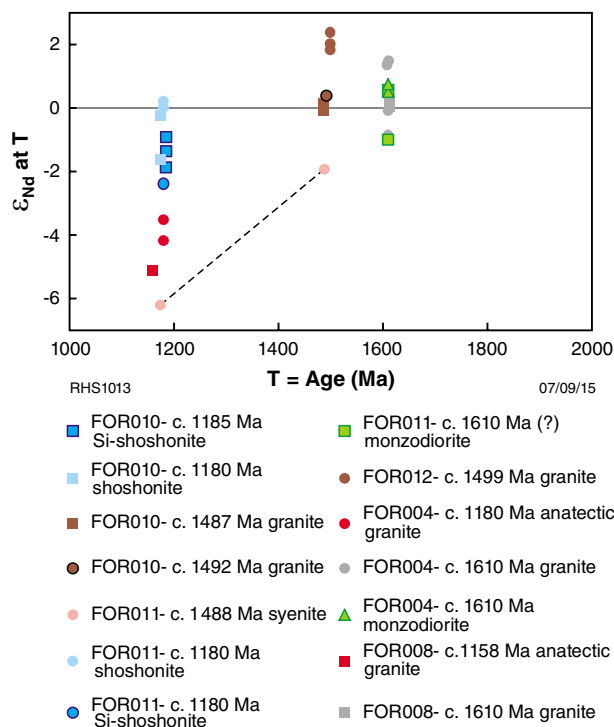


Figure 1. Nd-isotope data for rocks of the Forrest Zone displayed on a  $\epsilon_{\text{Nd}(t)}$  vs age (Ma) diagram.

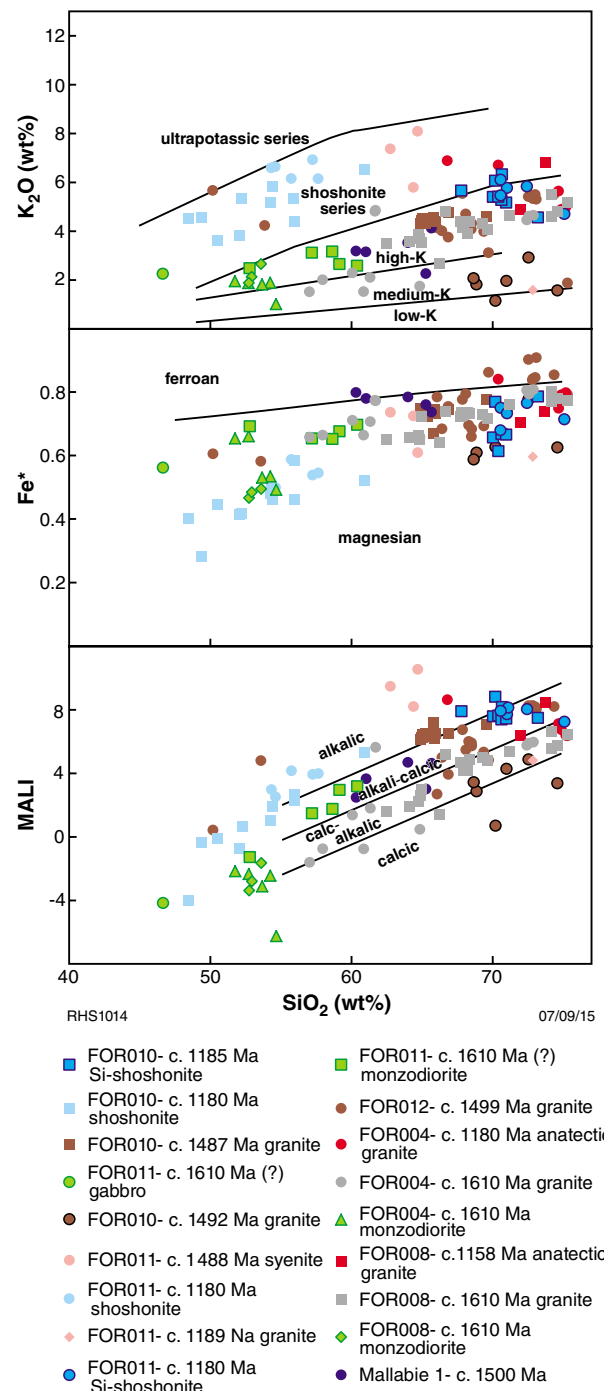
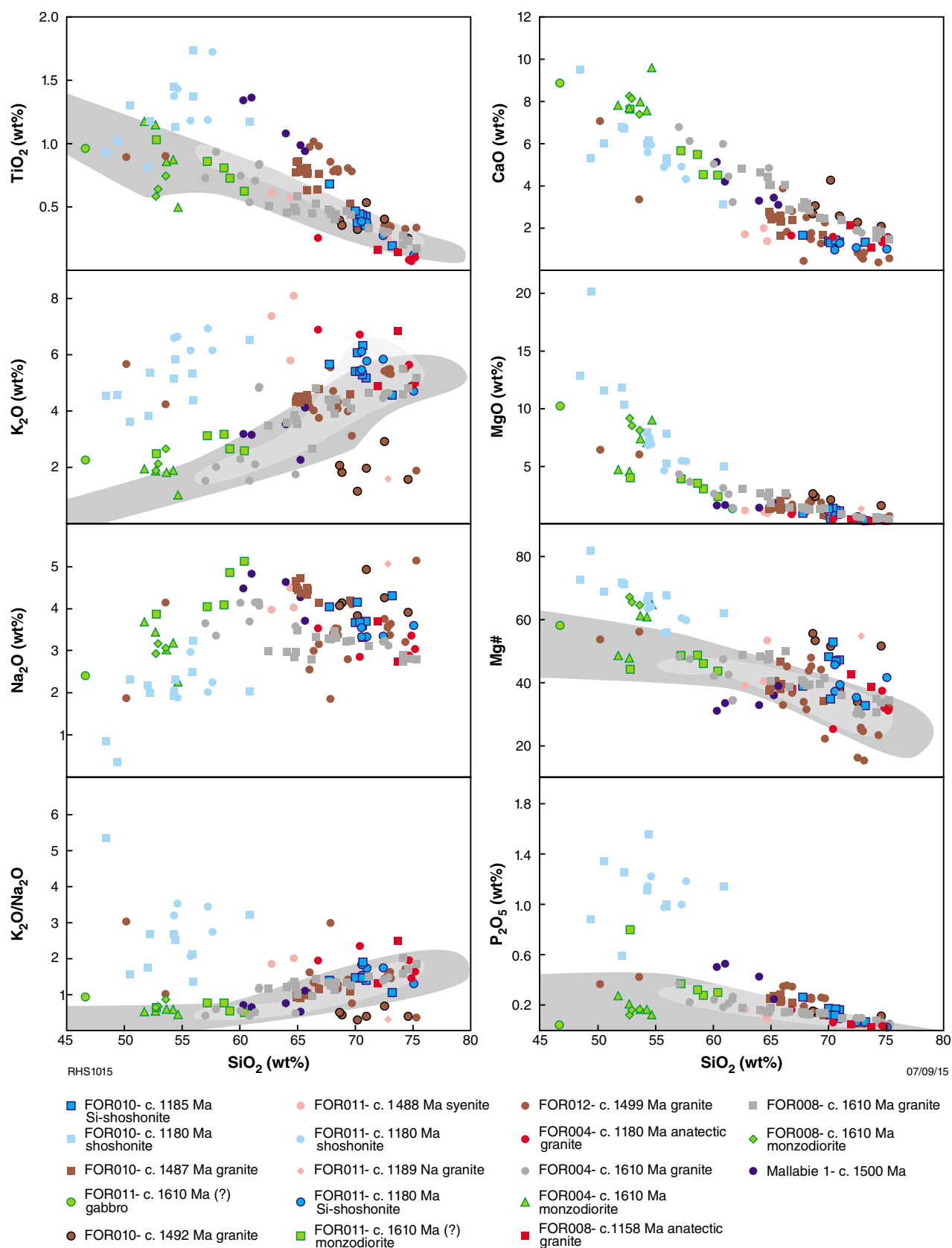
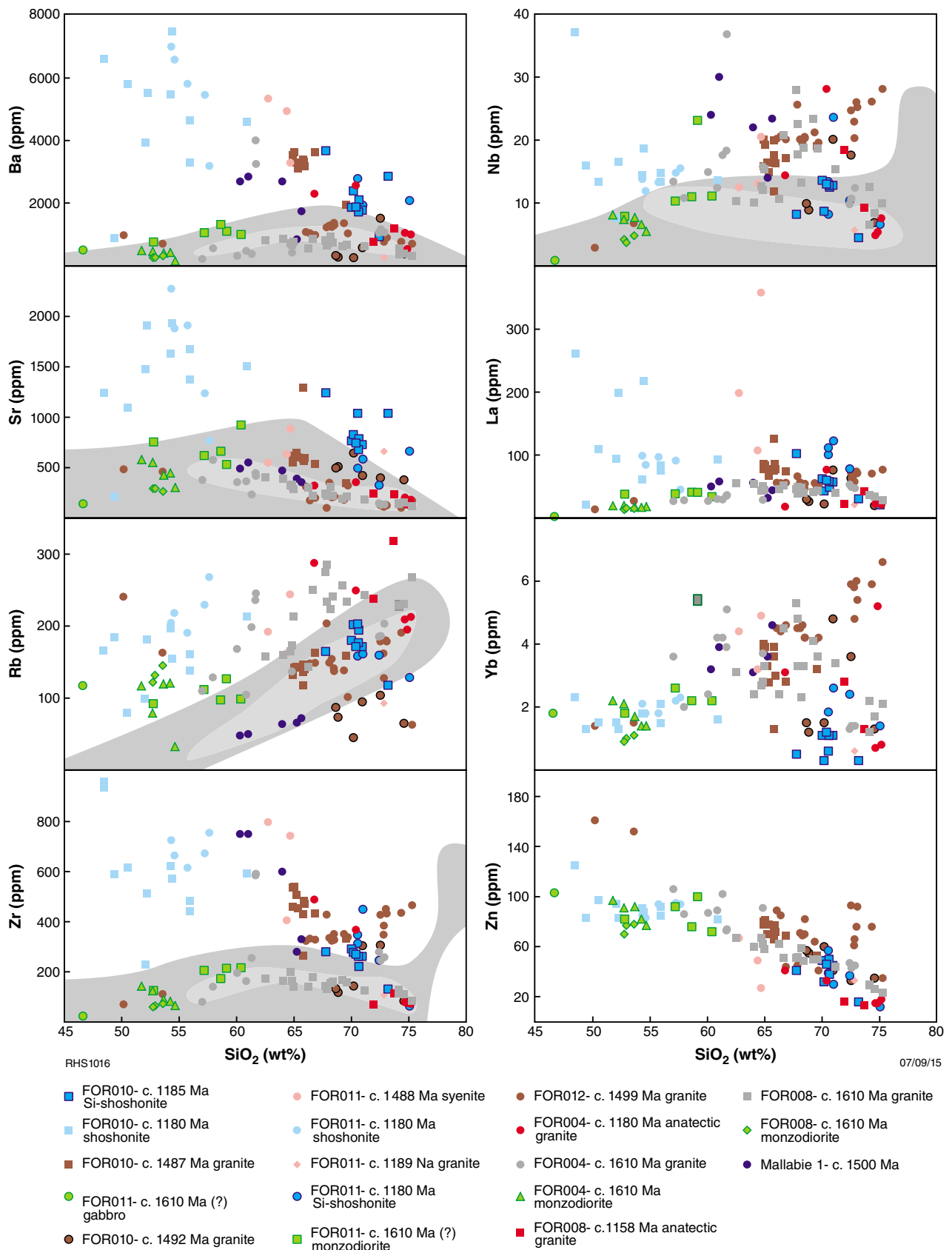


Figure 2. Analyses of Forrest Zone rocks displayed on various classification diagrams;  $\text{K}_2\text{O}$  vs  $\text{SiO}_2$  (after Peccerillo and Taylor, 1976);  $\text{Fe}^*$  ( $= \text{FeO}^\text{T}/(\text{FeO}^\text{T} + \text{MgO})$ ) vs  $\text{SiO}_2$  and MALI ( $= \text{Na}_2\text{O} + \text{K}_2\text{O} - \text{CaO}$ ) vs  $\text{SiO}_2$  (after Frost et al., 2001). Data for Mallabie 1 are from Wade et al. (2007).





**Figure 3.** Major element variation vs SiO<sub>2</sub> for rocks of the Forrest Zone. Also shown for comparison are fields for subduction-related rocks of the c. 1300 Ma Wankanki Supersuite of the Musgrave Province and rocks of the c. 1600–1640 Ma Saint Peters Suite of the Gawler Craton (field for the Saint Peters Suite courtesy D. Champion written comm., 2015).



**Figure 4.** Variation in the concentrations of various trace elements vs  $\text{SiO}_2$  for rocks of the Forrest Zone. Also shown for comparison are fields for subduction-related rocks of the c. 1300 Ma Wankanki Supersuite of the Musgrave Province and rocks of the c. 1600–1640 Ma Saint Peters Suite of the Gawler Craton (field for the Saint Peters Suite courtesy D. Champion written comm., 2015).

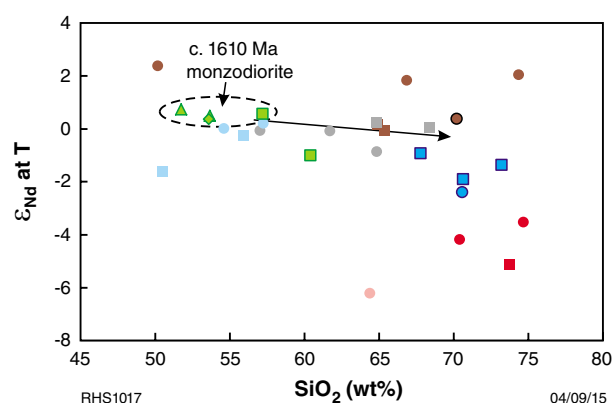


Figure 5.  $\epsilon_{Nd(t)}$  vs  $SiO_2$  diagram for rocks of the Forrest Zone. Symbols as for Fig. 2.

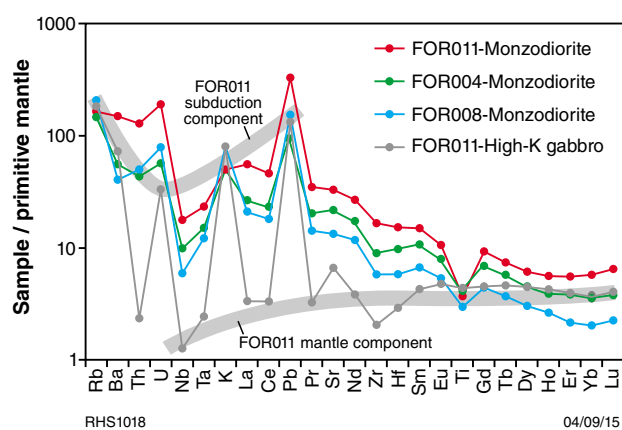


Figure 6. Primitive mantle normalized trace element diagrams for c. 1610 Ma mafic rocks of the Forrest Zone. Normalization factors are from Sun and McDonough (1989).

## Undated rocks in FOR011 likely to be c. 1610 Ma in age

FOR011 contains several mafic units that remain undated radiometrically and that are potentially an ‘early’ component of the drill core based on textural relationships (pre-dates development of the earliest preserved deformation fabrics). In addition, Nd-isotope data from younger granites in FOR011 suggest a c. 1600 Ma mafic crustal basement component (see below).

The first of these is a series of low- $SiO_2$  (52.78 – 60.39 wt%) monzodiorites. These are sodic ( $Na_2O = 3.87 - 5.13$  wt% and  $K_2O/Na_2O < 0.8$ ) (Fig. 3) but also high-K, magnesian and alkali-calcic (Fig. 2) and show close compositional similarities with the c. 1610 Ma primitive monzodiorites from FOR004 and FOR008 (Fig. 6), including equivalent Nd-isotope compositions (data with all of these rocks being isotopically equivalent at 1600 Ma — FOR011;  $\epsilon_{Nd(1600Ma)} +0.46 - -1.11$ ; FOR004 and FOR008  $\epsilon_{Nd(1600Ma)} +0.65 - 0.24$ ).

The second undated mafic component is a high-K gabbro (46.63 wt%  $SiO_2$ , 2.26 wt%  $K_2O$ ) containing 10.22 wt% MgO. With a  $Mg^\#$  of 58 it has undergone a degree of fractionation, although Ni concentration of 295 ppm suggests the rock remains relatively primitive. Mantle-normalised trace element patterns for this sample (Fig. 6) identify a depleted mantle source, but also significant enrichment in fluid-mobile trace elements. No crustal addition is recognised. This pattern strongly resembles arc or fore-arc basalt derived from a previously depleted mantle source re-fertilised with a fluid-mobile (i.e. shallow) subduction component. The fluid-mobile enrichment pattern strongly resembles enrichment patterns in the c. 1610 Ma monzodiorites.

## Summary of c. 1610 Ma units

These rocks have suffered element mobility through high-grade metamorphism (local anatexis) but still preserve compositions that favour a subduction (rather than intra-plate or syn-collisional) origin. Granite and monzodiorite are likely to be co-genetic. The monzodiorite is primitive (almost primary) and its trace element enrichments and un-radiogenic isotopic compositions are more likely to have occurred in the mantle source (mantle wedge or as modified lithosphere) than during intrusion.

## 1510–1480 Ma rocks from FOR012 and FOR010

Material of 1510–1480 Ma age forms the sole magmatic component in FOR012 and both a magmatic and inherited component in FOR010. Dates of c. 1492 and c. 1487 Ma from metagranites in FOR010 relate to two compositionally discrete groups, although the two ages are within uncertainty and the contact relationships suggest the c. 1492 Ma group is actually younger than the c. 1487 Ma group.

The c. 1492 Ma group is silica rich (68.65 – 74.58 wt%), medium-K, calc-alkalic and magnesian (Fig. 2). It typically has amongst the highest MgO,  $Na_2O$  and CaO contents and lowest FeO and  $K_2O$  all of the FOR-prefix granites at a given silica content (Fig. 3). These sodic granites are enriched in Sr (378–645 ppm) and depleted in Pb (mainly <23 ppm) and Rb (<104 ppm) (Fig. 4). Whereas low concentrations of Yb (<1.5 ppm) (Fig. 4) and Y (< 13 ppm) and high La/Yb [ $>15$  (La up to 30 ppm)] and Sr/Y ratios (38–54) (Fig. 7) suggest a broadly adakitic paragenesis. However, the c. 1492 Ma granites rocks have low Dy/Yb and Sr/Y ratios compared with true adakites (such as those from MAD002) and are more indicative of moderate- to low-pressure hornblende fractionation.

The c. 1487 Ma granites from FOR010 have a narrower and lower silica range (mainly 64.89 – 66.86 wt%), are high-K to shoshonitic but remain magnesian (Fig. 2). They are  $TiO_2$ -rich, CaO-poor, have high  $Na_2O$  (4.73 – 4.14 wt%) and  $K_2O/Na_2O$  (~0.9 – 1.1) and are enriched in  $P_2O_5$  over nearly all other FOR-prefix granites except for the c. 1499 Ma granites from FOR012 (Fig. 3).

They have high Ba, Sr and Pb concentrations but are relatively depleted in Rb, and show weak to moderate enrichments in Nd and Ta and strong enrichments in Zr, Hf and REE (Fig. 4). Overall, they show A-type characteristics (including high Ga and Zn) but are distinct in that they remain magnesian.

The c. 1492 and 1487 Ma granites are isotopically similar and their isotopic composition could result through reworking of c. 1600 Ma crust, similar to that found in FOR004, FOR008, and FOR011. If an A-type petrogenetic interpretation is correct, a lack of c. 1600 Ma zircon inheritance in the c. 1487 Ma granites might be related to high melting temperatures. Alternatively, the melting source might have been at the zircon-poor mafic end of the c. 1600 Ma material (or its source!).

The c. 1499 Ma rocks that form FOR012 include strongly deformed, fine-grained rocks in the lower section of the core that might be volcanic or volcanoclastic in origin. Several of these are strongly depleted in alkalis (particularly in the silica range from 66–70 wt%) and are peraluminous — probably as a result of alteration. The c. 1499 Ma rocks share many compositional features with the c. 1487 Ma granites from FOR010, but they are slightly less alkali (mainly alkali-calcic), are high-K (rather than ‘shoshonitic’), and trend to more ferroan compositions at silica above 70 wt% (Fig. 2). They show significant enrichments (over most other FOR-prefix rocks) in HFSE and REE (particularly HREE) (Fig. 4) and have A-type granite compositions. Extended trace element trends, high trace element concentrations, significant Sr and Eu anomalies suggest these rocks are more fractionated than those of the c. 1487 Ma granites. Nd-isotopic compositions also indicate a greater juvenile component ( $\epsilon_{\text{Nd}(1500\text{Ma})} +0.82 - 1.51$  c.f.  $-0.95$  for the c. 1487 Ma rocks) (Fig. 1). Whereas the c. 1492 and 1487 Ma rocks could be a result of remelting c.1600 Ma crust (or its source), formation of the c. 1499 Ma rocks would require the addition of a more radiogenic component (e.g. mantle) — consistent with their more ferroan, A-type compositions.

Both the c. 1499 and 1487 Ma rocks show similarities to c. 1500 Ma granites sampled from the Mallabie drill core in the Coompana Province of South Australia (Wade et al., 2007) (Figs. 2–4). These are also isotopically primitive ( $\epsilon_{\text{Nd}(1500\text{Ma})} +1.2 - 3.3$ ) marginally ‘A-type’ in composition and straddle the ferroan/magnesian boundary.

The A-type signature of the c. 1500 Ma FOR-Mallabie granites is interesting given the large proportions of magnesian compositions — and suggests a strongly magnesian and likely oxidised and hydrated crustal source. It is very difficult to interpret these compositions without additional information (e.g. structural data etc.) but we have three instances of similarly aged rocks with similar compositional features that distinguish them from other magma compositions including typical subduction compositions. In many respects these resemble post-collisional granites, with the more magnesian compositions (of the c. 1487 Ma rocks in particular) perhaps correlating with their more crustal isotopic compositions. It is inviting to suggest that these rocks formed through high temperature melting of juvenile mafic arc-related crust during extensional collapse.

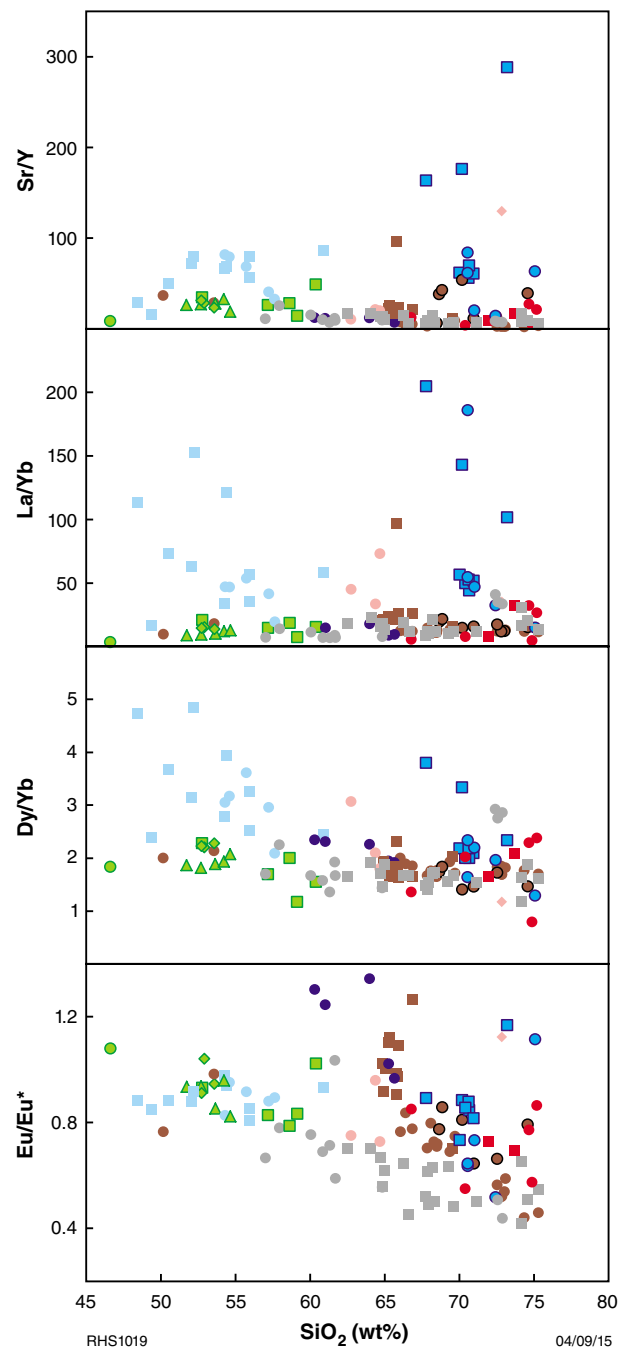


**Figure 7.** Ratios of various incompatible trace elements against  $\text{SiO}_2$  for rocks of the Forrest Zone. Symbols as for Fig. 2.

## A c. 1488 Ma component in FOR011

FOR011 includes a small group of alkali-rich syenites and leucosyenogranites. One of these contains two distinct zircon age populations; rims dated at  $1174 \pm 12$  Ma, and cores dated at  $1488 \pm 4$  Ma. Younger rims have very low Th/U ratios and comprise only 12% of the dated zircon population. If the c. 1174 Ma age is interpreted to represent the age of igneous crystallization, the overwhelming dominance of the c. 1488 Ma zircon age component (which could be interpreted as inheritance) suggests felsic crust of that age was the main Zr-contributing component of the melting source. Irrespective of how the age data are interpreted, it appears likely that c. 1488 Ma crust was quite proximal, if not a significant component of FOR011.

The syenites have a narrow silica range (62.75 – 64.68 wt%) but with very high  $K_2O$  (5.80 – 8.09 wt%), high  $Na_2O$  (3.98 – 4.50 wt%) and low CaO (Fig. 3). They are magnesian and ‘alkaline’, lying at the upper end on the ‘shoshonite’ field near the ultrapotassic series (Fig. 2). They are strongly enriched in Ba (and to a lesser degree Sr, Rb and Pb), LREE ( $> MREE > HREE$ ) and Zr and Hf, but don’t show significant enrichments in Nb, Ta, Y, Ga or Zn expected of typical A-type magmas (Fig. 4). Their non-radiogenic Nd ( $\epsilon_{Nd(1500Ma)} -1.87$ ;  $\epsilon_{Nd(1200Ma)} -5.86$ ) require a dominantly ‘crustal’ origin — possibly strongly metasomatised crust. Whereas c. 1488 Ma crust is the main source of Zr, the non-radiogenic Nd-isotope composition is not consistent with derivation from known c. 1500 Ma sources (which are too radiogenic) (Fig. 8). However, it is consistent with derivation from c. 1610 Ma crust. Although no inherited zircons of that age are found in the syenite, it is possible that the source was c. 1610 Ma mafic crust (monzodiorite?). Thus, possible scenarios for these rocks are c. 1610 Ma mafic crust strongly alkali-metasomatised and partially melted at c. 1488 Ma, and then either remelted and remobilised, or simply recrystallised, at c. 1174 Ma. Although strongly alkali-rich, these syenites are not quite peralkaline. Their relatively low Nb (Ta) and Y concentrations distinguish them from typical sodic A-type felsic rocks often associated with alkali-magmatism in rift settings, but this could be a reflection of a particularly juvenile (and Nb, Ta etc – depleted) subduction-related crustal source component, and it is interesting that the syenites do show strong enrichments in Zr and LREE (Fig. 4).

## 1192–1150 Ma rocks

Rocks with ages within this range occur in FOR004, FOR008, FOR010 and FOR011. Nd-isotope data immediately distinguish two groups (Fig. 1): 1) evolved (un-radiogenic) samples from FOR004, FOR008 and FOR011; 2) primitive samples from FOR010 and FOR011. The isotopically primitive group can be broadly grouped into a ‘shoshonite’ series. Ages from the un-radiogenic group reflect either crustal melting or metamorphic resetting.

## 1192–1150 Ma crustal melting or metamorphic resetting

A granite vein (sample 213838 – no Nd-isotope data) cross cuts all other lithological and structural components in FOR011. This is a sodic (5.07 wt%  $Na_2O$ ) high-silica (72.85 wt%  $SiO_2$ ) granite with low  $K_2O$  (1.59 wt%), high Sr (661 ppm), Sr/Y (129) and La/Yb (35), and low Y (5.1 ppm) and Yb (0.6 ppm) (Figs. 2–4, 7) strongly reminiscent of adakite. However, it has amongst the lowest Dy/Yb of all FOR-prefix rocks (Fig. 7), reflecting a strong hornblende rather than garnet control. It is likely a low- to moderate-pressure melt of mafic basement (arguments presented above would point to a c. 1600–1500 Ma crustal source).

Schlieric leucogranites in FOR004 form a distinct geochemical group — one sample has zircon grains and rims dated at  $1179 \pm 10$  Ma. This is interpreted as the age of in-situ leucosome development in the c. 1613 Ma host. These leucogranites are silica-rich ( $>66$  wt% and most  $\sim 75$ ), have low  $TiO_2$ , FeO, MgO (even for a given silica content), CaO, have similar  $Na_2O$  to the host but are enriched in  $K_2O$ , Ba, and Rb (but not Sr or Pb) (Figs. 2–4). The lack of Sr- and Pb-enrichment and the distinctly un-radiogenic Nd isotope compositions ( $\epsilon_{Nd(1200Ma)} -4.56$  –  $-3.28$ ) clearly distinguish these rocks from the silica-rich members of the shoshonite series (see below). At c. 1200 Ma the leucogranites are isotopically equivalent to c. 1600–1500 Ma crust. Similarly, two leucogranites in FOR008 are migmatitic melts of the c. 1600 Ma host, formed between c. 1158 and 1150 Ma (Fig. 9).

## Shoshonite series intrusions

These form a major component (up to 25%) of both FOR010 and FOR011 and can be broadly divided into mafic samples ( $SiO_2$  48.45 – 60.87 wt%) and felsic samples ( $SiO_2$  67.78 – 75.08 wt%), each type occurring in both cores.

The mafic group (Figs. 2–4) typically has between 5.0 and 10.0 wt% MgO but up to 20.18 wt% (aMgO with LOI of 2.18 wt%). Corresponding  $Mg^\#$  are mainly  $> 66$  and up to 82 in FOR010 and between 56 and 65 in FOR011, with high Ni (1019–80 ppm in FOR010; 181–71 ppm in FOR011) and Cr (987–93 ppm in FOR010; 216–60 ppm in FOR011). Mafic shoshonites from FOR011 typically overlap the less primitive end of the range for the mafic shoshonites from FOR010. The mafic shoshonites lie within the upper part of the ‘shoshonite series’ field in the  $K_2O$  vs  $SiO_2$  diagram of Peccerillo and Taylor (1976) although none cross into the ultrapotassic field (Fig. 2). They are strongly enriched in  $TiO_2$ ,  $P_2O_5$ , LILE (particularly Ba and Sr), Zr, Hf, (to a lesser extent Nb, Ta) Th, U, and L-MREE but are depleted (or at least not enriched) in HREE, with correspondingly high La/Yb ratios. Their Dy/Yb ratios are high but decrease rapidly with increasing silica suggesting a strong role for hornblende fractionation, but Eu/Eu\* remain constant at  $\sim 1.0$  – 0.8 (Fig. 7), suggesting either relatively oxidized (and wet?) conditions or no feldspar fractionation — or



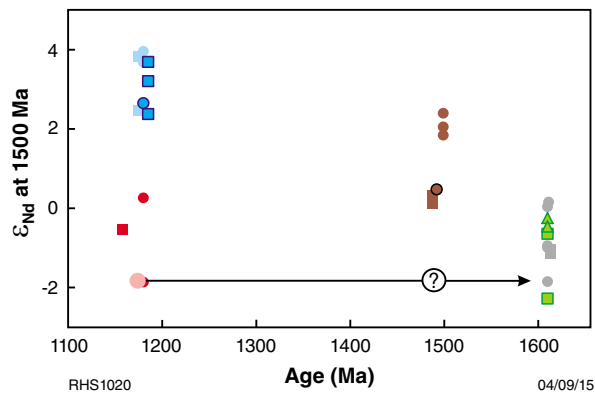


**Figure 8.**  $\epsilon_{\text{Nd}}(1500 \text{ Ma})$  vs  $\text{SiO}_2$  diagram for rocks of the Forrest Zone. Symbols as for Fig. 2.

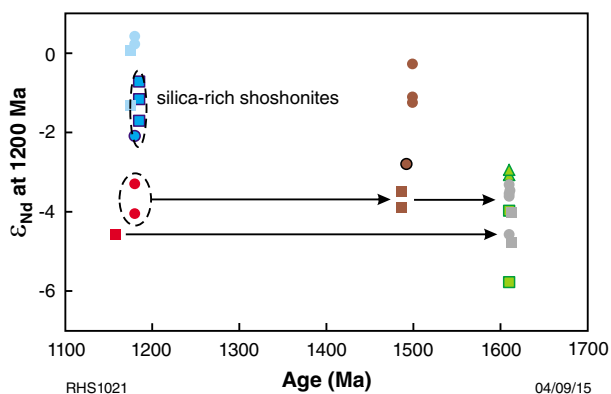


**Figure 9.**  $\epsilon_{\text{Nd}}(1200 \text{ Ma})$  vs  $\text{SiO}_2$  diagram for rocks of the Forrest Zone. Symbols as for Fig. 2.

all of these. The high  $\text{La/Yb}$ ,  $\text{Dy/Yb}$ ,  $\text{Sr/Yb}$  ratios and low Yb support a deep melting source with residual garnet, but not plagioclase. The evidence for wet and oxidised magmatism favours a garnet amphibolite source rather than an eclogite.

Scattered, to decreasing,  $\text{La/Nb}$  and  $\text{Th/Nb}$  with increasing silica or decreasing  $\text{Mg}^\#$  (Fig. 10) are inconsistent with a direct crustal contribution (e.g. AFC) to the mafic shoshonites. Models for shoshonite petrogenesis typically emphasize post-orogenic extensional melting of subduction-modified lithosphere as a resulting of upwelling asthenosphere. The extent to which the asthenosphere supplies material (melt), or just heat, is unclear. Nd isotope data for the FOR-prefix shoshonites appears to require a source component slightly more radiogenic than any sampled FOR-prefix material at c. 1200 Ma (Fig. 9), and slightly more radiogenic than bulk-earth — i.e. likely an asthenospheric component. Nevertheless, any asthenospheric material contribution is likely to have been greatly exceeded by melting of a less radiogenic mafic lithospheric melt component, candidates for which include the source of subduction-derived c. 1600 Ma monzodiorite.

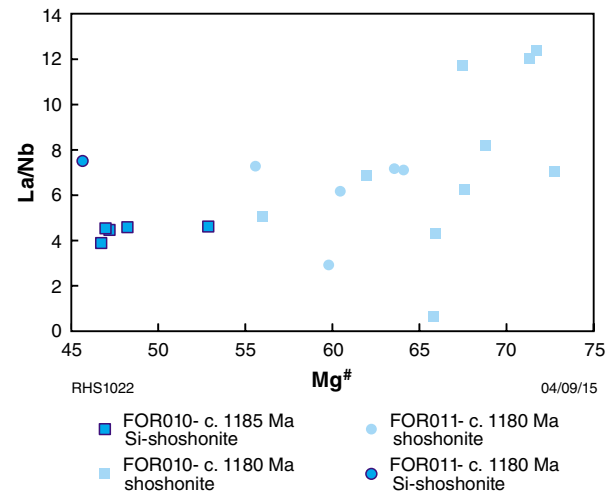


**Figure 10.**  $\text{La/Nb}$  vs  $\text{Mg}^\#$  diagram showing variation in shoshonites of the Bottle Corner Suite. Symbols as for Fig. 2.

Mafic shoshonite also forms a minor component of the Loongana core in the Madura Province where it cuts c. 1400 Ma rocks. Compared with the FOR-prefix mafic shoshonites, the MAD-prefix shoshonites are less enriched in  $\text{TiO}_2$  and  $\text{P}_2\text{O}_5$  and in the range of typically incompatible trace elements, except the HREE (Fig. 11). The lower  $\text{La/Yb}$ ,  $\text{Dy/Yb}$  and  $\text{Sr/Y}$  (36 c.f. 65) associated with the MAD-prefix shoshonite possibly indicate derivation from thinner crust and the different trace element concentrations (at equivalent  $\text{MgO}$  and  $\text{Mg}^\#$ ) reflect a less subduction-modified source.

The more felsic rocks of the shoshonite group show slight enrichments in  $\text{TiO}_2$  and  $\text{P}_2\text{O}_5$  compared with all other FOR-prefix granites (except those with A-type affinity) at similar silica levels, have higher  $\text{Mg}^\#$  (53–33) than most FOR-prefix granites, are distinctly magnesian and alkali-calcic to alkali and straddle the shoshonite series – high-K boundary (Fig. 2). Compared to other FOR-prefix granites at similar silica, the felsic shoshonites are also enriched in LILE (except Rb), Zr and Hf (but not Nb and Ta) and LREE (but not HREE) and hence show the same enrichment patterns as the mafic shoshonites. The less radiogenic Nd isotope compositions of the felsic shoshonites (Fig. 9) are consistent with the presence of inherited zircons, but there is no clear correlation between  $\text{SiO}_2$  and  $\epsilon_{\text{Nd}}$  that would indicate significant contamination or AFC style processes.

## Summary of Forrest Zone geochemistry and some preliminary tectonic interpretations

Magmatism at c. 1610 Ma included co-genetic suites that cover an extended silica range. The mafic end-members are monzodiorite with compositions in equilibrium with

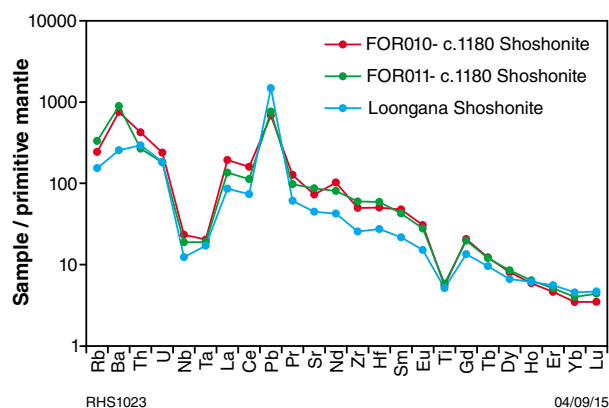


**Figure 11. Primitive mantle normalized trace element diagrams comparing shoshonites of the Forrest Zone with rare shoshonite from the Madura Province. Normalization factors are from Sun and McDonough (1989).**

mantle peridotite and with trace element enrichments unlikely to reflect contamination in the crust. Thus, the c. 1610 Ma rocks are most likely subduction-related. Rare zircon inheritance suggests the age of the crust they intrude was c. 1724–1671 Ma (or older if it was mafic and contained no zircon), but probably no older than c. 1950 Ma based on depleted mantle model ages. It was also isotopically juvenile. Isotopic and zircon-age data require that c. 1610 Ma basement occurs throughout the entire sampled portion of the Forrest Zone. Geochemical and isotopic similarities with the Saint Peters Suite, along the southern and western edge of the Gawler Craton, permit the interpretation of a much more regionally extensive primitive arc-related suite.

Most units dated at c. 1500 Ma, including rocks from Mallabie 1 in the Coompana Province of South Australia (Wade et al., 2007), are transitional A-type felsic rocks with a crustal source component that was primitive, MgO-rich, and likely hydrated and oxidized (potentially c. 1610 Ma monzodioritic crust), and a mantle component comprising upwelled asthenosphere. These rocks reflect extension of the 1724–1610 Ma (to 1950 Ma) arc-complex.

Magmatism during the 1192–1150 Ma period is diverse, ranging from in-situ anatectic melting of basement to the southeast (FOR004, FOR008) to higher degree melting and melt migration of sodic granites in the northwestern part of the sampled region (FOR010, FOR011). Also in the northwestern part, extensive partial melting of lithosphere, significantly enriched during formation of the c. 1724–1610 Ma (or older) arc complex, resulted in voluminous mafic – felsic shoshonitic magmatism. This likely also reflects extensional destabilization of the lithosphere and asthenospheric upwelling, and the thermally anomalous period relates directly with processes occurring in the Madura Province and in the Albany–Fraser Orogen and Musgrave Province.

## Comparisons between the Madura Province and the Forrest Zone.

Both the Madura Province and the Forrest Zone are isotopically identical pieces of crust which, at c. 1.95 Ga were essentially entirely juvenile. Geochemical, and Hf- and Nd-isotopic data indicate that juvenile, depleted mantle material was periodically added (e.g. at c. 1600, 1500, 1400, 1200 Ma). However, the compositional evolution does not require the addition or contribution from older, non-radiogenic sources, and the only physical evidence for such material is in the form of rare inherited zircons, mainly in samples from regions presently proximal to major tectonic boundaries (e.g. the Rodona Shear Zone). In all of these regards, the Madura Province and the Forrest Zone are indistinguishable from the Musgrave Province, to the northeast. However, whereas the Forrest Zone and Madura Province potentially formed from the same piece of crust, they are lithologically and geochemically very different (Fig. 12), reflecting a very different history.

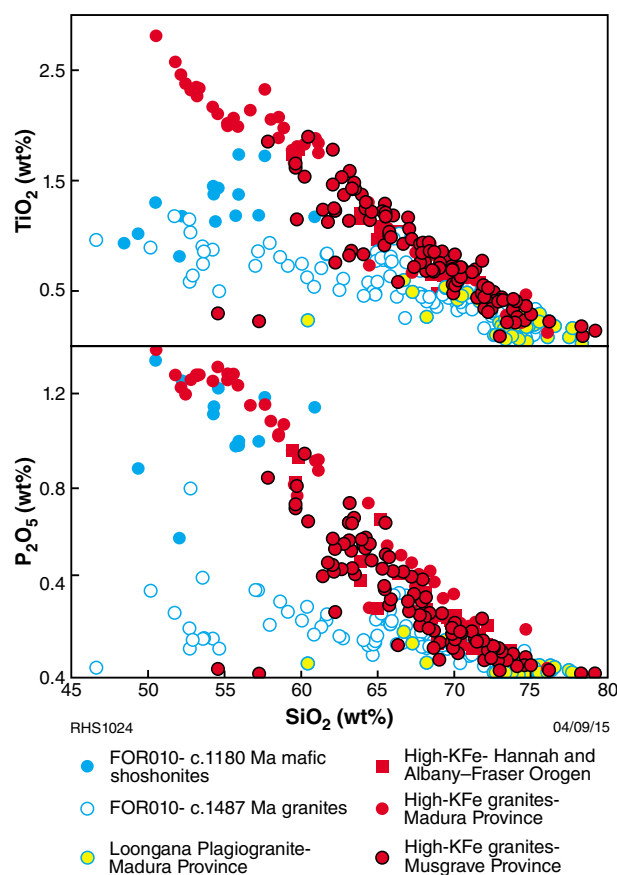


**Figure 12.  $\text{TiO}_2$  and  $\text{P}_2\text{O}_5$  vs  $\text{SiO}_2$  variation diagram comparing rocks of the Forrest Zone with high-KFe series rocks from the Madura Province, Musgrave Province and the Albany–Fraser Orogen.**

The Forrest Province underwent early and probably multi-phased subduction recycling, potentially starting at 1720 Ma (or older) and extending to at least c. 1610 Ma, and synchronous with juvenile magmatism along the southwestern Gawler Craton. A notable feature of nearly all FOR-prefix magmatism, irrespective of age, are the magnesian and very-likely subduction-related (or recycled subduction-related material) compositions. Nowhere in the Forrest Zone do we find the equivalents of the MAD-prefix high-KFe rocks at any age. There is little evidence of magmatic activity from c. 1500 Ma to 1192 Ma. Magmatism at c. 1192 Ma is shoshonitic and represents deep melting of earlier subduction-metasomatism lithosphere. Hence, the Forrest Zone underwent early subduction/accretion and then developed and retained thick lithosphere.

In contrast with the Forrest Zone, the Madura Province records very little magmatic activity between 1950 and c. 1400 Ma. It remains oceanic to oceanic-arc — like in nature, and generally more 'tholeiitic' until a very late-stage, when, at c. 1400 Ma it undergoes subduction reworking prior to accretion to the eastern Nornalup Zone. The lithosphere either remains thin or is removed at c. 1180 Ma, so a 'tholeiitic' asthenospheric component plays a much greater role in c. 1180 Ma magmatism — which is high-KFe rather than high-KMg.

## References

- Frost, BR, Barnes, CG, Collins, WJ, Arculus, RJ, Ellis, DJ and Frost, CD 2001, Ageochemical classification for granitic rocks: *Journal of Petrology*, v. 42, p. 2033–2048.
- Peccerillo, A, and Taylor, SR, 1976, Geochemistry of Eocene calc-alkaline volcanic rocks from the Kastamonu area, Northern Turkey: *Contribution to Mineralogy and Petrology*, v. 58, p. 63–81.
- Smithies, RH, Howard, HM, Evins, PM, Kirkland, CL, Kelsey, DE, Hand, M, Wingate, MTD, Collins, AS and Belousova, E 2011, High-temperature granite magmatism, crust–mantle interaction and the Mesoproterozoic intracontinental evolution of the Musgrave Province, central Australia: *Journal of Petrology*, v. 52(5), p. 931–958.
- Sun, S-S and McDonough, WF 1989, Chemical and isotopic systematics of oceanic basalts: implications for mantle compositions and processes, *in* *Magmatism in the Ocean Basins* edited by AD Saunders and MJ Norry: Geological Society, London, Special Publication 42, p. 313–345.
- Wade, BP, Payne, JL, Hand, M, and Barovich, KM, 2007, Petrogenesis of ca 1.50 Ga granitic gneiss of the Coompana Block: filling the 'magmatic gap' of Mesoproterozoic Australia: *Australian Journal of Earth Science*, v. 54, p. 1089–1102.

# Forrest Zone: isotopes and crustal evolution

by

CL Kirkland<sup>1</sup>, RH Smithies, CV Spaggiari, and MTD Wingate

Time-constrained isotopic datasets permit the evaluation of tectonic processes, including continental collision, rifting, and the origins of crustal blocks by addressing important questions such as: when was material added to the crust, how did it get there — juvenile addition from the mantle or reworking of older crust, and what was the likely geodynamic environment? Hf behaves incompatibly and as a result is enriched in the continental crust with crustal  $^{176}\text{Lu}/^{177}\text{Hf}$  values typically ranging from c. 0.008 to 0.025. Evolution arrays normally assume an average bulk crustal composition of  $^{176}\text{Lu}/^{177}\text{Hf} = 0.015$ , implying a single source repeatedly tapped during magmatism (crustal reworking). However in many cases evolution arrays are better interpreted as being influenced by mixing processes as additional juvenile (depleted mantle, DM) input is frequently necessary as the thermal impetus for magmatism. The form of such mixing processes can lead to ranges of  $^{176}\text{Lu}/^{177}\text{Hf}$  ratios that are distinctive for a specific geodynamic setting.

The Forrest Zone is currently defined as the basement east of the Mundrabilla Shear Zone, and as part of the Coompana Province that extends into South Australia. Magmatic rocks in this zone indicate crystallization ages of principally c. 1610 Ma (granitic gneiss), c. 1500 Ma (metagranites), and c. 1180 Ma (metagranite and shoshonite). As with the Musgrave Province of Central Australia the apparent isotopic evolution array of the Forrest Zone lie on an intermediate composition slope extrapolating back to depleted mantle values at c. 1950 Ma. However, this is not just a simple reworking process in that new DM input is also demonstrated at various points in its geological evolution, especially at c. 1180 Ma. The observed dataset implies a mixing array localised around a  $^{176}\text{Lu}/^{177}\text{Hf}$  ratio of 0.018 with scatter to higher  $^{176}\text{Lu}/^{177}\text{Hf}$ .

The  $^{176}\text{Lu}/^{177}\text{Hf}$  profile of specific geodynamic environments is highly distinctive. For example, convergent margins peak at about 0.018, rifted continents at about 0.02, back-arcs at > 0.02, and old oceanic crust at about 0.03. The Kerguelen Plateau, in the southern Indian Ocean, has a similar  $^{176}\text{Lu}/^{177}\text{Hf}$  profile to the Forrest Zone with a peak at about 0.018 and scatter to higher (more mafic)  $^{176}\text{Lu}/^{177}\text{Hf}$ . The Kerguelen Plateau is interpreted to reflect hot spot magmatism in oceanic crust, including rifted continental elements, with intrusive thickening of oceanic crust leading to internal differentiation of the mafic crust. Elements of the geological evolution of the Kerguelen Plateau appear to share similarities to the processes recorded by isotope geochemistry in the Madura Province, Musgrave Province, and Forrest Zone. A fundamental observation on the Forrest and Madura isotopic datasets is the general lack of evidence for old evolved crust. Instead, magmatism has repeatedly tapped new DM along with reworking of young crust formed through slightly older DM-tapping events commencing at c. 1950 Ma. Magmatism within the c. 1950–1900 Ma time interval is globally significant in terms of juvenile magmatism. However, in an Australian context igneous rocks of this age are very rare and the legacy of this period is retained mainly in cryptic isotopic trends of the northern Gawler margin, Musgrave and Rudall Provinces, and in the basement to the Eucla and Bight Basins.

---

<sup>1</sup> Centre for Exploration Targeting – Curtin Node, Department of Applied Geology, Curtin University, Bentley WA 6845

# Eucla basement results: implications for geodynamics and mineral prospectivity

by

CV Spaggiari, RH Smithies, CL Kirkland<sup>1</sup>, RN England<sup>2</sup>, SA Occhipinti<sup>3</sup>, and MTD Wingate

## Introduction

In this contribution we integrate the available data and interpretations from the cores, and speculate on potential geodynamic settings. We also look at the alteration footprints, their potential relevance to prospectivity, and significance in terms of the geodynamics. We address how the results and knowledge gained improves our understanding of the evolution of the Albany–Fraser Orogen, and potential links to the Gawler Craton. We do this by presenting a series of interpretations of the geodynamics in broad time slices, from oldest to youngest.

None of the stratigraphic cores were drilled as economic targets, yet although sparsely distributed, all cores contain sulfides — most commonly pyrite and chalcopyrite with Cu values up to 2146 ppm in MAD002 and 1172 ppm in FOR012 — and all have alteration features. Magnetite altered to hematite, and pink to reddish colouration of the metagranites is a common feature in the Forrest Zone.

## 2000–1600 Ma

This period marks major crustal evolution in the Albany–Fraser Orogen by modification of the Yilgarn Craton and its continental crust. This took place during formation of the Barren Basin accompanied by voluminous, dominantly felsic magmatism, in either a continental rift or back-arc setting (Fig. 1; Spaggiari et al., 2015; Smithies et al., 2015). The period also encompasses much of the formation of the Gawler Craton post the Sleaford Orogeny, including the Kararan and Kimban Orogenies (e.g. Betts and Giles, 2006).

In contrast, in both the Madura Province and the Forrest Zone, geochemical and isotopic data point to a common, juvenile crustal basement. A primitive isotopic array, anchored at depleted mantle at 2.0–1.9 Ga, is interpreted to reflect a complex mix of new and progressively reworked oceanic-plate magmas, and is inferred to also include the basement to the Musgrave Province (Kirkland et al., 2015).

In the Albany–Fraser Orogen, the end of the Biranup Orogeny at c. 1600 Ma is interpreted to record a transition to quiescence and formation of a passive margin setting. It is suggested that as the Barren Basin evolved, from at least 1800 Ma, an ocean-continent transition (OCT) was formed that extended from the eastern Nornalup Zone through to, and probably including, the Madura Province (Spaggiari et al., 2014a, 2015). The production of E-MORB/OIB (undated basalts in MAD002 and NSD) proto-oceanic crust in the Madura Province is interpreted as associated with this OCT phase, probably around 1600 Ma, during lithospheric extension on the continent edge. It is suggested that extension and juvenile crust formation were the dominant processes from 1600 Ma (or earlier) to c. 1450 Ma, and at least in the early stages tapped deep-mantle melting sources. High Ti/Yb ratios in the most primitive basalts from MAD002 confirm melting of a deep (>2.8 GPa = > 100 km) garnet-bearing mantle source. In the later stages, however, it appears that juvenile crustal additions were primarily from a source similar to that from N-MORB.

The E-MORB/OIB basaltic crust, and potential overlying sedimentary rocks, could be considered prospective for VMS-style mineralisation or exhalative deposits. The disseminated sulfides (pyrite, variably pyritised pyrrhotite, and chalcopyrite) and high Cu values (GSWA 206770, 2146 ppm) in the MAD002 basalt could be indicative of such prospectivity, although it is not clear whether the sulfides were introduced later during intrusion of the adakite at c. 1389 Ma, which also contains sulfides, or were remobilised during intrusion.

In MAD002 mineralisation consisting of chalcopyrite, pyrite and magnetite is also associated with plagioclase-rich, quartz-rich, and epidote-rich veins that were present

1 Centre for Exploration Targeting – Curtin Node, Department of Applied Geology, Curtin University, Bentley WA 6845

2 Petrology Services, Duncraig, WA 6023

3 Centre for Exploration Targeting, University of Western Australia, Crawley WA 6009



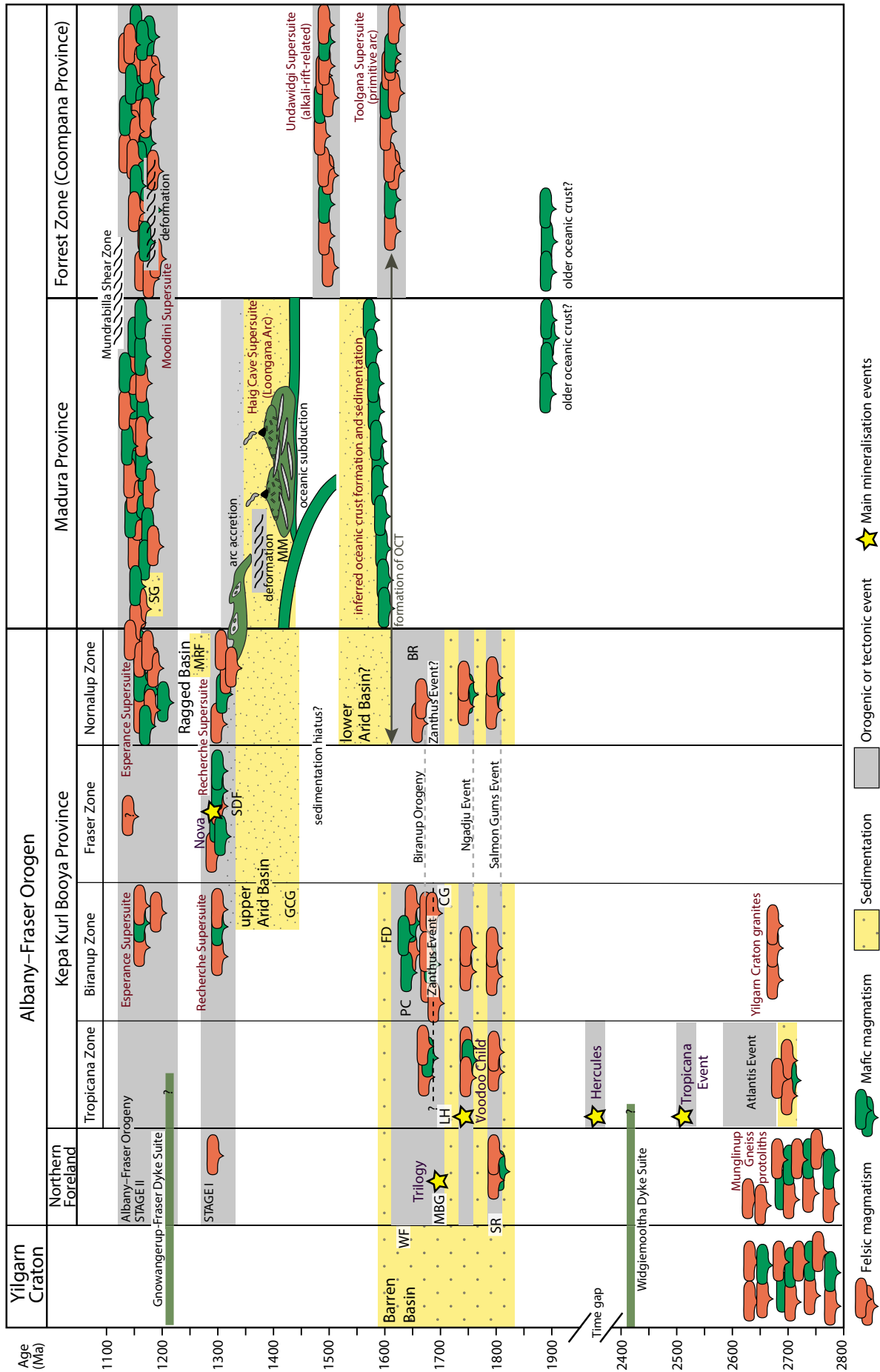


Figure 1. Time-space diagram of the Albany–Fraser Orogen, Madura Province and Forrest Zone. Abbreviations used: FD – Fly Dam Formation; GCG – Gwynne Creek Gneiss; MM – Malcolme Metamorphics; MRF – Mount Ragged Formation; SDF – Snowys Dam Formation; SG – Salisbury Gneiss; WF – Woodline Formation. Modified from Spaggiari et al. (2014c).

at the metamorphic peak, and are probably related to emplacement of adakites. Cu was possibly remobilised into these veins during metamorphism and deformation, which are interpreted to have occurred during adakite intrusion. However, petrographic work also suggests that the basalts could be a fertile, primary source of Cu, and that at an early stage the basaltic fragmental material, especially glass containing tiny sulfide grains, would have been reactive, permeable, and amenable to mobilisation of Cu.

## Forrest Zone: c. 1610 Ma Toolgana Supersuite

Granitic and likely co-genetic monzodioritic rocks of the Toolgana Supersuite (FOR004 and FOR008, southeast Forrest Zone) preserve compositions that suggest a subduction-modified mantle source. In particular, the primitive monzodiorite shows trace element and isotopic variations consistent with derivation from a mantle wedge or subduction-modified lithosphere. This suggests subduction- or arc-related mineral prospectivity, and the presence of Cu in chlorite–epidote–sericite alteration in these rocks is encouraging. It is worth noting that the Toolgana Supersuite is the same age as and geochemically and isotopically similar to the St Peters Suite, along the southern and western edge of the Gawler Craton, which is also interpreted as arc-related (Swain et al., 2008). Although no rocks of c. 1600 Ma age have as yet been found in the northwestern portion of the Forrest Zone, the geochemistry of FOR012, FOR011 and FOR010 rocks suggest Toolgana Supersuite or equivalents were a recycled component.

## 1500–1450 Ma

So far there is little direct record of activity in the Madura Province during this period, nor within the Albany–Fraser Orogen, suggesting it continued to be in a passive margin setting. It is also possible that lithospheric extension and oceanic crust formation in the Madura Province continued until c. 1450 Ma. In the Burkin prospect (Fig. 1 in Preface) a date of c. 1478 Ma in a poorly understood, quartzofeldspathic gneiss could be indicative of the maximum depositional age of the sedimentary rocks it cuts. These sedimentary rocks include fine-grained layers of plagioclase–chlorite–hornblende–epidote and magnetite, interpreted to be metamorphic mafic sedimentary or volcanosedimentary rocks. The magnetite layers contain up to 8.6 wt% MnO, and previous geochemical data identified several horizons of anomalous copper (up to ~1000 ppm). These features could indicate the potential for exhalative or VMS-style deposits, perhaps in the fore-arc position of the early stages of formation of the c. 1400 Ma Loongana Arc. Alternatively, the Burkin date of c. 1478 Ma could record a younger phase of lithospheric extension of the OCT substrate near the continental edge, perhaps related to the formation of the Undawidgi Supersuite in the Forrest Zone.

## Forrest Zone: c. 1500 Ma Undawidgi Supersuite

Meta-granitic rocks, and possible felsic (bimodal?) metavolcanic rocks of the Undawidgi Supersuite are interpreted as due to melting of lower mafic crust and introduction of a mantle component, in a rift setting. These rocks occur in the northwestern part of the Forrest Zone, and their chemistry suggests they have recycled c. 1600 Ma arc crust. Including the c. 1500 Ma granodiorite gneiss from Mallabie 1 (Wade et al., 2007), this event could be interpreted as widespread, c. 1500–1488 Ma lithospheric extension of the oceanic basement and subduction-related magmatic arcs (Toolgana Supersuite, St. Peters Suite?) to produce a suite of high-K rift-related, intrusions and volcanics.

The presence of Cu in these rocks (up to 1172 ppm in FOR012, GSWA 206795), and the significant alteration including chlorite–epidote–sericite, could indicate a potential for VMS deposits. These alkali-rich, magnetite-bearing, and probable high-level intrusions or volcanics that formed from melting of alkali-metasomatised, subduction-related mafic crust could also indicate the potential for IOCG-type mineralisation in the region. The presence in FOR011 of syenites, most likely of c. 1488 Ma crystallization age, with near peralkaline compositions, also suggests the possibility for Nb, Ta, REE mineralization in rift-related alkaline magmatic settings.

Spatially, there appears to be a division between the dominance of c. 1500 Ma Undawidgi Supersuite to the northwest, and c. 1600 Ma Toolgana Supersuite to the southeast, possibly separated by a major, northeasterly trending shear zone, between the mylonites in FOR012 and the granite gneiss in FOR008. The granite gneiss in FOR008 contains kinematic indicators that indicate top to the northwest tectonic transport on a shallowly-dipping structure. The timing of this deformation is probably c. 1180–1150 Ma, but the structure could be an inverted, c. 1500 Ma rift-related feature that extended arc rocks of the Toolgana Supersuite. It is interesting to note the presence of pyrite and carbonate in mylonitic rocks in FOR012, which could be indicative of orogenic gold related to this structure.

## 1450–1330 Ma

During this period major activity appears to be focussed in the Madura Province, and so far there is no further record of tectonic activity after c. 1500 Ma in the Forrest Zone until c. 1190 Ma. The interpretation of an oceanic arc, the Loongana Arc (Haig Cave Supersuite) has been described previously, and has been dated between 1410–1400 Ma (Spaggiari et al., 2014a; Smithies et al., this volume; Wingate et al., this volume). Metasedimentary and basaltic rocks exposed at Point Malcolm (and possibly basaltic rocks drilled at the Burkin prospect) are interpreted to be fore-arc deposits associated with the formation of the Loongana Arc (see Smithies et al., this volume).

This, and the uncontaminated crustal character of the Loongana Arc, suggest southeast-dipping subduction of oceanic crust away from the continental edge (Spaggiari et al., 2015).

The interpretation of oceanic subduction is supported by the presence of the c. 1398 Ma adakites in MAD002, which indicate that subduction was required prior to or during their formation. The adakites are interpreted as melts of subducting oceanic lithosphere, but geochemistry and Nd-isotope data indicate this was not related to the EMORB/OIB basaltic crust they intrude. Their formation was probably linked to formation of the Loongana Arc, and their present (structural/accreted) position west of the Loongana Arc suggests they intruded the MAD002 basalt close to, or within the fore-arc. The adakites in MAD002 are interpreted to be emplaced at a high level, but from deep (~ 52 km) source melting, potentially during folding and lower amphibolite facies metamorphism.

At c. 1330 Ma the Loongana Arc is interpreted to have collided with the passive margin of the Albany–Fraser Orogen, resulting in accretion of the EMORB/OIB rocks of MAD002 and NSD — potentially as topographic highs — and the fore-arc and arc. This event marks the onset of Stage I of the Albany–Fraser Orogeny, and formation of the southeast-dipping Rodona Shear Zone as a major crustal boundary (Spaggiari et al., 2014b, 2015; Kirkland et al., 2015; Smithies et al., 2015).

Despite the widespread younger intrusions of the Moodini Supersuite, the Madura Province represents the preservation of a large, at least 200 km wide, relatively intact, portion of Mesoproterozoic crust with a history of oceanic crust, OCT, and oceanic-arc evolution, thrust over the continental edge of a modified Archean craton as an ophiolite complex. The formation of these oceanic-arc and related rocks have potential for subduction-related mineralization, including PGEs and Ni, preserved within this accreted ophiolite complex.

It is worth noting that so far no c. 1330 to 1260 Ma rocks have been found in the Madura Province or Forrest Zone, and therefore Stage I of the Albany–Fraser Orogeny appears to be restricted to the accretion event itself. This suggests that the Stage I event is not continental collision, but is simply arc accretion. A lack of c. 1300 Ma rocks in the Madura Province also suggests that a switch to west-dipping subduction placing the Albany–Fraser Orogen in a back-arc setting at c. 1300 Ma, to accommodate intrusion of the Fraser Zone gabbros (Clark et al., 2014; Spaggiari et al., 2015), may be incorrect. It is feasible that extensional relaxation, possibly combined with delamination, is all that was required to intrude the remainder of Recherche Supersuite rocks and the Fraser Zone gabbros. This model fits with spatial patterns observed in the ages and geochemistry of the Recherche Supersuite (Smithies et al., 2015). It is suggested that as accretion progressed, thrusting, over-riding and burying of the craton edge led to progressive, westwards crustal thickening. This was followed by westward migrating delamination of the lower crust, with associated magmatism culminating in intrusion of the Fraser Zone gabbros against the more robust portion (older crustal ramp?) of the Yilgarn Craton

(Biranup–Nornalup Zone boundary). This would also allow the Snowys Dam Formation (Arid Basin/Fraser Zone) to quickly get buried due to thrusting and folding.

The prospectivity of the Fraser Zone is well known, however the large, crustal-scale structure (Rodona Shear Zone) that separates Yilgarn Craton-modified crust from dominantly oceanic crust, or OCT crust of the Madura Province, could also be prospective as it also formed during Stage I of the Albany–Fraser Orogeny. Recherche Supersuite intrusions are widespread, particularly in the eastern Nornalup Zone, and intrude sedimentary rocks of the Arid Basin, and it is tempting to suggest that Ni–Cu deposits similar to Nova could be located within the eastern Nornalup Zone. The Rodona Shear Zone could also have facilitated the formation of clastic-dominated (CD) deposits hosting base metals, perhaps within the overlying Arid Basin. Alternatively, the Rodona Shear Zone and surrounding areas could be prospective for orogenic Au, or remobilised Cu–Au sourced from the Madura Province.

## 1200–1100 Ma

This period coincides with Stage II of the Albany–Fraser Orogeny (1225–1140 Ma) and the Musgrave Orogeny (1220–1150 Ma). Intervening crust between the West Australian Craton (WAC) and the South Australian Craton (SAC) is a large, well-preserved remnant of a primitive ‘oceanic domain’ comprising oceanic crust, oceanic arcs, accreted oceanic arcs and reworked oceanic arc crust. The Moodini Supersuite is the expression of the final massive melting event at c. 1225–1130 Ma. In the Madura Province the Moodini Supersuite comprises high-KFe series mafic to felsic magmas. These are geochemically quite highly specialised, high-temperature A-type magmas. However, there are synchronous, compositionally equivalent, magmas forming a voluminous and widespread component of the contiguous Albany–Fraser Orogen and Musgrave Province. The evolution of these rocks reflects high-temperature melting of thinned primitive crust and we suggest this huge regional extent of juvenile high-KFe magmatism relates to an ocean that was not completely destroyed by amalgamation of the WAC the SAC, and remained relatively thin compared to its neighbouring cratons. In fact, it appears that continental collision between the WAC and SAC never actually occurred, at least in the western and southern parts of central Australia, and the two cratons are instead regarded as juxtaposed, but separated by the Madura and Coompana Provinces.

The Madura high-KFe series show regional compositional and Nd-isotopic variations. Rocks of the Booanya Suite (e.g. Hannah 1) marginal to the Madura Province are less radiogenic ( $\epsilon_{\text{Nd}(1200\text{Ma})}$  -4.95 – -7.34) than those from within the Madura Province (e.g. MAD014 ( $\epsilon_{\text{Nd}(1200\text{Ma})}$  -3.7 – -4.8), which in turn are less radiogenic than rocks from Moodini and MAD011 ( $\epsilon_{\text{Nd}(1200\text{Ma})}$  -1.85 – -2.7). This represents a systematic west-northwesterly increase in the proportion of non-radiogenic source material, a trend continued into the eastern Nornalup Zone of the Albany–Fraser Orogen (Smithies et al., 2015). It is also interesting to note that

the more juvenile magmatism in the east-southeast of the Madura Province (MAD011 and Moodini) is younger (c. 1144–1125 Ma) than magmatism to the west-northwest (Booanya, Hannah 1 and MAD014; c. 1181–1172 Ma), reflecting a greater mantle contribution with decreasing age. Similar trends are observed in the Pitjantjatjara Supersuite high-KFe magmas of the Musgrave Province.

The metagranite intersected in the drill holes at Moodini has A-type granite geochemistry, similar in many respects to the contemporaneous Esperance Supersuite granites of the Albany–Fraser Orogen. Both supersuites are a result of mantle-derived melts mixing with remnant extended lower crust, but in the case of the Moodini Supersuite, this lower crust was juvenile Madura Province crust rather than the reworked Archean crust beneath the Albany–Fraser Orogen.

Although essentially recycling crust of the same (or very similar) origins, 1200–1100 Ma magmatism in the Forrest Zone and Madura Province are compositionally extremely different — the high-KFe magmas of the latter contrasting with the high-KMg magmas of the former. Apart from local anatexitic melts expressing high geotherms related to the same thermal anomaly driving high-KFe processes in the Madura Province and Musgrave Province, 1200–1100 Ma magmatism in the Forrest Zone is essentially shoshonitic. It includes both mafic, primitive shoshonite and high silica derivatives of these, forming intrusions that make up to 25% of the crust sampled by FOR010 and FOR011. Their compositions reflect deep melting of wet, oxidized, modified mantle lithosphere and so their presence indicates that the Forrest Zone retained a thick lithosphere up to and into the 1200–1100 Ma event. This contrasts strongly with the Madura Province (and Musgrave Province), where crustal melting components and asthenospheric mantle additions strongly suggest highly extended, dry and reduced crust with little or no remaining lithosphere.

Importantly, the Bottle Corner Shoshonite in the Forrest Zone shows, as a suite, many of the compositional attributes considered indicative as magmas potentially prospective for Cu and Cu–Au mineralisation, including high Sr/Y and evidence for extensive amphibole fractionation.

Rocks from drill cores FOR011 and FOR010, from the northwestern part of the Forrest Zone, share a similar history. These drill sites are located in a distinct northeasterly trending belt that includes the rift-related c. 1490 Ma Undawidgi Supersuite granites intruded by c. 1180 Ma Bottle Corner Shoshonite, and were most likely deformed together during various pulses of shoshonitic magmatism producing northeasterly trending folds, in the low to middle amphibolite facies. These rocks are cut by veins of Moodini Supersuite, hematite altered granites (also c. 1180 Ma), which contain sulfides — pyrite (possibly after pyrrhotite) and chalcopyrite, and locally molybdenite, and galena. Late retrogression is marked by chlorite and epidote alteration. These rocks, and the c. 1500 Ma high-level intrusive and possible felsic volcanic rocks intersected in FOR012, are considered prospective for intrusion-related Cu–Au (or non-

subduction-related porphyry Cu–Au), especially where they occur in the vicinity of large faults or shear zones.

## 1200–1100 Ma deformation

Geochronology and structural analyses of cores FOR011 and FOR010 indicate at least one deformation event, bracketed by the age of the Bottle Corner Shoshonite ( $1180 \pm 6$  Ma in both cores) and an interpreted metamorphic age from crosscutting metagranite dated at  $1174 \pm 12$  Ma, potentially due to late-stage recrystallization or recovery after the foliation-forming event (Fig. 1). This deformation event is interpreted as syn-magmatic, possibly occurring between pulses of shoshonite emplacement, with magmatism outlasting deformation.

## Mundrabilla Shear Zone

The Mundrabilla Shear Zone (Fig. 1 in Preface) is currently defined as the boundary between the Madura Province and the Forrest Zone of the Coompana Province, although based on geochemical and isotopic considerations, it is likely that at least the Madura Province and the Forrest Zone, but possibly also part of the Coompana Province further east (e.g. Mallabie 1), formed on similar juvenile basement. A maximum age of sinistral movement on the Mundrabilla Shear Zone is provided by metagranite in the Moodini prospect drill cores, which contains a strong subhorizontal fabric and yielded identical magmatic crystallization dates of  $1125 \pm 7$  Ma and  $1132 \pm 9$  Ma (GSWA 192565 and 192566, respectively). These dates are similar to the Eucla 1 granite crystallization date of  $1140 \pm 8$  Ma to the east, within the Forrest Zone (Kirkland et al., 2011). It is unknown whether the Mundrabilla Shear Zone initiated at this late stage, or whether it represents a more fundamental, earlier structure and is truly a major province boundary. Regardless of this, it is clear that significant displacement has occurred (c.f. Aitken et al., 2015) as the shear zone separates two crustal entities that are likely to have a common juvenile basement, but preserve different components of the geological history.

## References

- Aitken, ARA, Betts, PG, Young, DA, Blankenship, DD, Roberts, JL, Siegert, MJ 2015, The Australo-Antarctic Columbia to Gondwana transition. *Gondwana Research*, <http://dx.doi.org/10.1016/j.gr.2014.10.019>
- Betts, PG and Giles, D 2006, The 1800–1100 Ma tectonic evolution of Australia: *Precambrian Research*, v. 144, p. 92–125.
- Clark, C, Kirkland, CL, Spaggiari, CV, Oorschot, C, Wingate, MTD and Taylor, R 2014, Proterozoic granulite formation driven by magmatism: an example from the Fraser Range Metamorphics, Western Australia: *Precambrian Research*, v. 240, p. 1–21.
- Kirkland, CL, Smithies, RH and Spaggiari, CV 2015, Foreign contemporaries – Unravelling disparate isotopic signatures from Mesoproterozoic Central and Western Australia: *Precambrian Research special issue*, v. 265, p. 218–231.

- Kirkland, CL, Wingate, MTD, Spaggiari, CV and Tyler, IM 2011, 194773: granitic rock, Eucla No. 1 drillhole; Geochronology Record 1001: Geological Survey of Western Australia, 4p.
- Smithies, RH, Spaggiari, CV and Kirkland, CL 2015, Building the crust of the Albany–Fraser Orogen; constraints from granite geochemistry: Geological Survey of Western Australia, Report 150, 49p.
- Spaggiari CV, Kirkland CL, Smithies RH, and Wingate MTD, 2014a, Tectonic links between Proterozoic sedimentary cycles, basin formation and magmatism in the Albany–Fraser Orogen, Western Australia Geological Survey of Western Australia Report 133, 63p.
- Spaggiari, CV, Occhipinti, SA, Korsch, RJ, Doublier, MP, Clark, DJ, Dentith, MC, Gessner, K, Doyle, MG, Tyler, IM, Kennett, BLN, Costelloe, RD, Fomin, T and Holzschuh, J 2014b, Interpretation of Albany–Fraser seismic lines 12GA-AF1, 12GA-AF2 and 12GA-AF3: implications for crustal architecture, *in* Albany-Fraser Orogen seismic and magnetotelluric (MT) workshop 2014: extended abstracts: *compiled by* CV Spaggiari and IM Tyler Geological Survey of Western Australia, Record 2014/6, p. 28–51.
- Spaggiari, CV, Kirkland, CL, Smithies, RH, Occhipinti, SA and Wingate, MTD 2014c, Geological framework of the Albany–Fraser Orogen, *in* Albany–Fraser Orogen seismic and magnetotelluric (MT) workshop 2014: extended abstracts *compiled by* CV Spaggiari and IM Tyler: Geological Survey of Western Australia, Record 2014/6, p. 12–27.
- Spaggiari, CV, Kirkland, CL, Smithies, RH, Wingate, MTD, and Belousova, EA 2015, Transformation of an Archean craton margin during Proterozoic basin formation and magmatism: The Albany–Fraser Orogen, Western Australia: Precambrian Research, v. 266, p. 440–466.
- Swain, G, Barovich, K, Hand, M, Ferris, G and Schwartz, M 2008, Petrogenesis of the St Peter Suite, southern Australia: Arc magmatism and Proterozoic crustal growth of the South Australian Craton: Precambrian Research, v. 166, p. 283–296.
- Wade, BP, Payne, JL, Hand, M, and Barovich, KM, 2007, Petrogenesis of ca 1.50 Ga granitic gneiss of the Coompana Block: filling the ‘magmatic gap’ of Mesoproterozoic Australia: Australian Journal of Earth Science, v. 54, p. 1089–1102.



## **Appendix 1**

**Graphic summary logs of the stratigraphic cores and Haig cores**

Madura Province

Hole ID: Haig HDDH001    Azimuth: 315    Inclination: -80    Total depth: 636m    EIS co-funded core drilled by Teck Australia Pty Ltd



Depth	Sample	Unit	Graphic log	Lithology	Structure	Alteration	Comment
390		Madura Formation		Dark grey carbonaceous mudstone to siltstone.	Undeformed		Locally derived from basement; contains c. 1410 Ma detrital zircons only
395				Dark, thinly-bedded quartz-mica sandstone with black organic matter.			
400		Disconformity		Polymictic conglomerate mixed with coarse sands, black organic layers.	Undeformed	Minor hematite	
405		Shanes Dam Conglomerate		Polymictic conglomerate: clast-supported, average size 1-20 mm, up to 40-60 mm. Clasts are sandstone, claystone, vein quartz, mafic rock and granite.			
410							
415							
420	199456						
425		Haig Cave Supersuite: c. 1410 Ma (Loongana Arc)		Angular unconformity at 426 m	Foliated		
430				Intensely weathered, veined metagabbro and leucogranite.			
435							
440							Geochronology sample 192560; leucogranite interlayered with leucogabbro; sample submitted
445				Grey, weathered and variably altered metagabbro and leucogranite			
450	201299			Coarse- to medium-grained leucogranite (sample) interlayered with leucogabbro.	Localised, weak to moderate gneissosity	Feldspar-amphibole veins with minor pyrite and chlorite-sericite alteration	
455							
460	201175,6			Medium-grained meso- melanocratic gabbro cut by veins of medium- to coarse-grained acicular leucogabbro (e.g. 201175).		Feldspathic veins, minor	
465						K-feldspar alteration, actinolite, epidote, hematite	
470					Semi-brittle fault zone	Actinolite, chlorite, epidote, hematite, pyrite	
475	201177			Acicular leucogabbro of variable grainsizes; contorted layering.			
480							
485					Localised, weak to moderate gneissosity		
490	201300			Coarse- to medium-grained leucogranite interlayered with fine- to medium-grained leucogabbro; some acicular hornblende to 8 mm.	Semi-brittle fault zone	Actinolite, chlorite, epidote, hematite, pyrite	
495	201178						
495	201179						
500	201180						
505							
510	201181,2			Acicular leucogabbro of variable grainsizes.		K-feldspar alteration, biotite, chlorite, epidote, hematite, pyrite	
515							
520	201183,4			Fine-grained gabbro with veins of acicular leucogabbro of variable grainsizes.		Chlorite, amphibole, sericite, pyrite	
525	201185					Hematite, chlorite	
530	201186					K-feldspar, chlorite, epidote, hematite, pyrite	
535				Mesocratic homogeneous gabbro; well layered coarse-grained to fine-grained acicular gabbro.		Epidote, feldspar, hematite, pyrite	
540	201187					K-feldspar, epidote, chlorite	
545	213804			Coarse- to medium-grained leucogranite (213804) interlayered with acicular leucogabbro.	Localised, weak to moderate gneissosity	Chlorite, epidote, feldspar, sericite, pyrite	
550							
555	201188						
560	201189			Medium- to coarse-grained acicular leucogabbro.		K-feldspar, epidote, pyrite to E.O.H.	
565							
570	201190			Interlayered medium-grained leucogabbro and mesocratic gabbro			
575	213801			Coarse- to medium-grained leucogranite (213801) interlayered with leucogabbro.	Localised, weak to moderate gneissosity		
580	201191,2						
585	213802			Coarse- to medium-grained leucogranite (213802), interlayered with leucogabbro, locally coarse-grained acicular-textured (201190).			
590	201193				Localised, weak to moderate gneissosity		
595							
600				Coarse- to medium-grained leucogranite interlayered with leucogabbro, locally acicular - more intense alteration to E.O.H.			
605							
610					Semi-brittle fault zone		
615					Semi-brittle fault zone		
620							
625							
630							
635							
640							
							Additional information: Tillick 2011, Report A091287; Reynolds 2014, Curtin Honours thesis

# Madura Province

Hole ID: Haig HDDH002 Azimuth: 315 Inclination: -70 Total depth: 483.7m EIS co-funded core drilled by Teck Australia Pty Ltd

[illegible]

## Hole ID: MAD002

Azimuth: 290    Inclination: -80    Total depth: 591.6 m

## GSWA–EIS stratigraphic hole

[illegible]

## Hole ID: MAD011

Azimuth: 140    Inclination: -75    Total depth: 641.15 m

GSWA–EIS stratigraphic hole

[illegible]



## Hole ID: MAD014

Azimuth: 340    Inclination: -80    Total depth: 459.5 m

GSWA–EIS stratigraphic hole

[illegible]



Forrest Zone, Coompana Province

Hole ID: FOR011

Azimuth: 010    Inclination: -80    Total depth: 500.1 m

GSWA–EIS stratigraphic hole



Depth	Sample	Unit	Graphic log	Lithology	Structure	Alteration	Comment
250		Madura Formation		Dark grey carbonaceous mudstone to siltstone.			Mafic layers hbl- and bt-rich
255							
260		Loongana Formation		Poorly consolidated, quartz-dominated feldspathic sandstone; angular, poorly sorted. Locally coarse-grained.			
265							
270							
275							
280				Unconformity at about 285 m.			
285		Undawidgi Supersuite: metamonzodiorite, metasyenite c.1488 Ma		Weathered foliated metagranite.			
290							
295							
300		Moodini Supersuite: Bottle Corner Shoshonite c. 1180 Ma (some evolved Si-rich), Na-rich pegmatite					Breccia with K-feldspar-rich fragments in a bt-chl-ep matrix.
305				Seriate-to equigranular, fine- to medium-grained, red metagranite with mafic and felsic layering; foliation cut by thin pegmatite.	Moderate foliation; cut by veins	Thin quartz-carbonate veins.	
310							
315							
320				Seriate-to equigranular, fine- to medium-grained, red metagranite with mafic and felsic layering; foliation cut by thin pegmatite.			
325							
330							
335				Fine-grained grey metagranite with sparse bt-rich layers – silicified?	Moderate foliation; shallow to moderate NW dip.	Thin quartz-carbonate or chlorite veins Pyrite in bt-rich contact; breccia.	
340				Red equigranular, fine- to medium-grained metagranite, locally with mafic and felsic layering.		Thin quartz-carbonate veins.	
345							
350				Layers of fine-grained bt-hbl metadiorite to metamonzodiorite (shoshonite) in red equigranular metagranite.	Moderate foliation; cut by veins	Thin quartz-carbonate veins; red speckled texture.	Prominent titanite (213836)
355							
360				Red sparsely porphyritic, fine- to medium-grained metagranite.	Moderate foliation; cut by thin pegmatite		
365							
370	213839			Seriate-to equigranular, fine- to medium-grained, red metagranite with mafic and felsic layering.	Small-scale, northeast-plunging antiform	Thin carbonate and chl-bt veins	
375	213836						
380				Distinct mafic amphibolite layer (213837) – older host rock?	Moderate to strong foliation; shallow to moderate SE dip.	Thin quartz-carbonate veins.	
385	213837			Coarse (3-10 mm) quartz-rich cross-cutting granitic vein, cuts S1.		Disseminated pyrite (alt pyrrhotite?), chalcopyrite (alt to bornite).	
390	213840			Seriate-to equigranular, fine- to medium-grained, red metagranite with variable proportions of mafic and felsic layering.	Shallow NE dip - fold hinge.		
395	213841						
400	213842			Seriate-to equigranular, fine- to medium-grained, red metagranite with variable proportions of mafic and felsic layering.	Weak to moderate foliation; moderate NW dip.	Thin chlorite veins.	Geochronology sample 213838 (late pegmatite) 1189 ± 6 Ma
405	213843						
410	213844			Seriate-to equigranular, fine- to medium-grained, red metagranite with variable proportions of mafic and felsic layering.			
415	213845						
420	213846			Layers of fine-grained bt-hbl metadiorite to metamonzodiorite (shoshonite) in red equigranular metagranite.		Disseminated pyrite, minor molybdonite and chalcopyrite.	
425	213847						
430	213848						
435	213849			Seriate-to equigranular, fine- to medium-grained, red metagranite with variable proportions of mafic and felsic layering.	Moderate foliation; moderate NW or NE dip.	Breccia and alteration zone; chlorite veins	
440	213850						
445	213851						
450	213852			Distinct mafic amphibolite layer – older host rock?	Weak to moderate foliation; moderate NW or NE dip.	Thin quartz-carbonate veins, zones of chlorite alteration and breccia, magnetite to hematite	Geochronology samples 206729 (shoshonite) 1180 ± 6 Ma and 206730 (metasyenite) 1488 ± 4 Ma, metamorphic date 1174 ± 12 Ma
455				Seriate-to equigranular, fine- to medium-grained, red metagranite with variable proportions of mafic and felsic layering.		Broken core, clay-rich	
460							
465					Weak to moderate foliation; moderate NW or NE dip.	Thin quartz-carbonate veins, zones of chlorite alteration and breccia.	
470	192596			Seriate-to equigranular, fine- to medium-grained, red metagranite with variable proportions of mafic and felsic layering.		Broken core, clay-rich	
475							
480							
485						Thin quartz-carbonate veins, zones of chlorite alteration and breccia.	
490				Seriate-to equigranular, fine- to medium-grained, red metagranite with variable proportions of mafic and felsic layering.			
495							
500							
505							

## Hole ID: FOR010

Azimuth: 140

Inclination: -80

Total depth: 527.8 m

GSWA–EIS stratigraphic hole

[illegible]

## Hole ID: FOR012

Azimuth: 150

Inclination: -75

Total depth: 510.60 m

GSWA-EIS stratigraphic hole

[illegible]



Hole ID: FOR008

Azimuth: 105

Inclination: -75

Total depth: 585.50 m

GSWA–EIS stratigraphic hole

[illegible]

# Forrest Zone, Coompana Province

Hole ID: FOR004

Azimuth: 070

Inclination: -80

Total depth: 570.40 m

## GSWA–EIS stratigraphic hole

[illegible]

This Record is published in digital format (PDF) and is available as a free download from the DMP website at  
<[www.dmp.wa.gov.au/GSWApublications](http://www.dmp.wa.gov.au/GSWApublications)>.

Further details of geological products produced by the Geological Survey of Western Australia can be obtained by contacting:

Information Centre  
Department of Mines and Petroleum  
100 Plain Street  
EAST PERTH WESTERN AUSTRALIA 6004  
Phone: +61 8 9222 3459 Fax: +61 8 9222 3444  
[www.dmp.wa.gov.au/GSWApublications](http://www.dmp.wa.gov.au/GSWApublications)

